Theory of the Cosmic Microwave Background (CMB)

Mini-course for the Heidelberg Grad-days 2023

Ruth Durrer

Département de Physique Théorique de l'Université de Genève
Quai E. Ansermet 24, 1211 Genève 4, Suisse

Contents

Chapter 1

The expanding Universe

1.1 Homogeneity and Isotropy

I assume that you all are more or less familiar with General Relativity, i.e. that you know what a metric is, what a geodesic is and how Christoffel symbols, curvature and the Einstein tensor are defined. Einstein's equations are

$$G_{\mu\nu} = \frac{8\pi G}{c^4} T_{\mu\nu} + \Lambda g_{\mu\nu} \,, \tag{1.1}$$

where $G_{\mu\nu}(g_{\mu\nu}, \partial_\alpha g_{\mu\nu}, \partial_\alpha \partial_\beta g_{\mu\nu})$ is the Einstein tensor determined by the metric, $g_{\mu\nu}$ and its derivatives, $T_{\mu\nu}$ is the energy momentum tensor determined by the matter content of the Universe, Λ is the cosmological constant and G is Newton's constant.

In cosmology we search for spatially homogeneous and isotropic solutions of these equations. This means, in a first attempt we neglect the irregularities of the matter distribution in the Universe and approximate it by a spatially homogeneous and isotropic distribution. This is often called the 'cosmological principle': on large enough scales, the Universe looks the same in every position and in all directions. In a second step we shall study fluctuation mainly within linear perturbation theory. On sufficiently large scales this agrees surprisingly well with observations as we shall see.

The first difficulty we encounter is how to define spatial homogeneity and isotropy. For this we assume that the spacetime $\mathcal{M}$ admits a foliation into 3-manifolds with a timelike unit normal u, $u^2 = g_{\mu\nu} u^\mu u^\nu = -1$. Since u is hypersurface orthogonal it is proportional to the gradient of some function τ on $\mathcal{M}$ which we call cosmic time, $u = f\partial_\tau$. Since we assume spatial homogeneity f cannot depend of the position on the hypersuface Σ_τ hence it can at best be a function of τ. We can get rid of this dependence by a simple redefinition of τ such that $u = \partial_\tau$. This time coordinate is called cosmic time.

Spacetime is now of the form

$$\mathcal{M} = \Sigma \times I \tag{1.2}$$

where $I \subset \mathbb{R}$ is an interval and Σ is a 3-manifold which we request to be homogeneous and isotropic. More precisely, the isometry group of the metric

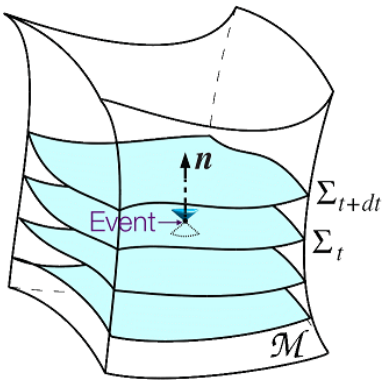

Figure 1.1: A foliation of spacetime. The unit normal n is called u in the text.

induced on Σ, g_Σ contains the rotations and translations. One can now show that this implies that Σ is a space of constant curvature K with metric

$$g_\Sigma = a^2 \gamma_{ij} dx^i dx^j \, . \tag{1.3}$$

The time dependence can be absorbed into the dependence of the scale factor $a(\tau)$. One can choose coordinates on Σ such that γ takes one of the following forms.

$$\gamma_{ij} dx^i dx^j = \frac{\delta_{ij} dx^i dx^j}{(1 + \frac{K}{4}\rho^2)^2} \tag{1.4}$$

$$\gamma_{ij} dx^i dx^j = dr^2 + \chi^2(r) \left(d\theta^2 + \sin^2(\theta) d\varphi^2 \right) \tag{1.5}$$

$$\gamma_{ij} dx^i dx^j = \frac{dR^2}{1 - KR^2} + R^2 \left(d\theta^2 + \sin^2(\theta) d\varphi^2 \right) \tag{1.6}$$

where in Eq. (1.4)

$$\rho^2 = \sum_{i,j=1}^{3} \delta_{ij} x^i x^j \ , \text{ and } \delta_{ij} = \begin{cases} 1 & \text{if } i = j \\ 0 & \text{else,} \end{cases} \tag{1.7}$$

and in Eq. (1.5)

$$\chi(r) = \begin{cases} r & \text{in the Euclidean case,} \quad K = 0 \\ \frac{1}{\sqrt{K}} \sin(\sqrt{K} r) & \text{in the spherical case,} \quad K > 0 \\ \frac{1}{\sqrt{|K|}} \sinh(\sqrt{|K|} r) & \text{in the hyperbolic case,} \quad K < 0. \end{cases} \tag{1.8}$$

Often, one normalizes the scale factor such that $K = \pm 1$ whenever $K \neq 0$. One has, however, to keep in mind that in this case r and K become dimensionless and the scale factor a has the dimension of length. If $K = 0$ we can normalize a arbitrarily. We shall usually normalize the scale factor such that $a(\tau_0) = 1$ and the curvature is not dimensionless. Here and in the following, the subscript 0, (if not denoting the component of a 4-vector) indicates the value of a quantity at present time.

Exercice 1 Coordinates
Find the coordinate transformation leading from the coordinates used in Eq. (1.5) to those of Eq. (1.6) and finally to those of Eq. (1.4).

Instead of cosmic time τ we shall often also use conformal time t which is defined by $dt = d\tau/a(\tau)$. The 4d metric in cosmic and conformal time is given by

$$ds^2 = g_{\mu\nu}dx^\mu dx^\nu = -d\tau^2 + a^2(\tau)\gamma_{ij}dx^i dx^j \,, \tag{1.9}$$
$$= a^2(t)\left(-dt^2 + \gamma_{ij}dx^i dx^j\right) \,. \tag{1.10}$$

A spacetime with a metric of this form is called a Friedmann-Lemaître (FL) universe.

Exercice 2 Cosmic flow

i) Using cosmic time, (1.9) compute the Christoffel symbols in terms of the Christoffels of the spatial metric γ_{ij} which we denote ${}^3\Gamma^k_{ij}$.

ii) Use the result of i) to show that the vector field $u = \partial_\tau$ is a geodesic,

$$\nabla_u u = 0, \qquad i.e.\ (\nabla_u u)^\mu = u^\nu\partial_\nu u^\mu + \Gamma^\mu_{\alpha\beta}u^\alpha u^\beta = 0\,. \tag{1.11}$$

1.2 The Friedman equations

A Universe with homogeneous and isotropic spatial sections is called a Friedmann-Lemaître universe. Friedmann was the first to discuss these solutions of Einstein's equations and Lemaître was the first to interpret the observable Universe as close to such a solution. (Later Robertson and Walker refined and extended the discussion of homogeneous and isotropic geometries).

1.2.1 Derivation

Due to the symmetry of spacetime, the energy–momentum tensor can only be of the form

$$(T_{\mu\nu}) = \begin{pmatrix} -\rho g_{00} & \mathbf{0} \\ \mathbf{0} & P g_{ij} \end{pmatrix} \,. \tag{1.12}$$

There is no additional assumption going into this ansatz, such as the matter content of the Universe being an ideal fluid. It is a simple consequence of homogeneity and isotropy and is also verified for scalar field matter, a viscous fluid or free-streaming particles in a FL universe. As usual, the energy density ρ and the pressure P are defined as the time- and space-like eigenvalues of (T^μ_ν).

The Einstein tensor can be calculated from the definition (A.12) and Eqs. (A.31)—

(A.38) given in the appendix,

$$G_{00} = 3\left[\left(\frac{a'}{a}\right)^2 + \frac{K}{a^2}\right] \quad \text{(cosmic time)} \tag{1.13}$$

$$G_{ij} = -\left(2a''a + a'^2 + K\right)\gamma_{ij} \quad \text{(cosmic time)} \tag{1.14}$$

$$G_{00} = 3\left[\left(\frac{\dot{a}}{a}\right)^2 + K\right] \quad \text{(conformal time)} \tag{1.15}$$

$$G_{ij} = -\left(2\left(\frac{\dot{a}}{a}\right)^{\bullet} + \left(\frac{\dot{a}}{a}\right)^2 + K\right)\gamma_{ij} \quad \text{(conformal time)}\ . \tag{1.16}$$

The Einstein equations relate the Einstein tensor to the energy–momentum content of the Universe via $G_{\mu\nu} = 8\pi G T_{\mu\nu} - g_{\mu\nu}\Lambda$. Here Λ is the so called cosmological constant. In a FL universe the Einstein equations become

$$\left(\frac{a'}{a}\right)^2 + \frac{K}{a^2} = \frac{8\pi G}{3}\rho + \frac{\Lambda}{3} \quad \text{(cosmic time)} \tag{1.17}$$

$$2\frac{a''}{a} + \frac{(a')^2}{a^2} + \frac{K}{a^2} = -8\pi G P + \Lambda \quad \text{(cosmic time)} \tag{1.18}$$

$$\left(\frac{\dot{a}}{a}\right)^2 + K = \frac{8\pi G}{3}a^2\rho + \frac{a^2\Lambda}{3} \quad \text{(conformal time)} \tag{1.19}$$

$$2\left(\frac{\dot{a}}{a}\right)^{\bullet} + \left(\frac{\dot{a}}{a}\right)^2 + K = -8\pi G a^2 P + a^2\Lambda \quad \text{(conformal time)}\ . \tag{1.20}$$

Energy 'conservation', $T^{\mu\nu}_{;\mu} = 0$ yields

$$\dot{\rho} = -3(\rho + P)\left(\frac{\dot{a}}{a}\right) \quad \text{or, equivalently} \quad \rho' = -3(\rho + P)\left(\frac{a'}{a}\right)\ . \tag{1.21}$$

This equation can also be obtained by differentiating Eq. (1.17) or (1.19) and inserting (1.18) or (1.20); it is a consequence of the contracted Bianchi identities. Eqs. (1.17)—(1.20) are the Friedmann equations. The quantity

$$H(\tau) \equiv \frac{a'}{a} = \frac{\dot{a}}{a^2} \equiv \mathcal{H}a^{-1} \tag{1.22}$$

is called the Hubble rate or the Hubble parameter, where $\mathcal{H}$ is the comoving Hubble parameter. At present, the universe is expanding, so that $H_0 > 0$. We parameterize it by

$$H_0 = 100h \text{ km/sec/Mpc} \simeq 3.241 \times 10^{-18} h \text{ sec}^{-1} \simeq 1.081 \times 10^{-28} h \text{ cm}^{-1}\ .$$

For the last equation we set, as for the rest of this course,
the speed of light, $c = 1$.

Observations show that $0.66 < h < 0.75$. More precisely, latest local observations from supernovae (see Section 1.3) give $h = 0.7304 \pm 0.0104$ [1], while parameter estimation from the cosmic microwave background give $h = 0.674 \pm 0.005$ (assuming minimal neutrino masses) [2]. This discrepancy of about 5σ is called the 'Hubble tension'.

1.2.2 Some solutions

Eq. (1.21) is easily solved in the case $w = P/\rho =$ constant. Then one finds

$$\rho = \rho_0 (a_0/a)^{3(1+w)} \ , \tag{1.23}$$

where ρ_0 and a_0 denote the value of the energy density and the scale factor at present time, τ_0. For non-relativistic matter, $P_m = 0$, we therefore have $\rho_m \propto a^{-3}$ while for radiation (or any kind of massless particles) $P_r = \rho_r/3$ and hence $\rho_r \propto a^{-4}$. A cosmological constant corresponds to $P_\Lambda = -\rho_\Lambda$ and we obtain, as expected $\rho_\Lambda =$constant. If the curvature K can be neglected and the energy density is dominated by one component with $w =$ constant, inserting Eq. (1.23) into the Friedmann equations yields the solutions

$$K = 0\,, \qquad w = \text{const.}$$

$$a \propto \tau^{2/3(1+w)} \propto t^{2/(1+3w)} \qquad w = \text{constant} \neq -1 \tag{1.24}$$

$$a \propto \tau^{2/3} \propto t^2 \qquad w = 0, \quad \text{(dust)} \tag{1.25}$$

$$a \propto \tau^{1/2} \propto t \qquad w = 1/3, \quad \text{(radiation)} \tag{1.26}$$

$$a \propto \exp(H\tau) \propto 1/|t| \qquad w = -1, \quad \text{(cosmol. const.)} \tag{1.27}$$

Exercice 3 Some solutions to the Friedmann equation
Using the Friedmann eqns. (1.17) and (1.19), verify solutions (1.24) to (1.27).

It is interesting to note that if $w < -1$, so-called 'phantom matter', we have to choose $\tau < 0$ to obtain an expanding universe and the scale factor diverges in finite time, at $\tau = 0$. This is the so-called 'big rip'. Phantom matter has many problems but it is discussed in connection with the supernova type 1a (SN1a) data, which are compatible with an equation of state with $w < -1$ or with an ordinary cosmological constant [3]. For $w < -1/3$ the time coordinate t has to be chosen negative for the universe to expand and spacetime cannot be continued beyond $t = 0$. But $t = 0$ corresponds to a cosmic time, the proper time of a static observer, $\tau = \infty$; this is not a singularity. (The geodesics can be continued until affine parameter ∞.)

We also introduce the adiabatic sound speed c_s determined by

$$c_s^2 = \frac{P'}{\rho'} = \frac{\dot{P}}{\dot{\rho}} \ . \tag{1.28}$$

From this definition and Eq. (1.21) it is easy to see that

$$\dot{w} = 3\mathcal{H}(1+w)(w - c_s^2) \ . \tag{1.29}$$

Hence $w =$ constant if and only if $w = c_s^2$ or $w = -1$. Note that already in a simple mixture of matter and radiation $w \neq c_s^2 \neq$constant.

Exercice 4 Matter and radiation mixture
Consider a FL universe containing a mixture of non-relativistic matter (dust)

and radiation with vanishing curvature. The respective densities and pressures are ρ_m, ρ_r and $P_m = 0$, $P_r = \rho_r/3$. We denote the ratio of radiation to matter by $R = \rho_r/\rho_m$.

(a) Determine w and c_s^2 as functions of R. What is the time dependence of R?

(b) For a given redshift $z_{\rm eq} \gg 1$ of matter and radiation equality determine the scale factor as a function of conformal and of physical time; normalize the scale factor to 1 at equality, $a_{\rm eq} = 1$.

(c) Determine $t_{\rm eq}$ and $\tau_{\rm eq}$ as functions of $z_{\rm eq}$, and H_0.

(d) Express $z_{\rm eq}$ in terms of Ω_r and Ω_m (today). Compute $z_{\rm eq}$, $t_{\rm eq}$ and $\tau_{\rm eq}$ numerically for $\Omega_m = 0.3$, $\Omega_r = 8.51 \times 10^{-5}$ and $H_0 = 70 km/s/Mpc$. (You may neglect neutrino masses.)

Exercice 5 Cosmological constant

Investigate the dynamics of a FL universe with matter ($P = 0$) and a cosmological constant Λ.

(i) Show that for a sufficiently small cosmological constant and positive curvature that the Universe re-collapses in a 'big crunch', while for a larger cosmological constant or non-positive curvature, the Universe expands forever.

(ii) Show furthermore that for an even higher cosmological constant there are solutions which have no big bang in the past, but issue from a previous contracting phase. The transition from the contracting to an expanding phase is called the 'bounce'.

(iii) Make a qualitative plot in the plane $(\Omega_m, \Omega_\Lambda)$ distinguishing the regimes determined above.

(iv) For case (ii), determine (numerically, with Mathematica) the redshift of the bounce as a function of Ω_Λ for fixed $\Omega_m = 0.1$. Discuss.

Eq. (1.17) implies that for a critical value of the energy density given by

$$\rho(\tau) = \rho_c(\tau) = \frac{3H^2}{8\pi G} \tag{1.30}$$

the curvature and the cosmological constant vanish. The value ρ_c is called the critical density. The ratio $\Omega_X = \rho_X/\rho_c$ is the 'density parameter' of the component X. It indicates the fraction that the component X contributes to

the expansion rate of the Universe. We shall make use especially of

$$\Omega_r \equiv \Omega_r(\tau_0) = \frac{\rho_r(\tau_0)}{\rho_c(\tau_0)} \tag{1.31}$$

$$\Omega_m \equiv \Omega_m(\tau_0) = \frac{\rho_m(\tau_0)}{\rho_c(\tau_0)} \tag{1.32}$$

$$\Omega_K \equiv \Omega_K(\tau_0) = \frac{-K}{a_0^2 H_0^2} \tag{1.33}$$

$$\Omega_\Lambda \equiv \Omega_\Lambda(\tau_0) = \frac{\Lambda}{3H_0^2} \ . \tag{1.34}$$

$$\tag{1.35}$$

1.2.3 The 'big bang' and 'big crunch' singularities

We can absorb the cosmological constant into the energy density and pressure by redefining

$$\rho_{\rm eff} = \rho + \frac{\Lambda}{8\pi G} \ , \qquad P_{\rm eff} = P - \frac{\Lambda}{8\pi G} \ .$$

Since Λ is a constant and $\rho_{\rm eff}+P_{\rm eff} = \rho+P$, the conservation equation (1.21) still holds. A first interesting consequence of the Friedmann equations is obtained when subtracting Eq. (1.17) from (1.18). This yields

$$\frac{a''}{a} = -\frac{4\pi G}{3}(\rho_{\rm eff} + 3P_{\rm eff}) \ . \tag{1.36}$$

Hence if $\rho_{\rm eff} + 3P_{\rm eff} > 0$, the Universe is decelerating. Furthermore, Eqs. (1.21) and (1.36) then imply that in an expanding and decelerating Universe

$$\frac{\rho'_{\rm eff}}{\rho_{\rm eff}} < -2\frac{a'}{a} \ ,$$

so that ρ decays faster than $1/a^2$. If the curvature is positive, $K > 0$, this implies that at some time in the future, $\tau_{\rm max}$, the density has dropped down to the value of the curvature term, $K/a^2(\tau_{\rm max}) = 8\pi G\rho_{\rm eff}(\tau_{\rm max})$. Then the Universe stops expanding and recollapses. Furthermore, independent of curvature, as a' decreases the curve $a(\tau)$ is concave and thus cuts the $a = 0$ line at some finite time in the past. This moment of time is called the 'big bang'. The spatial metric vanishes at this value of τ, which we usually choose to be $\tau = 0$; and spacetime cannot be continued to earlier times. This is not a coordinate singularity. From the Ricci tensor given in Eqs. (A.31) and (A.32) one obtains the Riemann scalar

$$R = 6\left[\frac{a''}{a} + \left(\frac{a'}{a}\right)^2 + \frac{K}{a^2}\right] \ ,$$

which also diverges if $a \to 0$. Also the energy density, which grows faster than $1/a^2$ as $a \to 0$ diverges at the big bang.

If the curvature K is positive, the Universe contracts after $\tau = \tau_{\rm max}$ and, since the graph $a(\tau)$ is convex, reaches $a = 0$ at some finite time τ_c, the time of the 'big crunch'. The big crunch is also a physical singularity beyond which spacetime cannot be continued.

It is important to note that this behavior of the scale factor can only be implied if the so-called 'strong energy condition' holds, $\rho_{\rm eff} + 3P_{\rm eff} > 0$. It is illustrated in Fig. 1.2.

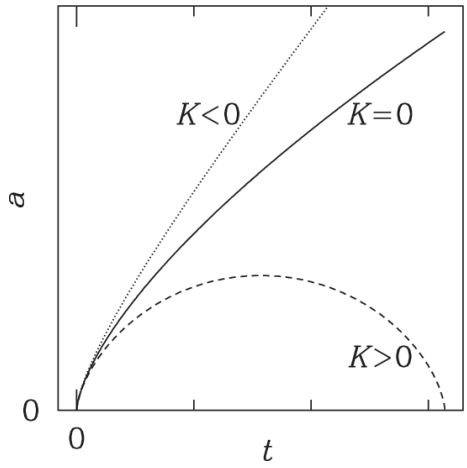

Figure 1.2: The kinematics of the scale factor in a Friedmann–Lemaître universe which satisfies the strong energy condition, $\rho_{\rm eff} + 3P_{\rm eff} > 0$.

1.3 Distances in cosmology

It is notoriously difficult to measure distances in the Universe. The position of an object in the sky gives us its angular coordinates, but how far away is the object from us? This problem has plagued cosmology for centuries. It was only Hubble, who discovered around 1915–1920 that the 'spiral nebulae' are actually not situated inside our own galaxy but much further away. This then led to the discovery of the expansion of the Universe.

For cosmologically distant objects, a third coordinate, which is nowadays relatively easy to obtain, is the redshift z experienced by the photons emitted from the object. A given spectral line with intrinsic wavelength λ is redshifted due to the expansion of the Universe. If it is emitted at some time τ, it reaches us today with wavelength $\lambda_0 = \lambda a_0/a(\tau) = (1+z)\lambda$. This leads to the definition of the cosmic redshift

$$z(\tau) = \frac{a_0}{a(\tau)} - 1 \ . \tag{1.37}$$

On the other hand, an object at physical distance $d = a_0 r$ away from us, at redshift $z \ll 1$, recedes with speed $v = H_0 d$. To the lowest order in z, we have $\tau_0 - \tau \approx d$ and $a(\tau) \approx a_0 + a'(\tau_0)(\tau - \tau_0)$, so that

$$1 + z \approx 1 + \frac{a'(\tau_0)}{a_0}(\tau_0 - \tau) \approx 1 + H_0 d.$$

For objects that are sufficiently close, $z \ll 1$, we therefore have $v \approx z$ and hence $H_0 = v/d$. This is the method usually applied to measure the Hubble constant. I requires measuring not only the redshift but also the distance to far away objects.

There are different ways to measure distances in cosmology all of which give the same result in a Minkowski universe but differ in an expanding universe. They are, however, simply related as we shall see.

One possibility is to define the distance D_A to a certain object of given physical size Δ seen at redshift z_1 such that the angle subtended by the object is given by

$$\vartheta = \Delta/D_A \ , \quad D_A = \Delta/\vartheta \ . \tag{1.38}$$

This is the angular diameter distance or area distance, see Fig. 1.3.

Figure 1.3: The two ends of the object emit a flash simultaneously from A and B at z_1 which reaches us today. The angular diameter distance to A (or B) is defined by $D_A = \Delta/\vartheta$.

We now derive the expressions

$$D_A(z) = \frac{1}{\sqrt{|\Omega_K|}H_0(1+z)}\chi\left(\sqrt{|\Omega_K|}H_0\int_0^z \frac{dz'}{H(z')}\right) \tag{1.39}$$

for the angular diameter distance to redshift z. In a given cosmological model, this allows us to express the angular diameter distance for a given redshift as a function of the cosmological parameters.

To derive (1.39) we use the coordinates introduced in (1.5). Without loss of generality we set $r = 0$ at our position. We consider an object of physical size Δ at redshift z_1 simultaneously emitting a flash at both ends A and B. Hence $r = r_1 = t_0 - t_1$ at the position of the flashes, A and B at redshift z_1. If Δ denotes the physical arc length between A and B we have $\Delta = a(t_1)\chi(r_1)\vartheta = a(t_1)\chi(t_0 - t_1)\vartheta$, i.e.,

$$\vartheta = \frac{\Delta}{a(t_1)\chi(t_0 - t_1)} \ . \tag{1.40}$$

According to Eq. (1.38) the angular diameter distance to t_1 or z_1 is therefore given by

$$a(t_1)\chi(t_0 - t_1) \equiv D_A(z_1) \ . \tag{1.41}$$

To obtain an expression for $D_A(z)$ in terms of the cosmic density parameters and the redshift, we have to calculate $(t_0 - t_1)(z_1)$.

Note that in the case $K = 0$ we can normalize the scale factor a as we want, and it is convenient to choose $a_0 = 1$, so that comoving scales become physical scales today. However, for $K \neq 0$, we have already normalized a such that $K = \pm 1$ and $\chi(r) = \sin r$ or $\sinh r$. In this case, we have no normalization constant left and a_0 has the dimension of a length. The present spatial curvature of the Universe then is $\pm 1/a_0^2$.

The Friedmann equation (1.19) reads

$$\dot{a}^2 = \frac{8\pi G}{3}a^4\rho + \frac{1}{3}\Lambda a^4 - Ka^2, \tag{1.42}$$

where $\dot{a} = da/dt$. To be specific, we assume that ρ is a combination of dust, cold, non-relativistic 'matter' of $P_m = 0$ and radiation of $P_r = \rho_r/3$.

Since $\rho_r \propto a^{-4}$ and $\rho_m \propto a^{-3}$, we can express the terms on the r.h.s. of (1.42) as

$$\frac{8\pi G}{3} a^4 \rho = H_0^2 \left(a_0^4 \Omega_r + \Omega_m a a_0^3 \right) \tag{1.43}$$

$$\frac{1}{3}\Lambda a^4 = H_0^2 \Omega_\Lambda a^4 \tag{1.44}$$

$$-Ka^2 = H_0^2 \Omega_K a^2 a_0^2 \; . \tag{1.45}$$

The Friedmann equation then implies

$$\frac{da}{dt} = H_0 a_0^2 \left(\Omega_r + \frac{a}{a_0}\Omega_m + \frac{a^4}{a_0^4}\Omega_\Lambda + \frac{a^2}{a_0^2}\Omega_K \right)^{\frac{1}{2}} \tag{1.46}$$

so that

$$t_0 - t_1 = \frac{1}{H_0 a_0} \int_0^{z_1} \frac{dz}{\left[\Omega_r (z+1)^4 + \Omega_m (z+1)^3 + \Omega_\Lambda + \Omega_K (z+1)^2\right]^{\frac{1}{2}}} . \tag{1.47}$$

Here we have used $z + 1 = a_0/a$ so that $da = -dz a_0/(1+z)^2$.

In principle, we could of course also add other matter components like, e.g. 'quintessence' [4], which would lead to a somewhat different form of the integral (1.47), but for definiteness, we remain with matter, radiation and a cosmological constant.

From $\frac{-K}{H_0^2 a_0^2} = \Omega_K$ we obtain $H_0 a_0 = \frac{1}{\sqrt{|\Omega_K|}}$ for $\Omega_K \neq 0$. The expression for the angular diameter distance thus becomes

$$D_A(z) = \begin{cases} \frac{1}{\sqrt{|\Omega_K|} H_0 (z+1)} \chi \left(\sqrt{|\Omega_K|} \int_0^z \frac{dz'}{\left[\Omega_r (z'+1)^4 + \Omega_m (z'+1)^3 + \Omega_\Lambda + \Omega_K (z'+1)^2\right]^{\frac{1}{2}}} \right) \\ \qquad \text{if } K \neq 0 \\ \\ \frac{1}{H_0 (z+1)} \int_0^z \frac{dz'}{\left[\Omega_r (z'+1)^4 + \Omega_m (z'+1)^3 + \Omega_\Lambda\right]^{\frac{1}{2}}} \\ \qquad \text{if } K = 0 \; . \end{cases} \tag{1.48}$$

Using again the Friedmann equation, this formula can also be written in the form of Eq. (1.39).

In general, the above integral has to be solved numerically. It determines the angle $\vartheta(\Delta, z) = \Delta / D_A(z)$ under which an object of size Δ placed at redshift z is seen (see Figs. 1.3 and 1.4).

If we are able to measure the redshifts and the angular extensions of a certain class of objects at different redshifts, of which we know the intrinsic size Δ, comparing with Eq. (1.48) allows in principle to determine the parameters Ω_m, Ω_Λ, Ω_K and H_0.

Observationally we know for certain that $10^{-5} < \Omega_r \leq 10^{-4}$ as well as $0.1 \leq \Omega_m \lesssim 1$, $|\Omega_\Lambda| \lesssim 1$ and $|\Omega_K| \lesssim 1$.

If we are interested in small redshifts, $z_1 \lesssim 10$, we may therefore safely neglect Ω_r. In this region, Eq. (1.48) is very sensitive to Ω_Λ and provides an excellent mean to constrain the cosmological constant.

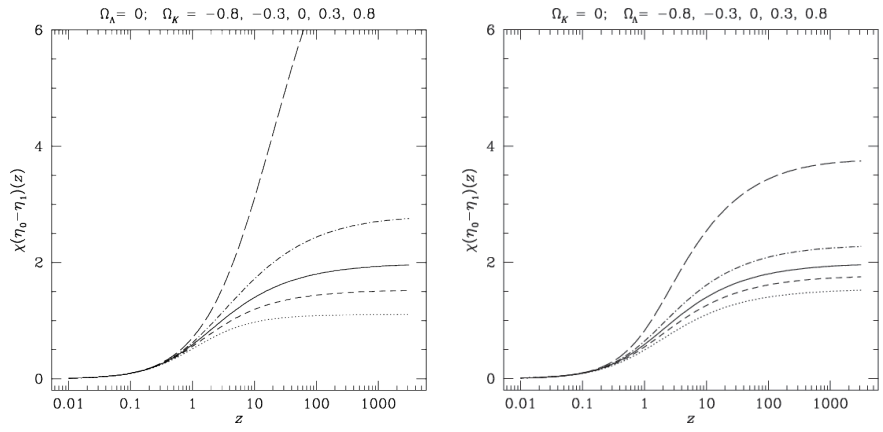

Figure 1.4: The function $\chi(t_0 - t_1)$ as a function of the redshift z for different values of the cosmological parameters Ω_K (left, with Ω_Λ=0) and Ω_Λ (right, with Ω_K=0), namely -0.8 (dotted), -0.3 (short-dashed), 0 (solid), 0.3 (dot-dashed), 0.8 (long-dashed).

At high redshift, $z_1 \gtrsim 1000$, neglecting radiation is no longer a good approximation.

We shall later also need the opening angle of the *horizon* distance,

$$\vartheta_H(z_1) = \frac{t_1}{\chi(t_0 - t_1)}, \tag{1.49}$$

$$t_1 = \frac{1}{H_0 a_0} \int_{z_1}^{\infty} \frac{dz}{[\Omega_r(z+1)^4 + \Omega_m(z+1)^3 + \Omega_\Lambda + \Omega_K(z+1)^2]^{\frac{1}{2}}}. \tag{1.50}$$

(Clearly this integral diverges if $\Omega_r = \Omega_m = 0$. This is exactly what happens during an inflationary period and leads there to the solution of the horizon problem.)

Neglecting Ω_r, for $\Omega_\Lambda = 0$ and small curvature, $0 < |\Omega_K| < \Omega_m(1 + z_1)$ at high enough redshift, $z_1 \geq 10$, one has $t_0 - t_1 \simeq 2\sqrt{|\Omega_K|/\Omega_m} = 2/(H_0 a_0 \sqrt{\Omega_m})$. With $\chi(x) \simeq x$ which is valid for small curvature, this yields $\vartheta(\Delta, z_1) \simeq \sqrt{\Omega_m} H_0 a_0 \Delta/(2a_1) = \frac{1}{2}\sqrt{\Omega_m} H_0 \Delta/(z_1 + 1)$.

Another important distance measure in cosmology is the luminosity distance. It is defined as follows. Let L be the luminosity (energy emitted per second) of a source at redshift z_1 and F its flux (energy received per second per square centimetre) arriving at the observer position. We define the luminosity distance to the source by

$$D_L(z_1) \equiv \left(\frac{L}{4\pi F}\right)^{1/2}. \tag{1.51}$$

We now want to show that $D_L(z_1) = (1 + z_1)^2 D_A(z_1)$.

In a proper time interval of the emitter, $d\tau_1 = a(t_1)dt$, the source emits the energy $La(t_1)dt$. This energy is redshifted by a factor $(1 + z_1)^{-1} = a(t_1)/a(t_0)$.

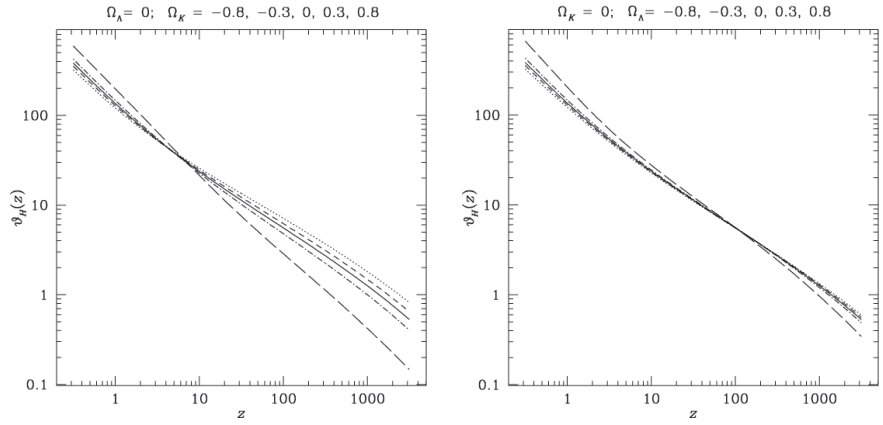

Figure 1.5: $\vartheta_H(z_1)$ (in degrees) for different values of the cosmological parameters Ω_K and Ω_Λ the line styles are as in Fig. 1.4.

It is then distributed over a sphere with radius $a(t_0)\chi(t_0 - t_1)$. So that the flux per proper time of the observer $d\tau_0 = a(t_0)dt$ becomes

$$F = \frac{La^2(t_1)}{4\pi a^4(t_0)\chi^2(t_0 - t_1)}$$

leading to

$$D_L(z_1) = \frac{a(t_0)^2}{a(t_1)}\chi(t_0 - t_1) = (1 + z_1)^2 D_A(z_1) \; . \tag{1.52}$$

The luminosity distance hence contains two additional factors $(1 + z)$ compared to the angular diameter distance. One of them is due to the 'redshift' of proper time and the other is due to the redshift of photon energy.

A standard candle is a source of which the absolute luminosity is known (usually from having observed such sources nearby where the distance is known e.g. by paralax measurements or by other means). By measuring the flux from standard candles, Eq. (1.51) allows to infer the luminosity distance $D_L(z)$. The observation of hundreds of supernovae type Ia which are 'modified' standard candles, has allowed during the last 20 years to infer that the Universe is presently dominated by a cosmological constant Λ or some other form of dark energy with $w \sim -1$, see Figs. 1.6 and 1.7 .

1.4 The thermal history of the Universe

We assume that, at sufficiently early times, reaction rates for particle interactions are much faster than the expansion rate, so that the cosmic fluid is in thermal equilibrium. During its expansion, the Universe then cools adiabatically. At early times, it is dominated by a relativistic radiation background with

$$\rho = C/a^4 = \frac{g_{\rm eff}}{2} a_{\rm SB} T^4 \, . \tag{1.53}$$

This behaviour implies that $T \propto a^{-1}$. Here $g_{\rm eff}$ is the effective number of degrees of freedom, which we define below and $a_{\rm SB}$ is the Stefan–Boltzmann constant,

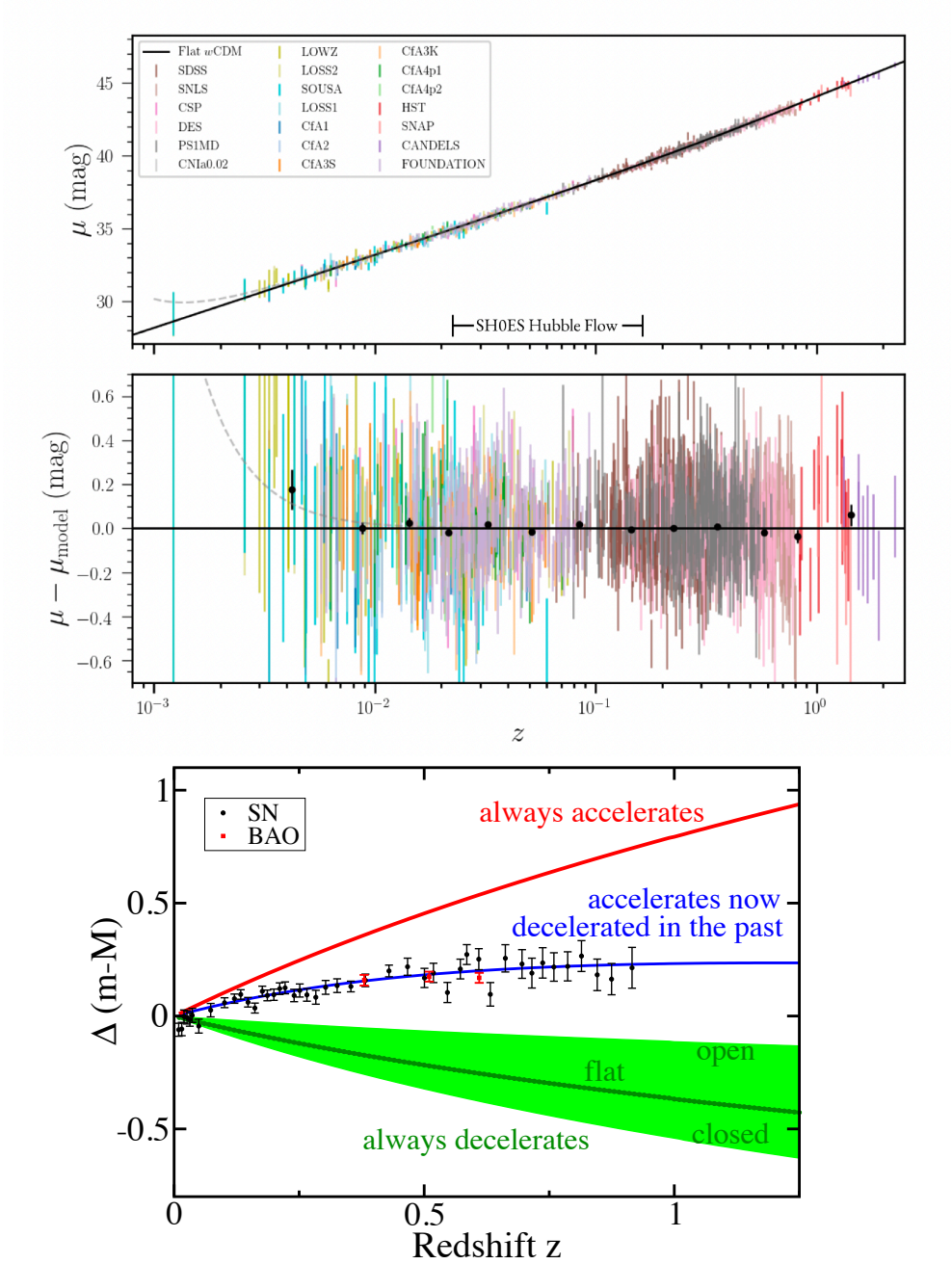

Figure 1.6: The Pantheon+ data, Brout et al.. (2022) (top).
The resulting acceleration of the Universe, Huterer and Shafer (2018) (bottom).

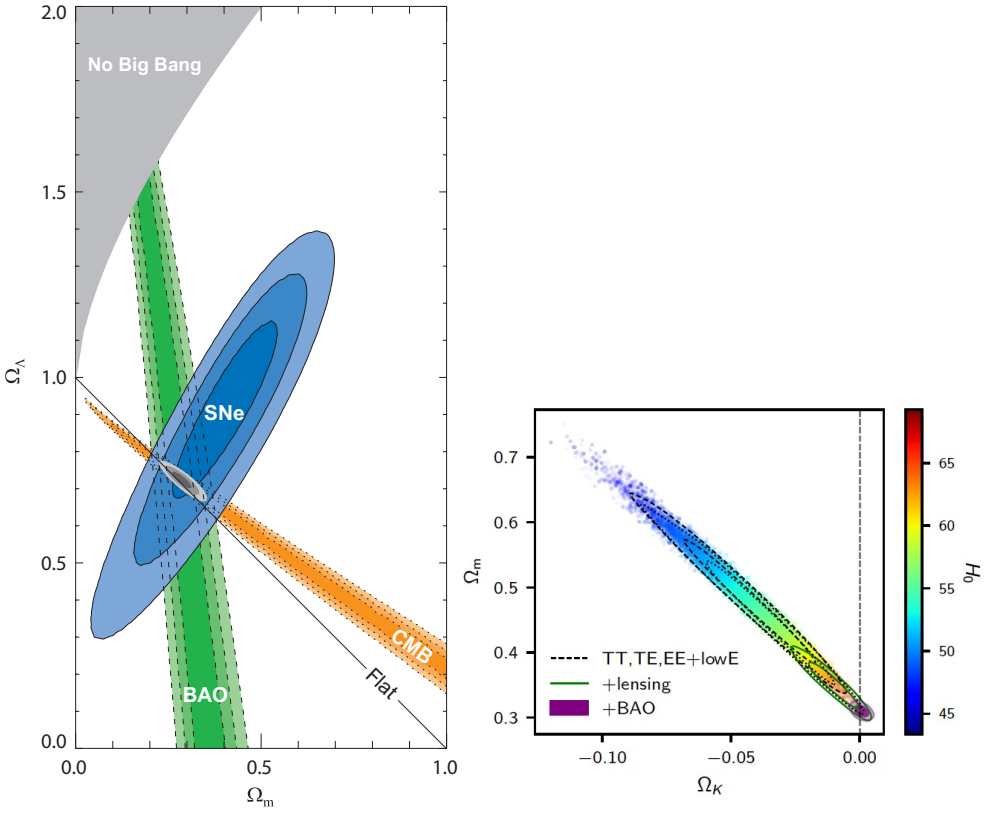

Figure 1.7: **Left:** The observationally preferred values from Ω_Λ and Ω_m from type Ia Supernovae (blue) baryon acoustic oscillations (green) and the CMB (orange), from Suzuki et al. (2011) .
Right: The same result (plotting Ω_m vertically and $\Omega_K = 1 - \Omega_m - \Omega_\Lambda$ horizontally) without SN data from the more recent Planck satellite (2018) [2].

$a_{\rm SB} = \pi^2/15$ in our units ($\hbar = k_B = c = 1$). For massless (or extremely relativistic) fermions and bosons in thermal equilibrium at temperature T with N_b respectively N_f spin degrees of freedom we have

$$\begin{aligned}\rho_b &= \frac{N_b 4\pi}{(2\pi)^3}\int_0^\infty \frac{p^3\,dp}{\exp(p/T)-1} = \frac{N_b T^4}{2\pi^2}\int_0^\infty \frac{x^3\,dx}{\exp(x)-1} \\ &= \frac{N_b T^4}{2\pi^2}\Gamma(4)\zeta(4) = \frac{N_b T^4\pi^2}{30}\,, \qquad (1.54)\\ \rho_f &= \frac{N_f 4\pi}{(2\pi)^3}\int_0^\infty \frac{p^3\,dp}{\exp(p/T)+1} = \frac{N_f T^4}{2\pi^2}\int_0^\infty \frac{x^3\,dx}{\exp(x)+1} \\ &= \frac{N_f T^4}{2\pi^2}\Gamma(4)\zeta(4)\frac{7}{8} = \frac{7}{8}\frac{N_f T^4\pi^2}{30}\,, \qquad (1.55)\end{aligned}$$

where Γ denotes the Gamma-function and ζ is the Riemann zeta-function and we make use of the integrals [5]

$$I_b(\alpha) = \int_0^\infty \frac{x^\alpha\,dx}{\exp(x)-1} = \Gamma(\alpha+1)\zeta(\alpha+1)\,, \qquad (1.56)$$

$$I_f(\alpha) = \int_0^\infty \frac{x^\alpha\,dx}{\exp(x)+1} = \left[1-\left(\frac{1}{2}\right)^\alpha\right]\Gamma(\alpha+1)\zeta(\alpha+1)\,. \qquad (1.57)$$

Furthermore, $\zeta(2) = \pi^2/6$, $\zeta(4) = \pi^4/90$, and $\Gamma(n) = (n-1)!$ for $n \in \mathbb{N}$, see [6].

Hence $\rho = \rho_b + \rho_f = \frac{g_{\rm eff}}{2} a_{SB} T^4$ for $a_{SB} = \pi^2 k_B^4/(15\,\hbar^3 c^2) = \pi^2/15$ and $g_{\rm eff} = N_b + 7/8 N_f$, if all the particles are at the same temperature T. If the temperatures are different, like e.g., the neutrino temperature after electron–positron annihilation as we shall see below, this has to be taken into account with a factor $(T_\nu/T_\gamma)^4$ multiplying N_ν in $g_{\rm eff}$.

At temperatures below the electron mass, $T < m_e \sim 0.5$ MeV only neutrinos and photons are still relativistic. Very recently, $T \lesssim 0.05$ eV ~ 580K at least some of the neutrinos also become non-relativistic so that the density parameter of relativistic particles today is probably given only by the photon density[1],

$$\Omega_{\rm rel} = \Omega_\gamma = \frac{8\pi G}{3H_0^2} a_{\rm SB} T_0^4 = 2.49\times 10^{-5} h^{-2}\,. \qquad (1.58)$$

Here we have set $T_0 = 2.725\,{\rm K}$ (see [8]).

The pressure of relativistic particles is given by $P = T_i^i/3 = \rho/3$. The thermodynamic relation $dE = T\,dS - P\,dV$ therefore gives for the entropy density $s = dS/dV$

$$s = \frac{dS}{dV} = \frac{1}{T}\left(\frac{dE}{dV} + P\right) = \frac{\rho + P}{T} = \frac{4\rho}{3T}\,. \qquad (1.59)$$

Using the expression for the energy density (1.54) and (1.55) this gives for each particle species X

$$s_X = \begin{cases} \frac{2\pi^2}{45} N_X T^3 & \text{for bosons}\,, \\ \frac{7\pi^2}{180} N_X T^3 & \text{for fermions}\,. \end{cases} \qquad (1.60)$$

[1] At present only neutrino mass differences are known from oscillation experiments. The lowest neutrino mass could still be zero or at least lower than T_0. From oscillation experiments, however, we know that the heaviest neutrino mass is at least 0.05eV (see [7]).

The particle density for relativistic particles is given by

$$n_X = \frac{N_X}{2\pi^2}\int \frac{p^2}{\exp(p/T)\pm 1}\,dp = \begin{cases} T^3\frac{N_X}{\pi^2}\zeta(3) & \text{for bosons ,} \\ T^3\frac{N_X}{\pi^2}\zeta(3)\frac{3}{4} & \text{for fermions .} \end{cases} \tag{1.61}$$

The particle and entropy densities both scale like T^3. Using $\zeta(3) \simeq 1.202\,057$ we obtain

$$s_X \simeq \begin{cases} 3.6\cdot n_X & \text{for bosons ,} \\ 4.2\cdot n_X & \text{for fermions .} \end{cases} \tag{1.62}$$

The photons obey a Planck distribution ($\epsilon = ap$ = the photon energy),

$$f(\epsilon) = \frac{1}{e^{\epsilon/T}-1}\ . \tag{1.63}$$

1.4.1 Recombination

At a temperature of about $T \sim 4000\,\mathrm{K} \sim 0.4$ eV, the number density of photons with energies above the hydrogen ionization energy ($= \Delta = 1\,\mathrm{Ry} = 13.6$ eV) drops below the baryon density of the Universe, and the protons begin to (re)combine to neutral hydrogen. Even though electrons and protons where not combined to neutral hydrogen before, this process is called 'recombination' rather than 'combination'.

Helium has already recombined earlier. The binding energy of the first electron to the He nucleus is $4\Delta = 54.4$eV. The recombination of the first electron $\mathrm{He}^{+2} \to \mathrm{He}^{+}$, takes place at $T_{2\to1} \simeq 1.4\times10^4$K. The binding energy of the second electron to the He nucleus is 24.6eV and, a the transition $\mathrm{He}^{+} \to \mathrm{He}$ takes place at $T_{1\to0} \simeq 0.5\times10^4$K (see [9] where this temperatures are derived using the Saha equation).

Photons and baryons are tightly coupled before (re)combination by Thomson scattering of electrons. During recombination the free electron density drops sharply and the mean free path of the photons grows larger than the Hubble scale. At the temperature $T_{\mathrm{dec}} \sim 3000\,\mathrm{K}$ (corresponding to the redshift $z_{\mathrm{dec}} \simeq 1100$ and the physical time $\tau_{\mathrm{dec}} \simeq a_{\mathrm{dec}}t_{\mathrm{dec}} \simeq 10^5\,\mathrm{yr}$) photons decouple from the electrons and the Universe becomes transparent.

The process of recombination happens quite rapidly and leaves the photon distribution virtually unchanged. After that, it is modified only by the redshift of the photon momenta. Therefore, scaling the 'temperature' in the distribution function like $T \propto 1/a$, it remains a Planck distribution even if the function $T(a)$ not longer represents a thermodynamical temperature but rather a parameter of the distribution function. These photons are redshifted at the present day to $T_0 = 2.728$K, see Fig. 1.8. The thermal photons represent what we call the 'Cosmic Microwave Background (CMB). No deviation from a thermal spectrum is found until today. For examples the limits on a possible chemical potential or a Compton y parameter are

$$|\mu| < 9\times10^{-5}, \quad |y| < 1.2\times10^{-5}. \tag{1.64}$$

The CMB photons not only have a very thermal spectrum, but they are also distributed very isotropically, apart from a dipole which is (most probably) mainly due to our motion relative to the surface of last scattering.

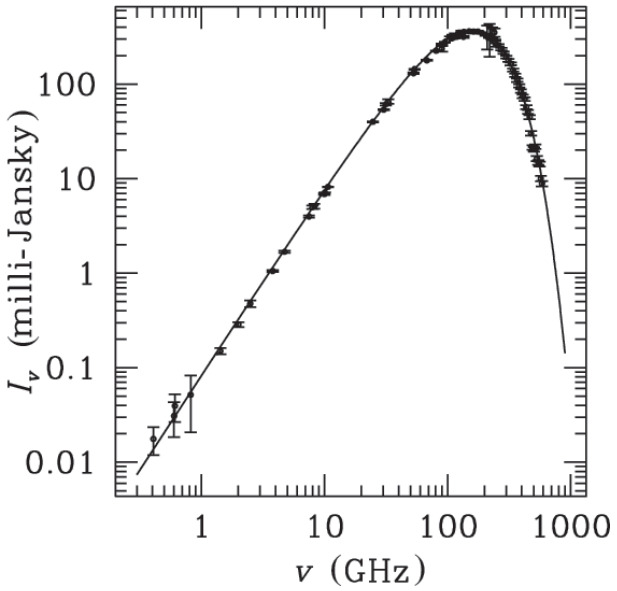

Figure 1.8: The spectrum of the cosmic background radiation. I_ν is the energy flux per frequency. The data are from many different measurements which are all compiled in [10]. The points around the top are the measurements from the FIRAS experiment on COBE [11]. The line traces a blackbody spectrum at a temperature of 2.728 K .

Indeed, an observer moving with velocity $\mathbf{v}$ relative to a source in direction $\mathbf{n}$ emitting a photon with proper momentum $\mathbf{p} = -\epsilon\mathbf{n}$ sees this photon redshifted with frequency

$$\epsilon' = \gamma\epsilon\,(1 - \mathbf{nv})\,, \tag{1.65}$$

where $\gamma = 1/\sqrt{1-v^2}$ is the relativistic γ-factor. For an isotropic emission of photons coming from all directions $\mathbf{n}$ this leads to a dipole anisotropy to first order in $\mathbf{v}$. This dipole anisotropy, which is of the order of

$$\left(\frac{\Delta T}{T}\right)_{\rm dipole} \simeq 1.2\times 10^{-3}\,,$$

has already been discovered in the seventies. Interpreting it as due to our motion with respect to the last scattering surface implies a velocity for the solar system barycentre of $v = 369 \pm 0.9\,{\rm km\,s^{-1}}$ at 68% CL ([12]).

In addition to this 'local' term, small fluctuations of the CMB which we discuss in detail in Chapter 3. Their theoretical study and experimental measurement has led to the best determination of cosmological parameters and can be called the 'success story of modern cosmology'.

For more details and the calculation of the remaining reionisation fraction see [9].

1.4.2 Nucleosynthesis and neutrino decoupling

At high temperatures, $T > 30$ MeV, none of the light nuclei (deuterium, ^{2}H, helium-4, ^{4}He, helium-3, ^{3}He or lithium, ^{7}Li) are stable. At these temperatures, we expect the baryons to form a simple mixture of protons and neutrons in thermal equilibrium with each other and with electrons, photons and neutrinos. The highest binding energy is the one of ^{4}He which is about 28 MeV. Nevertheless, ^{4}He cannot form at this temperature since the baryon density of the Universe is not high enough for three- or even four-body interactions to occur in thermal equilibrium. Therefore, before any nucleosynthesis can occur, the temperature has to drop below the binding energy of deuterium which is about 2.2 MeV. But even at this temperature there are still far too many high-energy photons around for deuterium to be stable. This is due to the very low baryon to photon ratio $\eta_B \equiv n_B/n_\gamma \simeq 10^{-10}$. Just as recombination is delayed from the naively expected temperature $T = 13.7$ eV to about $T_{\rm rec} \sim 0.3$ eV, nucleosynthesis does not happen at $T \sim 2.2$ MeV but around $T_{\rm nuc} \sim 0.1$ MeV. Most of the neutrons present at that temperature are converted into ^{4}He. Only small traces remain as deuterium or are burned into ^{3}He and ^{7}Li. The number of neutrons present at this temperature depends on the time at which β and inverse β decay drop out of equilibrium. This happens when the corresponding reaction rate Γ_β equals the expansion rate H,

$$\Gamma_\beta(t) = H(t)\,.$$

Hence this depends strongly on the expansion rate which in turn is given by the energy density,

$$\rho = \rho_{\rm rel}(t) = [\rho_\gamma(t) + \rho_\nu(t)] = \left[1 + N_\nu \frac{7}{8}(4/11)^{4/3}\right] \frac{\pi^2}{15} T^4\,, \tag{1.66}$$

where N_ν is the number of neutrino species, 3 in the standard model of particle physics (the factor $(4/11)^{4/3}$ is explained below). For this reason, the helium abundance, which is about $Y_{\rm He} \simeq 25\%$, depends on the number of neutrino families. Or more precisely on the number of light ($m < 1$MeV) particles with thermal abundance. We do not present the calculation of $Y_{\rm He}$ in detail here, it can be found in the literature, see e.g. [13, 9].

As a simple example we study the dropout of thermal equilibrium of neutrinos in some more detail. At the time of recombination, the relativistic particle species are the photon and, probably, three types of neutrinos. As we shall see, the neutrino temperature is actually a factor of $(4/11)^{1/3}$ lower than the temperature of the photons. With Eqs. (1.54) and (1.55), the energy density of these particles while they are relativistic is then given by

$$\begin{aligned}
\rho_{\rm rel}(t) &= [\rho_\gamma(t) + \rho_\nu(t)] = \left[1 + 3\frac{7}{8}(4/11)^{4/3}\right] \frac{\pi^2}{15} T^4\,, && (1.67)\\
&\simeq 10^{-33}\,{\rm g\,cm^{-3}} \left(\frac{T}{T_0}\right)^4\,, && (1.68)\\
&\simeq \rho_c(t_0)\Omega_{\rm rel} h^2 (1+z)^4\,, \text{ where}\\
\Omega_{\rm rel} h^2 &\simeq 4.4 \times 10^{-5}\,. && (1.69)
\end{aligned}$$

Note that at temperatures below the highest neutrino mass, this is no longer the energy density of relativistic particles, therefore $\Omega_{\rm rel}$ is not the density parameter

of relativistic particles today. Above the neutrino mass threshold and below the electron mass threshold we have

$$\frac{\rho_{\rm rel}}{\rho_m} = \frac{\Omega_{\rm rel}}{\Omega_m}(1+z) \simeq 4.4\times 10^{-5}\left(\frac{1}{\Omega_m h^2}\right)(1+z)\,, \tag{1.70}$$

Since $\Omega_m h^2 \simeq 0.14$, the redshift $z_{\rm eq}$ above which the Universe is dominated by relativistic particles is about

$$z_{\rm eq} \simeq 3.2\times 10^3\ , \quad T_{\rm eq} \simeq 1\,{\rm eV}\,. \tag{1.71}$$

At temperatures significantly above $T_{\rm eq}$, we can also neglect a possible contribution from curvature or a cosmological constant to the expansion of the Universe, so that for

$$z \gg z_{\rm eq} \qquad P = \frac{1}{3}\rho\,, \quad a \propto \tau^{1/2} \propto t\,. \tag{1.72}$$

At these high temperatures the energy density of the Universe is given by

$$\rho = g_{\rm eff}\frac{\pi^2}{30}T^4 \quad \text{where} \quad g_{\rm eff} = N_B(T) + \frac{7}{8}N_F(T)\,. \tag{1.73}$$

Here, N_B and N_F denote the number of bosonic and fermionic degrees of freedom of relativistic particles (i.e. particles with mass $m < T$) which are in thermal equilibrium at temperature T.

To discuss the physical processes at work at some temperature T, we need to know the spectrum of relativistic particles and their interactions at this temperature. Here, we shall study the Universe at $10\,{\rm keV} < T < 100\,{\rm MeV}$ where the physics is well known. The only relativistic particles present at these temperatures are electrons, positrons, photons and three types of neutrinos. (The muons have a mass of $m_\mu \simeq 105.66{\rm MeV}$. We neglect the small contribution from muon/anti-muon pairs which decay exponentially $\propto \exp(-m_\mu/T)$ via the reaction $\mu + \bar\nu_\mu \to e + \bar\nu_e$.) Even if the individual neutrino masses are not very well constrained, the oscillation experiments [14] imply that their masses are below 1 eV if there is no degeneracy. As we shall see later, also CMB data estimate masses below this value. Therefore, we may neglect the neutrino masses in our treatment. The baryon number is well conserved at these temperatures, so that we may set η_B equal to its present value, $\eta_B = n_B/n_\gamma \simeq 2.7\times 10^{-8}\Omega_B h^2 =$ constant.

Due to the neutrality of the Universe, the difference between the electron number and positron number is determined by the proton number which is given by $n_p \sim \eta_B n_\gamma \sim 10^{-10} n_\gamma$. Therefore the electron and positron chemical potential is very small. We assume that also the neutrino chemical potential can be neglected, but this assumption is not based on observations. At $1{\rm MeV} < T < 100{\rm MeV}$ the relativistic particles are the photons, neutrinos electrons and positrons with so that $N_B = 2$ and $N_F = 4 + 6$, hence

$$g_{\rm eff}(T \sim 100\,{\rm MeV}) = \frac{43}{4} = 10.75\,. \tag{1.74}$$

The Hubble parameter is given by

$$\left(\frac{a'}{a}\right)^2 = H^2 = \frac{1}{4\tau^2} = \frac{8\pi G}{3}\rho = \frac{8\pi^3 G}{90}g_{\rm eff}T^4\,.$$

With the Planck mass, m_P defined by $G = 1/m_P^2 = 1/(1.22 \times 10^{19}\,\mathrm{GeV})^2$, we find

$$H^2(T) \simeq 2.76 g_{\rm eff}(T) \left(\frac{T^2}{m_P}\right)^2 , \tag{1.75}$$

$$H \simeq 0.21\sqrt{g_{\rm eff}} \left(\frac{T}{1\,\mathrm{MeV}}\right)^2 \mathrm{s}^{-1} , \tag{1.76}$$

$$\tau = \frac{1}{2H} \simeq 0.3 g_{\rm eff}(T)^{-1/2} \left(\frac{m_P}{T^2}\right) \simeq 2.4\,\mathrm{s} \left(\frac{1\,\mathrm{MeV}}{T}\right)^2 g_{\rm eff}^{-1/2} . \tag{1.77}$$

For $c = \hbar = 1$, MeV's have the same units as mass or momentum which then is the inverse unit of length or time. Converting MeV to seconds^{-1} we obtain 1MeV$= 1.5192 \times 10^{21}\mathrm{s}^{-1}$. The temperature of $T \sim 100$ MeV corresponds thus to an age of $\tau \sim 7 \times 10^{-5}$ s, and $T = 1$ MeV corresponds to $\tau \sim 0.7$ s. The relations (1.76) and (1.77) can be applied as long as the Universe is dominated by relativistic particles.

Neutrinos are kept in thermal equilibrium via the exchange of a W-boson, $e + \bar{\nu} \longleftrightarrow e + \bar{\nu}$ and $\nu + \bar{e} \longleftrightarrow \nu + \bar{e}$, or a Z-boson, $e + \bar{e} \longleftrightarrow \nu + \bar{\nu}$. At low energies $E \ll m_{Z,W} \sim 100$ GeV, we can determine the cross sections within the 4-fermion theory of weak interaction. The cross section of the different processes above are identical within this approximation and they are given by

$$\sigma_F \simeq G_F^2 E^2 \sim G_F^2 T^2 ,$$

where the coupling parameter, G_F is the Fermi constant,

$$G_F = 1.166 \times 10^{-5}\,\mathrm{GeV}^{-2} = (293\,\mathrm{GeV})^{-2}. \tag{1.78}$$

The involved particle density is $n_F(T) = g_F(T)\zeta(3)T^3/\pi^2 \sim 1.3T^3$ where we have set $g_F(T) = 3/4 N_F(T) = 30/4$ for the three types of left-handed neutrinos and the $e^{\pm}$s. Since the particles are relativistic, we can set $v \sim 1$ so that we obtain an interaction rate of

$$\Gamma_F = \langle \sigma_F v \rangle n_F \simeq 1.3 G_F^2 T^5 .$$

Comparing this with the expansion rate H obtained in (1.75), we find

$$\frac{\Gamma_F}{H} \simeq 0.24 T^3 m_P G_F^2 \simeq \left(\frac{T}{1.4\,\mathrm{MeV}}\right)^3 . \tag{1.79}$$

At temperatures below $T_F \sim 1.4$ MeV the probability for a neutrino to interact within one Hubble time, H^{-1}, becomes less than unity and the neutrinos effectively decouple. The plasma becomes transparent to neutrinos which are no longer in thermal equilibrium with electrons and positrons and hence photons and baryons.

Even at temperatures far below their mass $m_\nu \gtrsim 0.05$ eV, their particle distribution remains an extremely relativistic Fermi–Dirac distribution with temperature

$$T_\nu = T_F \frac{a_F}{a} ,$$

since they are no longer in thermal equilibrium and their distribution is affected solely by redshifting of the momenta.

As long as the photon/electron/baryon temperature also scales like $1/a$, the neutrinos conserve the same temperature as the thermal plasma, but when the number of degrees of freedom, $g_{\rm eff}$, changes, the plasma temperature decays for a brief period of time less rapidly than $1/a$ and therefore remains higher than the neutrino temperature. This is exactly what happens at the electron–positron mass threshold, $T = m_e \simeq 0.5$ MeV. Below that temperature, only the process $e + \bar{e} \to 2\gamma$ remains in equilibrium while $2\gamma \to e + \bar{e}$ is exponentially suppressed. We calculate the reheating of the photons gas by electron–positron annihilation assuming that the process takes place in thermal equilibrium and that the entropy remains unchanged. This is well justified since the cross section of this process is very high. Denoting the entropy inside a volume of size Va^3 before and after electron–positron annihilation by S_i and S_f we therefore have $S_i = S_f$. With (1.59) this yields

$$S_i = \frac{2}{3} a_{\rm SB} g_{{\rm eff},i} (Ta)_i^3 V, \quad S_f = \frac{2}{3} a_{\rm SB} g_{{\rm eff},f} (Ta)_f^3 V \,.$$

The electron–positron degrees of freedom disappear in this process so that $g_{{\rm eff},f} = 2$ while $g_{{\rm eff},i} = 2 + 4(\frac{7}{8}) = 11/2$. From $S_i = S_f$ we therefore conclude

$$(Ta)_f = (Ta)_i \left(\frac{11}{4}\right)^{1/3} .$$

The neutrino temperature is not affected by $e^\pm$ annihilation, so that $(T_\nu a)_f = (T_\nu a)_i = (Ta)_i$. For the last equals sign we have used that the neutrino and photon temperatures are equal before $e^\pm$ annihilation. At temperatures $T \ll m_e$ we therefore have

$$T = \left(\frac{11}{4}\right)^{1/3} T_\nu \,. \tag{1.80}$$

Since there are no further annihilation processes, this relation remains valid until today and the present Universe not only contains a thermal distribution of photons, but also a background of cosmic neutrinos which have an extremely relativistic Fermi–Dirac distribution with temperature

$$T_\nu(\tau_0) = (4/11)^{1/3} T_0 = 1.95\,{\rm K} \,. \tag{1.81}$$

We set

$$g_0 = 2 + \frac{7}{8} 6 \left(\frac{4}{11}\right)^{4/3} \simeq 3.36 \,, \quad \text{and} \tag{1.82}$$

$$g_{0S} = 2 + \frac{7}{8} 6 \left(\frac{4}{11}\right) \simeq 3.91 \,. \tag{1.83}$$

These are respectively the effective degrees of freedom of the energy and entropy densities as long as all the neutrinos are relativistic. Until then we therefore have

$$\rho_{\rm rel}(T) = \frac{\pi^2}{30} g_0 T^4 \simeq 8.1 \times 10^{-34}\,{\rm g\,cm^{-3}} \left(\frac{T}{T_0}\right)^4 , \tag{1.84}$$

$$s(T) = \frac{2\pi^2}{45} g_{0S} T^3 \simeq 3 \times 10^3\,{\rm cm^{-3}} \left(\frac{T}{T_0}\right)^3 . \tag{1.85}$$

The neutrino cross section at low energies is extremely weak, and so far the neutrino background has not been observed directly.

Exercice 6 The neutrino background
Determine the neutrino cross section for the reaction $e^- + \bar{\nu} \rightarrow e^- + \bar{\nu}$ *at energy* $E_\nu = T_\nu(t_0)$. *Compare it with the cross section of the neutrinos detected in the super-Kamiokande experiment, assuming a solar neutrino flux of* $F = 10^9 cm^{-2} s^{-1}$ *at a neutrino energy* $\sim 1 MeV$. *Keeping the efficiency of super-Kamiokande, how large (roughly) a water tank would you need to detect neutrinos from the cosmic neutrino background?*

1.4.3 Phase transitions in the early Universe

At even higher temperatures other physical processes take place. For example at $T = T_{QCD} \simeq 100$MeV the chiral transition takes place. The quarks gluon plasma which previously permeated the Universe confines into hadrons, protons and neutrons. At $T = T_{EW} \simeq 200$GeV the Higgs becomes massive and the electroweak transition takes place. Lattice calculations have shown that within the standard model, both these transitions are cross-overs and not phase transitions. This makes it difficult to think of any possible observational signature, 'cosmic fossils' of these events. However, if neutrinos have a relatively large chemical potential or if there are deviations from the standard model, e.g. a second Higgs or SUSY, one or the other of these transitions can become a first order phase transition. A first order phase transition would also be required to generate a baryon or lepton asymmetry from a symmetric initial state. Furthermore, physics beyond the standard model is needed to provide the dark matter or to solve the hierarchy problem.

It is therefore not improbable to postulate that during its expansion and cooling by many orders of magnitude, the Universe underwent a first order phase transition and to study the 'fossils' of such a transition. These can be

- Topological defects (cosmic strings, global monopoles or textures) [15],
- Primordial black holes [16],
- Gravitational waves [17],
- Cosmic magnetic fields [17].

Quite some theoretical studies are devoted to these possibilities, but so far not observational evidence has been found.

Chapter 2

Linear perturbation theory

2.1 Basic perturbation equations

The fluctuations in the CMB are small. It is therefore justified to calculate them with perturbation theory. Nearly all the observational results for the CMB are in perfect agreement with linear and second order perturbation theory. We first give a brief introduction to linear cosmological perturbation theory.

The first attempt to relativistic cosmological perturbation theory was undertaken by Lifshitz (1946) [18]. There he found that the gravitational potential cannot grow within linear perturbation theory in an FL universe and he concluded that galaxies cannot have formed by gravitational instability.

Today we know that in order to form structures it is sufficient that matter density fluctuations can grow. Nevertheless, considerable initial fluctuations with amplitudes of the order of 10^{-5} are needed in order to reproduce the cosmic structures observed today. These are much larger than typical statistical fluctuations on scales of galaxies and we need an additional mechanism, like inflation, to generate them.

2.1.1 Gauge transformation, gauge invariance

The observed Universe is not perfectly homogeneous and isotropic. Matter is arranged in galaxies and clusters of galaxies and there are large voids in the distribution of galaxies. Let us assume, however, that these inhomogeneities grew out of small initial variations of the geometry and of the energy–momentum tensor which we shall study at first-order in perturbation theory. For this we define the perturbed geometry by

$$g_{\mu\nu} = \bar{g}_{\mu\nu} + \varepsilon a^2 h_{\mu\nu} \ , \tag{2.1}$$

$\bar{g}_{\mu\nu}$ being the unperturbed Friedmann metric defined in the previous chapter. We conventionally set (absorbing the 'smallness' parameter ε into $h_{\mu\nu}$)

$$\begin{aligned} &g_{\mu\nu} = \bar{g}_{\mu\nu} + a^2 h_{\mu\nu} \ , \qquad \bar{g}_{00} = -a^2 \ , \qquad \bar{g}_{ij} = a^2 \gamma_{ij} \ , \qquad |h_{\mu\nu}| \ll 1 \ , \\ &T^\mu_\nu = \overline{T}^\mu_\nu + \theta^\mu_\nu \ , \qquad\quad \overline{T}^0_{\ 0} = -\bar{\rho} \ , \qquad \overline{T}^i_{\ j} = \bar{P}\delta^i_j \ , \qquad |\theta^\mu_\nu|/\bar{\rho} \ll 1 \ . \end{aligned} \tag{2.2}$$

The first fundamental problem we want to discuss is the choice of gauge in cosmological perturbation theory.

For linear perturbation theory to apply, the spacetime manifold $\mathcal{M}$ with metric g and the energy–momentum tensor T of the real, observable Universe must be in some sense close to a FL universe, i.e. the manifold $\mathcal{M}$ with a Robertson–Walker metric $\bar{g}$ and a homogeneous and isotropic energy–momentum tensor $\overline{T}$. It is an interesting, non-trivial unsolved problem how to construct 'the best' $\bar{g}$ and $\overline{T}$ from the physical fields g and T in practice. There are two main difficulties: first, spatial averaging procedures depend on the choice of a hypersurface of constant time and they do not commute with derivatives, so that averaged fields $\bar{g}$ and $\overline{T}$ will, in general, not satisfy Einstein's equations. Second, averaging is in practice impossible over super-horizon scales.

Even though we cannot give a constructive prescription of how to define the nearly homogeneous and isotropic spatial slices from the physical spacetime, or the spatially averaged metric and energy–momentum tensor, we now assume that there exists an averaging procedure which leads to a FL universe with spatially averaged tensor fields $\overline{S}$, such that the deviations are small,

$$\frac{|T_{\mu\nu}-\overline{T}_{\mu\nu}|}{\max_{\{\alpha\beta\}}\{|\overline{T}_{\alpha\beta}|\}} \ll 1 \quad \text{and} \quad \frac{|g_{\mu\nu}-\overline{g}_{\mu\nu}|}{\max_{\{\alpha\beta\}}\{\overline{g}_{\alpha\beta}\}} \ll 1,$$

and where $\bar{g}$ and $\overline{T}$ satisfy Friedmann's equations. The latter condition can be achieved, e.g., by defining $\overline{T}$ via the Friedmann equations. Let us call such an averaging procedure 'admissible'. There may be many different admissible averaging procedures (e.g., over different hypersurfaces) leading to slightly different FL backgrounds.

But since $|g-\bar{g}|$ is small of order ε, the difference of the two FL backgrounds must also be small of order ε and we can interpret it as part of the perturbation.

We now consider a fixed admissible FL background $(\bar{g},\overline{T})$ as chosen. Since the theory is invariant under diffeomorphisms (coordinate transformations), the perturbations are not unique. For an arbitrary diffeomorphism ϕ and its push forward ϕ_*, the two metrics g and $\phi_*(g)$ describe the same geometry. Since we have chosen the background metric $\bar{g}$ we only allow diffeomorphisms which leave $\bar{g}$ invariant i.e. which deviate only at first order from the identity. Such an 'infinitesimal' diffeomorphism can be represented as the infinitesimal flow of a vector field X, $\phi = \phi_\varepsilon^X$. Remember the definition of the flow: for the integral curve, $\gamma_x(s)$, of X with starting point x, i.e. $\gamma_x(s=0)=x$ we have $\phi_s^X(x)=\gamma_x(s)$. In terms of the vector field X, to first order in ε, its push forward is then of the form

$$\phi_* = id + \varepsilon L_X + \mathcal{O}(\varepsilon^2)\ ,$$

where L_X denotes the Lie derivative in direction X (see Appendix A.2). The transformation $g \to \phi_*(g)$ is equivalent to $\bar{g}+\varepsilon a^2 h \to \bar{g}+\varepsilon(a^2 h + L_X\bar{g})+\mathcal{O}(\varepsilon^2)$. Under an 'infinitesimal coordinate transformation' the metric perturbation h therefore transforms as

$$h \mapsto h + a^{-2} L_X \bar{g}\ . \tag{2.3}$$

In the context of cosmological perturbation theory, infinitesimal coordinate transformations are called 'gauge transformations'. The perturbation of an arbitrary tensor field $S = \bar{S} + \varepsilon S^{(1)}$ obeys the gauge transformation law

$$S^{(1)} \mapsto S^{(1)} + L_X \bar{S}\ . \tag{2.4}$$

Since every vector field X generates a gauge transformation $\phi = \phi_\varepsilon^X$, we can conclude that only perturbations of tensor fields with $L_X\overline{S} = 0$ for all vector fields X, i.e. with vanishing (or constant) 'background contribution' are gauge invariant. This result is called the 'Stewart–Walker Lemma' [19].

The gauge dependence of perturbations has caused many controversies in the literature, since it is often difficult to extract the physical meaning of gauge-dependent perturbations, especially on super-horizon scales. This problem is solved by gauge-invariant perturbation theory which we are going to use throughout. The advantage of the gauge-invariant formalism is that the variables used have simple geometric and physical meanings and are not plagued by gauge modes. Although the derivation requires somewhat more work, the final system of perturbation equations is usually simple and well suited for numerical treatment. We shall also see, that on subhorizon scales, the gauge-invariant matter perturbation variables approach the usual, gauge-dependent ones. Since one of the gauge-invariant geometrical perturbation variables corresponds to the Newtonian potential, the Newtonian limit can be performed easily.

First we note that all relativistic equations are covariant and can therefore be written in the form $S = 0$ for some tensor field S. The corresponding background equation is $\overline{S} = 0$, hence $S^{(1)}$ is gauge invariant. It is thus always possible to express the corresponding perturbation equations in terms of gauge-invariant variables.

2.1.2 Perturbation variables

It is useful to decompose perturbations into components which transform irreducibly under the symmetry group of the background. In our case these are translations and rotations. For simplicity I only present the case $K = 0$, but $K \neq 0$ is not very different apart from technicalities. The irreducible representations of the translation group are the Fourier modes. Vectors and tensors can be further decomposed into helicity 0, 1 and 2 components. We define the Fourier decomposition of a function by

$$f(\mathbf{x}, t) = \frac{1}{(2\pi)^3} \int d^3k\, f(\mathbf{k}, t)\, e^{-i\mathbf{kx}} \ . \tag{2.5}$$

The spin decomposition of a spatial vector field is a decomposition into a gradient and a curl. For the Fourier components we set

$$V_j = i\hat{k}_j V^{(S)} + V_j^{(V)} \ , \quad \text{where} \quad k^j V_j^{(V)} = 0. \tag{2.6}$$

Here $\hat{\mathbf{k}} = \mathbf{k}/k$.

For a spatial symmetric tensor field we have

$$H_{ij} = H_L\delta_{ij} - \left(\frac{k_ik_j}{k^2} - \frac{1}{3}\delta_{ij}\Delta\right) H_T + \frac{i}{2}\left(\hat{k}_j H_i^{(V)} + \hat{k}_i H_{j,i}^{(V)}\right) + H_{ij}^{(T)} \ , \tag{2.7}$$

where

$$H_i^{(V),i} = H_i^{(T)\,i} = H_{ij}^{(T)\,,j} = 0 \ . \tag{2.8}$$

Here H_L and H_T are helicity-0 components, $H_i^{(V)}$ is the helicity-1 component and $H_{ij}^{(T)}$ is the helicity-2 component of the tensor field H

Metric perturbations

Perturbations of the metric are of the form

$$g_{\mu\nu} = \bar{g}_{\mu\nu} + a^2 h_{\mu\nu} \ . \tag{2.9}$$

We parametrize them as

$$h_{\mu\nu}\, dx^\mu\, dx^\nu = -2A\, dt^2 - 2B_i\, dt\, dx^i + 2H_{ij}\, dx^i\, dx^j, \tag{2.10}$$

and we decompose the perturbation variables B_i and H_{ij} according to (2.6) and (2.7).

Let us consider the behaviour of $h_{\mu\nu}$ under gauge transformations. We set the vector field defining the gauge transformation to

$$X = T\partial_t + L^i\partial_i \ . \tag{2.11}$$

Using the definition of the Lie derivative, we obtain (for details see exercises)

$$\begin{aligned} L_{\mathbf{X}}\bar{g} \;=\; & a^2\left[-2\left(\mathcal{H}T + \dot{T}\right)dt^2 + 2\left(\dot{L}_i - T_{,i}\right)dt\, dx^i \right. \\ & \left. + \left(2\mathcal{H}T\gamma_{ij} + L_{i|j} + L_{j|i}\right)dx^i\, dx^j\right]. \end{aligned} \tag{2.12}$$

Comparing this with (2.10) and using (2.4), we obtain

$$\begin{aligned} A &\rightarrow A + \mathcal{H}T + \dot{T} \ , \\ B_i &\rightarrow B_i - \dot{L}_i + T_{,i} \ , \\ H_{ij} &\rightarrow H_{ij} + \frac{1}{2}\left(L_{i|j} + L_{j|i}\right) + \mathcal{H}T\gamma_{ij} \ . \end{aligned}$$

Using the decompositions (2.6) for B_i and (2.7) for H_{ij} this implies the following behaviour of the perturbation variables under gauge transformations (we also decompose the vector $L_i = L\hat{k}_i + L^{(V)}e_i$, $\mathbf{k}\cdot\mathbf{e} = 0$):

$$A \rightarrow A + \mathcal{H}T + \dot{T} \ , \tag{2.13}$$

$$B \rightarrow B - \dot{L} - kT \ , \tag{2.14}$$

$$B^{(V)} \rightarrow B^{(V)} - \dot{L}^{(V)} \ , \tag{2.15}$$

$$H_L \rightarrow H_L + \mathcal{H}T + \frac{k}{3}L \ , \tag{2.16}$$

$$H_T \rightarrow H_T - kL \ , \tag{2.17}$$

$$H^{(V)} \rightarrow H^{(V)} - kL^{(V)} \ , \tag{2.18}$$

$$H^{(T)} \rightarrow H^{(T)} \ . \tag{2.19}$$

Two scalar and one vector variable can be set to zero by gauge transformations. We shall use this to choose the longitudinal gauge for scalar perturbations, $B = H_T = 0$. In this gauge, scalar perturbations of the metric are of the form ($H_T|_{\rm long} = B|_{\rm long} = 0$):

$$h^{(S)}_{\mu\nu}dx^\mu dx^\nu = -2\Psi\, dt^2 - 2\Phi\gamma_{ij}\, dx^i dx^j. \tag{2.20}$$

Ψ and Φ are the so-called *Bardeen* potentials. In a generic gauge the Bardeen potentials are given by

$$\Psi = A - \mathcal{H}k^{-1}\sigma - k^{-1}\dot{\sigma} \ , \tag{2.21}$$

$$\Phi = -H_L - \frac{1}{3}H_T + \mathcal{H}k^{-1}\sigma = -\mathcal{R} + \mathcal{H}k^{-1}\sigma \ , \tag{2.22}$$

where $\sigma = k^{-1}\dot{H}_T - B$, is the scalar potential for the shear of the hypersurface of constant time, and $\mathcal{R} = H_L + \frac{1}{3}H_T$ is proportional to the spatial curvature perturbation.

In a FL universe the Weyl tensor (see Appendix A.1) vanishes. Its perturbation is therefore gauge-invariant. For scalar perturbations one finds

$$E_{ij} \equiv C^{\mu}{}_{i\nu j}u_\mu u^\nu = -C^0{}_{i0j} = -\frac{1}{2}\left[(\Psi+\Phi)_{,ij} - \frac{1}{3}\Delta(\Psi+\Phi)\delta_{ij}\right] \ , \tag{2.23}$$

All other non-vanishing components are also given by E_{ij}. In particular the B-part of the Weyl tensor vanishes for scalar perturbations.

Matter perturbations

Not only the metric, but also the matter fields, i.e. the components of the energy momentum tensor are perturbed. et $T^\mu_\nu = \overline{T}^\mu_\nu + \theta^\mu_\nu$ be the full energy–momentum tensor. We define its energy density ρ and its energy flux 4-vector u as the time-like eigenvalue and eigenvector of T^μ_ν:

$$T^\mu_\nu u^\nu = -\rho u^\mu, \quad u^2 = -1 \ . \tag{2.24}$$

We then parametrize their perturbations by

$$\rho = \bar{\rho}\,(1+\delta)\,, \quad u = u^0\partial_t + u^i\partial_i \ . \tag{2.25}$$

The component u^0 is fixed by the normalization condition,

$$u^0 = \frac{1}{a}(1-A) \ . \tag{2.26}$$

We further set

$$u^i = \frac{1}{a}v^i = \frac{1}{a}\left(v^i + v^{(V)i}\right). \tag{2.27}$$

Here $\mathbf{v}$ is a gradient (scalar perturbation) and $\mathbf{v}^{(V)}$ is divergence free (vector perturbation) $P^\mu_\nu \equiv u^\mu u_\nu + \delta^\mu_\nu$ is the projection tensor onto the subspace of tangent space normal to u. We define the stress tensor

$$\tau^{\mu\nu} = P^\mu_\alpha P^\nu_\beta T^{\alpha\beta}. \tag{2.28}$$

With this we can write

$$T^\mu_\nu = \rho u^\mu u_\nu + \tau^\mu_\nu \ . \tag{2.29}$$

In the unperturbed case we have $\tau^0_\mu = \tau^\mu_0 = 0$ and $\tau^i_j = \bar{P}\delta^i_j$. Including first-order perturbations, the components $\tau_{0\mu}$ are determined by the perturbation variables which we have already introduced. We obtain

$$\tau^0_0 = 0 \ , \quad \text{and} \quad \tau^j_0 = -\bar{P}v^j \ , \qquad \tau^0_j = \bar{P}(v_j - B_j) \ . \tag{2.30}$$

But τ^i_j contains in general new perturbations. We define

$$\tau^i_j = \bar{P}\left[(1+\pi_L)\,\delta^i_j + \Pi^i_j\right], \quad \text{with} \quad \Pi^i_i = 0\ . \tag{2.31}$$

From our definitions we can determine the perturbations of the energy–momentum tensor. A short calculation gives

$$\begin{aligned} T^0_0 &= -\bar{\rho}(1+\delta)\ , & (2.32)\\ T^0{}_j &= (\bar{\rho}+\bar{P})(v_j - B_j)\ , & (2.33)\\ T^j{}_0 &= -(\bar{\rho}+\bar{P})v^j\ , & (2.34)\\ T^i{}_j &= \bar{P}\left[(1+\pi_L)\delta^i_j + \Pi^i{}_j\right]\ . & (2.35) \end{aligned}$$

The traceless part of the stress tensor, Π^i_j, is called the anisotropic stress tensor. In Fourier space we decompose it as

$$\Pi^i_j(\mathbf{k}) = \Pi\left(\frac{1}{3}\delta^i_j - \hat{k}^i\hat{k}_j\right) + \Pi^{(V)}\frac{1}{2}(e^i k_j + e_j k^i) + \Pi^{(T)} e^i_j. \tag{2.36}$$

Here $\mathbf{e}$ is a unit vector normal to $\hat{\mathbf{k}}$ and e_{ij} is one of the two helicity 2 polarisations (either circular or linear). We assume perturbations to obey parity symmetry so that we can work just with one polarisation and, in the end multiply the result for the power spectrum by a factor 2.

We now study the gauge transformation properties of these perturbation variables. First we note that ρ is a scalar and $L_X\bar{\rho} = \dot{\bar{\rho}}T = -3(1+w)\mathcal{H}\bar{\rho}T$. Here we made use of the energy conservation equation. The same is true for $\bar{P}(1+\pi_L)$ which is 1/3 of the trace of $\tau^\mu{}_\nu$. With the adiabatic sound speed defined by $c_s^2 = \dot{P}/\dot{\rho}$, we obtain $L_X\bar{P} = \dot{\bar{P}}T = -3\frac{c_s^2}{w}(1+w)\mathcal{H}\bar{P}T$. The background contribution to the anisotropic stress tensor, $\Pi^\mu_\nu = \tau^\mu_\nu - \frac{1}{3}\tau^\alpha_\alpha\delta^\mu_\nu$, vanishes, hence Π^μ_ν is gauge invariant (the Stewart–Walker lemma). For perfect fluids $\Pi^\mu_\nu = 0$. For the velocity we use $L_X\bar{u} = [X,\bar{u}] = (-T\dot{a}a^{-2} - a^{-1}\dot{T})\partial_t - a^{-1}\dot{L}^i\partial_i$. Inserting our decomposition into scalar, vector and tensor perturbation variables for a fixed mode $\mathbf{k}$, we obtain finally the following transformation behaviour

$$\begin{aligned} \delta &\to \delta - 3(1+w)\mathcal{H}T\ , & (2.37)\\ \pi_L &\to \pi_L - 3\frac{c_s^2}{w}(1+w)\mathcal{H}T\ , & (2.38)\\ v &\to v - \dot{L}\ , & (2.39)\\ \Pi &\to \Pi\ , & (2.40)\\ v^{(V)} &\to v^{(V)} - \dot{L}^{(V)}\ , & (2.41)\\ \Pi^{(V)} &\to \Pi^{(V)}\ , & (2.42)\\ \Pi^{(T)} &\to \Pi^{(T)}\ . & (2.43) \end{aligned}$$

Apart from the anisotropic stress perturbations, there is only one gauge-invariant variable which can be obtained from the energy–momentum tensor alone, namely

$$\Gamma = \pi_L - \frac{c_s^2}{w}\delta\ . \tag{2.44}$$

One can show [9] that Γ is proportional to the divergence of the entropy flux of the perturbations. Adiabatic perturbations are characterized by $\Gamma = 0$.

Gauge-invariant density and velocity perturbations can be found by combining δ, v and $v_i^{(V)}$ with metric perturbations. We shall use

$$V \equiv v - \frac{1}{k}\dot{H}_T = v^{\rm lo} \ , \tag{2.45}$$

$$D_s \equiv \delta + 3(1+w)\mathcal{H}(k^{-2}\dot{H}_T - k^{-1}B) \equiv \delta^{\rm lo} \ , \tag{2.46}$$

$$\begin{aligned} D &\equiv \delta^{\rm lo} + 3(1+w)\frac{\mathcal{H}}{k}V = \delta + 3(1+w)\frac{\mathcal{H}}{k}\,(v-B) \\ &= D_s + 3(1+w)\frac{\mathcal{H}}{k}V \ , \end{aligned} \tag{2.47}$$

$$\begin{aligned} D_g &\equiv \delta + 3(1+w)\left(H_L + \frac{1}{3}H_T\right) = \delta^{\rm lo} - 3(1+w)\Phi \\ &= D_s - 3(1+w)\Phi \ , \end{aligned} \tag{2.48}$$

$$V^{(V)} \equiv v^{(V)} - \frac{1}{k}\dot{H}^{(V)} = v^{(\rm vec)} \ , \tag{2.49}$$

$$\Omega \equiv v^{(V)} - B^{(V)} = v^{(\rm vec)} + \sigma^{(V)} \ , \tag{2.50}$$

$$\Omega - V^{(V)} = \sigma^{(V)} \ . \tag{2.51}$$

Here $v^{\rm lo}$, $\delta^{\rm lo}$ and $v^{(\rm vec)}$ are the velocity (and density) perturbations in the longitudinal and vector gauge[1] respectively, and $\sigma^{(V)}$ is the metric perturbation in vector gauge and the shear of the $t =$ constant hypersurfaces, see [9] for details.

These variables can be interpreted nicely in terms of gradients of the energy density and the shear and vorticity of the velocity field.

On scales much smaller than the Hubble scale, $k \gg \mathcal{H} \sim t^{-1}$, the metric perturbations are much smaller than δ and v and we can neglect the difference between different gauges and/or gauge-invariant perturbation variables of the energy momentum tenosr. This is especially important when comparing experimental results with gauge-invariant calculations. This can be seen by the following order of magnitude argument: The perturbations of the Einstein tensor are a combination of the second derivatives of the metric perturbations, $\mathcal{H}$ times the first derivatives and $\mathcal{H}^2$ or $\dot{\mathcal{H}}$ times metric perturbations. The first-order perturbation of Einstein's equations therefore generically yield the following order of magnitude estimate $8\pi G\delta T_{\mu\nu} = \delta G_{\mu\nu}$:

$$\mathcal{O}\left(\frac{\delta T_{\mu\nu}}{a^2\rho}\right) \underbrace{\mathcal{O}\left(8\pi G a^2\rho\right)}_{\mathcal{O}(\dot{a}/a)^2 = \mathcal{O}(1/t^2)} = \mathcal{O}\left(\frac{1}{t^2}h + \frac{k}{t}h + k^2 h\right) \ , \tag{2.52}$$

$$\mathcal{O}\left(\frac{\delta T_{\mu\nu}}{a^2\rho}\right) = \mathcal{O}\left(h + kth + (kt)^2 h\right) \ . \tag{2.53}$$

For $kt \gg 1$ this gives $\mathcal{O}(\delta, v) = \mathcal{O}\left(\delta T_{\mu\nu}/\rho\right) \gg \mathcal{O}(h)$. Therefore, on subhorizon scales the differences between δ, $\delta^{\rm lo}$, D_g and D are negligible as are the differences between v and V or $v^{(V)}$, $V^{(V)}$ and $\Omega^{(V)}$. Since observations of density and velocity perturbations can only be made on vastly subhorizon scales, we may therefore use any of the gauge-invariant perturbation variables to compare with observations. Actually, when we carefully analyse what is truly measured, this always turns out to be gauge invariant in first order perturbation theory.

[1] 'vector gauge' is defined by $H^{(V)} = 0$.

2.1.3 Perturbation equations

We do not derive the first-order perturbations of Einstein's equations. By elementary algebraic methods, this is quite lengthy and cumbersome. However, we recommend that the student simply determines $\delta G_{\mu\nu}$ in longitudinal gauge using some algebraic package like Maple or Mathematica and then writes down the resulting Einstein equations using gauge-invariant variables. Since we know that these variables do not depend on the coordinates chosen, the equations obtained in this way are valid in any gauge. Here, we just present the resulting equations in gauge-invariant form. A rapid derivation by hand is possible using the 3+1 formalism of general relativity and working with Cartan's formalism for the Riemann curvature, see [20]. In order to simplify the notation, we suppress the overbar on background quantities whenever this does not lead to confusion. We also do not present the vector perturbation equations and set $K = 0$ as before.

Einstein's equations

The Einstein equations $G_{0\mu} = 8\pi G T_{0\mu}$ lead to two scalar constraint equations,

$$\begin{aligned} 4\pi G a^2 \rho D &= -k^2\Phi \qquad (00) \\ 4\pi G a^2 (\rho + P) V &= k\left(\mathcal{H}\Psi + \dot{\Phi}\right) \qquad (0i) \end{aligned} \quad , \tag{2.54}$$

The dynamical Einstein equations, $G_{ij} = 8\pi G T_{ij}$, provide two scalar, one vector and one tensor perturbation equations. The scalar and tensor equations are

scalar:

$$k^2\left(\Phi - \Psi\right) = 8\pi G a^2 P \Pi^{(S)} \,, \tag{2.55}$$

$$\ddot{\Phi} + 2\mathcal{H}\dot{\Phi} + \mathcal{H}\dot{\Psi} + \left[2\dot{\mathcal{H}} + \mathcal{H}^2 - \frac{k^2}{3}\right]\Psi = 4\pi G a^2 \rho \left[\frac{1}{3}D + c_s^2 D_s + w\Gamma\right] \tag{2.56}$$

tensor:

$$\ddot{H}^{(T)} + 2\mathcal{H}\dot{H}^{(T)} + k^2 H^{(T)} = 8\pi G a^2 P \Pi^{(T)} \,. \tag{2.57}$$

The second dynamical scalar equation is somewhat cumbersome and not often used, since we may use one of the conservation equations given below instead. For the derivation of the perturbed Einstein equation the following relations are useful. They can be derived from the Friedmann equations; a possible cosmological constant is included in ρ and P.

$$4\pi G a^2 \rho (1+w) = \mathcal{H}^2 - \dot{\mathcal{H}} \,, \tag{2.58}$$

$$\dot{\mathcal{H}} = -\frac{1+3w}{2}\mathcal{H}^2 \,, \tag{2.59}$$

$$4\pi G a^2 \rho (1+w) 3c_s^2 = \frac{\ddot{\mathcal{H}}}{\mathcal{H}} - \dot{\mathcal{H}} - \mathcal{H}^2 \,, \tag{2.60}$$

$$c_s^2 = \frac{\frac{\ddot{\mathcal{H}}}{\mathcal{H}} - \dot{\mathcal{H}} - \mathcal{H}^2}{3[\mathcal{H}^2 - \dot{\mathcal{H}}]} \,. \tag{2.61}$$

For the calculations below we shall also make use of

$$\dot{w} = 3(w - c_s^2)(1+w)\mathcal{H} \,. \tag{2.62}$$

Note that for perfect fluids, where $\Pi^i_j \equiv 0$, we have $\Phi = \Psi$. As we shall see below, for perfect fluids with $\Gamma = \Pi = 0$, the behaviour of scalar perturbations is given by Ψ, which describes a damped wave propagating with speed c_s^2.

Tensor perturbations are given by $H^{(T)}$, which for perfect fluids also obeys a damped wave equation propagating with the speed of light. On small scales (over short time periods) when $t^{-2} \lesssim k^2$, i.e. sub-Hubble scales, the damping term can be neglected and H_{ij} represents propagating gravitational waves.

Energy–momentum conservation

The conservation equations, $T^{\mu\nu}_{\ ;\nu} = 0$ lead to the following scalar perturbation equations:

$$\dot{D}_g + 3\left(c_s^2 - w\right)\mathcal{H}D_g + (1+w)kV + 3w\mathcal{H}\Gamma = 0 \tag{2.63}$$

$$\dot{V} + \mathcal{H}\left(1 - 3c_s^2\right)V = k\left(\Psi + 3c_s^2\Phi\right) + \frac{c_s^2 k}{1+w}D_g \tag{2.64}$$

$$+ \frac{wk}{1+w}\left[\Gamma - \frac{2}{3}\left(1 - \frac{3K}{k^2}\right)\Pi\right] \tag{2.65}$$

It is sometimes also useful to express the energy conservation equation in terms of the variable pair (D, V). Using $D = D_g + 3(1+w)\left[\mathcal{H}k^{-1}V + \Phi\right]$ in (2.63) one obtains after some algebra and making use of the $(0i)$ constraint equation (2.54)

$$\dot{D} - 3w\mathcal{H}D = -\left[(1+w)kV + 2\mathcal{H}w\Pi\right] , \tag{2.66}$$

For scalar perturbations we can actually derive an evolution equation for Φ, where Γ and Π enter only as source terms. Replacing D and D_s in (2.56) by use of (2.47) and (2.54) and replacing Ψ by Π and Φ via Eq. (2.55) leads to

$$\ddot{\Phi} + 3\mathcal{H}(1+c_s^2)\dot{\Phi} + \left[3(c_s^2 - w)\mathcal{H}^2 + c_s^2k^2\right]\Phi$$
$$= \frac{8\pi G a^2 P}{k^2}\left[\mathcal{H}\dot{\Pi} + [2\dot{\mathcal{H}} + 3\mathcal{H}^2(1 - c_s^2/w)]\Pi - \frac{1}{3}k^2\Pi + \frac{k^2}{2}\Gamma\right]. \tag{2.67}$$

This is the Bardeen equation. To derive it we also made use of (2.59) to replace $\dot{\mathcal{H}}$.

Exercice 7 The Bardeen equation

1. *We consider the case $\Gamma = \Pi = 0$ and $w = c_s^2 =$constant.*

   (i) Solve the Bardeen equation. Discuss especially the cases $w = 1/3$ and $w = 0$.

   (ii) Compute also V, D and D_s, discuss again the cases $w = 1/3$ and $w = 0$.

   (iii) Concentrating on the 'growing' mode, solve the equation numerically in a matter radiation universe. Plot the resulting power spectrum, $P_\Psi = k^3|\Psi|^2(k, t_0)$ for scale invariant initial initial conditions,

   $$P_\Psi = k^3|\Psi|^2(k, t_{\rm in}) = \text{const.} ,$$

   given deep in the radiation era. Plot also the density power spectrum $P_D = k^3|D|^2(k, t_0)$. Discuss!

2. Derive the Bardeen eqn. as outlined above (this is a bit more difficult, maybe specialize on $\Gamma = \Pi = 0$ *and* $w = c_s^2 =$*constant.).*

Solving the above exercise you have seen that the Bardeen potential never grows. This fact (even though he used different variables) led Lifshitz [18] to the conclusion that perturbations do not grow in an expanding universe. It is actually interesting that the gravitational potential on all cosmological scales from galaxies ($\sim$ 10kpc) to the Hubble scale ($\sim$ 10Gpc) has about the same amplitude, $\Psi \sim 10^{-5}$.

Exercice 8 *Solve the tensor perturbation equation (2.57) in the case* $\Pi^{(T)} = 0$. *Discuss the behavior on super- and sub-Hubble scales.*

2.2 Perturbed photon geodesics

After decoupling, $t > t_{\rm dec}$, photons follow light-like geodesics. The temperature shift of a Planck distribution of photons is equal to the energy shift of any given photon. The relative energy shift, red- or blue shift, is independent of the photon energy (gravity is 'achromatic').

The unperturbed photon trajectory follows

$$(x^\mu(t)) \equiv \left(t, \int_t^{t_0} \mathbf{n}(t')\, dt' + \mathbf{x}_0\right),$$

where $\mathbf{x}_0$ is the photon position at time t_0 and $\mathbf{n}$ is the (parallel transported) photon direction. We determine the components of the photon momentum with respect to a geodesic basis $(\mathbf{e}_i)_{i=1}^3$ on the constant time hypersurfaces. We choose

$$\mathbf{e}_i = \frac{\partial}{\partial x^i} \tag{2.68}$$

Our metric is of the form

$$d\tilde{s}^2 = a^2 ds^2\ , \quad \text{with} \tag{2.69}$$

$$ds^2 = (\eta_{\mu\nu} + h_{\mu\nu})\, dx^\mu\, dx^\nu, \quad \eta_{00} = -1,\ \eta_{i0} = 0,\ \eta_{ij} = \delta_{ji}\ . \tag{2.70}$$

We make use of the fact that light-like geodesics are conformally invariant. More precisely, ds^2 and $d\tilde{s}^2$ have the same light-like geodesics, only the corresponding affine parameters are different. Let us denote the two affine parameters by λ and $\tilde{\lambda}$ respectively, and the tangent vectors to the unperturbed geodesic by

$$n = \frac{dx}{d\lambda}\,, \quad \tilde{n} = \frac{dx}{d\tilde{\lambda}}\ , \quad n^2 = \tilde{n}^2 = 0\ ,\ \ n^0 = 1\ ,\ \ \mathbf{n}^2 = 1\ . \tag{2.71}$$

The photon 4-momentum p^μ is then given by $p^\mu = \omega n$, where ω is the constant energy of the photon moving in the unperturbed metric ds^2. We have seen that in expanding space the photon momentum is redshifted. Actually, the components behave like $\tilde{n}^i \propto 1/a^2$ so that $\tilde{\mathbf{n}}^2 = a^2 \sum_i (\tilde{n}^i)^2 \propto 1/a^2$, hence we have to choose $\tilde{\lambda} = a^2\lambda$. As always for light-like geodesics, $\tilde{\lambda}$ and λ are only determined up to a multiplicative constant which we have fixed by the conditions $\mathbf{n}^2 = 1$ and $\tilde{\lambda} = a^2\lambda$.

Let us now introduce perturbations. We set $n^0 = 1 + \delta n^0$. The geodesic equation for the perturbed metric

$$ds^2 = (\eta_{\mu\nu} + h_{\mu\nu})\, dx^\mu\, dx^\nu \ , \tag{2.72}$$

yields, to first order,

$$\frac{d}{d\lambda}\delta n^\mu = -\delta\Gamma^\mu_{\alpha\beta} n^\alpha n^\beta \ . \tag{2.73}$$

For the energy shift, we have to determine δn^0. Since $g^{0\mu} = -\delta_{0\mu} + \text{first order}$, we obtain $\delta\Gamma^0_{\alpha\beta} = -\frac{1}{2}(h_{\alpha 0|\beta} + h_{\beta 0|\alpha} - \dot h_{\alpha\beta})$, so that

$$\frac{d}{d\lambda}\delta n^0 = h_{\alpha 0|\beta} n^\beta n^\alpha - \frac{1}{2}\dot h_{\alpha\beta} n^\alpha n^\beta \ . \tag{2.74}$$

Integrating this equation we use $h_{\alpha 0|\beta} n^\beta n^\alpha = \frac{d}{d\lambda}(h_{\alpha 0} n^\alpha)$, so that the change of n^0 between some initial time t_i and some final time t_f is given by

$$\delta n^0|_i^f = \left[h_{00} + h_{0j} n^j\right]_i^f - \frac{1}{2}\int_i^f \dot h_{\mu\nu} n^\mu n^\nu d\lambda \ . \tag{2.75}$$

The energy of a photon with 4-momentum $\tilde p^\mu$ as seen by an observer moving with 4-velocity $\tilde u$ is given by $E = -(\tilde u \tilde\cdot \tilde p)$. Hence, the ratio of the energy of a photon measured by some observer at t_f to the energy emitted at t_i is

$$\frac{E_f}{E_i} = \frac{(\tilde n \tilde\cdot \tilde u)_f}{(\tilde n \tilde\cdot \tilde u)_i} = \frac{a_i}{a_f}\frac{(n\cdot u)_f}{(n\cdot u)_i} \ , \tag{2.76}$$

where here $\tilde\cdot$ denotes the scalar product in an expanding universe, containing the factor a^2 and $\tilde u$ is the emitter and receiver 4-velocity in an expanding universe, $\tilde u = a^{-1}u$, while u_f and u_i are the 4-velocities of the observer and emitter respectively in the non-expanding conformally related geometry given by

$$u = (1 - A)\partial_t + v^i \mathbf{e}_i = a\tilde u \ . \tag{2.77}$$

Together with $\tilde n = a^{-2} n$ this implies the result (2.76). The ratio $a_i/a_f = T_f/T_i$ is the usual (unperturbed) redshift. An observer measuring a temperature T_0 receives photons that were emitted at the time $t_{\rm dec}$ of decoupling of matter and radiation, at the fixed temperature $T_{\rm dec}$. In first-order perturbation theory, we find the following relation between the unperturbed temperatures T_f, T_i, the true temperatures $T_0 = T_f + \delta T_f$, $T_{\rm dec} = T_i + \delta T_i$, and the photon energy density perturbation:

$$\frac{a_i}{a_f} = \frac{T_f}{T_i} = \frac{T_0}{T_{\rm dec}}\left(1 - \frac{\delta T_f}{T_f} + \frac{\delta T_i}{T_i}\right) = \frac{T_0}{T_{\rm dec}}\left(1 - \frac{1}{4}\delta_\gamma|_i^f\right) \ , \tag{2.78}$$

where δ_γ is the intrinsic energy density perturbation in the radiation and we have used $\rho_\gamma \propto T^4$ in the last equality. Inserting the above equation and Eq. (2.75) into Eq. (2.76), and using Eq. (2.10) for the definition of $h_{\mu\nu}$, as well as Eqs. (2.21), (2.22), (2.48) and (2.45) one finds, after integration by parts, the following result for scalar perturbations:

$$\frac{E_f}{E_i} = \frac{T_0}{T_{\rm dec}}\left\{1 - \left[\frac{1}{4}D_g^{(r)} + V_j^{(b)} n^j + \Psi + \Phi\right]_i^f + \int_i^f (\dot\Psi + \dot\Phi)\, d\lambda\right\} \ . \tag{2.79}$$

Here $D_g^{(r)}$ denotes the density perturbation in the radiation fluid, and $V^{(b)}$ is the peculiar velocity of the baryonic matter component (the emitter and observer of radiation).

Evaluating Eq. (2.79) at final time t_0 (today) and initial time $t_{\rm dec}$, we obtain the temperature difference of photons coming from different directions $\mathbf{n}_1$ and $\mathbf{n}_2$

$$\frac{\Delta T}{T} \equiv \frac{\Delta T(\mathbf{n}_1)}{T} - \frac{\Delta T(\mathbf{n}_2)}{T} \equiv \frac{E_f}{E_i}(\mathbf{n}_1) - \frac{E_f}{E_i}(\mathbf{n}_2) \ . \tag{2.80}$$

Direction-independent contributions to E_f/E_i do not enter in this difference.

The largest contribution to $\Delta T/T$ is the dipole term, $V_j^{(b)}(t_0)n^j$ which simply describes our motion with respect to the emission surface. Its amplitude is about 1.2×10^{-3} and it has been measured so accurately that even the yearly variation due to the motion of the Earth around the sun has been detected.

For the higher multipoles (polynomials in n^j of degree 2 and higher) we can set

$$\frac{\Delta T(\mathbf{n})}{T} = \left[\frac{1}{4}D_g^{(r)} + V_j^{(b)}n^j + \Psi + \Phi\right](t_{\rm dec}, \mathbf{x}_{\rm dec}) + \int_{t_{\rm dec}}^{t_0} (\dot\Psi + \dot\Phi)(t, \mathbf{x}(t))\, dt \ , \tag{2.81}$$

where $\mathbf{x}(t)$ is the unperturbed photon position at time t for an observer at $\mathbf{x}_0$, and $\mathbf{x}_{\rm dec} = \mathbf{x}(t_{\rm dec})$ (if $K = 0$ we simply have $\mathbf{x}(t) = \mathbf{x}_0 - (t_0 - t)\mathbf{n}$). The first term in Eq. (2.81) is the one we have discussed in the previous section. It describes the intrinsic inhomogeneities of the radiation density on the surface of last scattering, due to acoustic oscillations prior to decoupling, see Ex. 7. Depending on the initial conditions, it can also contribute significantly on super-horizon scales. This is especially important in the case of adiabatic initial conditions. As we have seen in Ex. 7, in a dust + radiation universe with $\Omega = 1$, adiabatic initial conditions imply $D_g^{(r)}(k,t) = -\frac{20}{3}\Psi(k,t)$ and $V^{(b)} = V^{(r)} \ll D_g^{(r)}$ when $kt \ll 1$. With $\Phi = \Psi$ the square bracket of Eq. (2.81) therefore gives for adiabatic perturbations

$$\left(\frac{\Delta T(\mathbf{n})}{T}\right)^{\rm (OSW)}_{\rm adiabatic} = \frac{1}{3}\Psi(t_{\rm dec}, \mathbf{x}_{\rm dec}) \ ,$$

on super-horizon scales. The contribution to $\Delta T/T$ from the last scattering surface on very large scales is called the 'ordinary Sachs–Wolfe effect' (OSW). It was derived for the first time by Sachs and Wolfe (1967).

The second term in (2.81) describes the relative motion of emitter and observer. This is the Doppler contribution to the CMB anisotropies. It appears on the same angular scales as the acoustic term; we call the sum of the acoustic and Doppler contributions 'acoustic peaks'.

The integral in Eq. (2.81) accounts for the red- or blue shifts caused by the time dependence of the gravitational potential along the path of the photon, and represents the so-called integrated Sachs–Wolfe (ISW) effect. In a $\Omega = 1$, pure dust universe, as we have seen, the Bardeen potentials are constant and there is no integrated Sachs–Wolfe effect; the blue shift which the photons acquire by falling into a gravitational potential is exactly cancelled by the redshift induced by climbing out of it. This is no longer true in a universe with substantial radiation contribution, curvature, or a cosmological constant. The sum of the ordinary Sachs–Wolfe term and the integral is the full Sachs–Wolfe contribution.

For **tensor** perturbations, i.e. gravitational waves, only the gravitational part remains:

$$\left(\frac{E_f}{E_i}\right)^{(T)} = \frac{a_i}{a_f}\left[1 - \int_i^f \dot{H}_{lj} n^l n^j d\lambda\right] . \tag{2.82}$$

Equations (2.79) and (2.82) are the manifestly gauge-invariant results for the energy shift of photons due to scalar and tensor perturbations. Disregarding again the dipole contribution due to our proper motion, Eq. (2.82) implies the tensor temperature fluctuations

$$\left(\frac{\Delta T(\mathbf{n})}{T}\right)^{(T)} = -\int_i^f \dot{H}_{lj}(t, \mathbf{x}(t)) n^l n^j \, d\lambda . \tag{2.83}$$

2.3 Power spectra

The quantities that we can determine from a given model are usually not the precise values of perturbation variables as $\Psi(\mathbf{k}, t)$, but only expectation values like $\langle \Psi(\mathbf{k}, t) \cdot \Psi^*(\mathbf{k}', t)\rangle$. In different realizations, e.g., of the same inflationary model, the 'phases' $\alpha(\mathbf{k}, t)$ given by $\Psi(\mathbf{k}, t) = \exp(i\alpha(\mathbf{k}))|\Psi(\mathbf{k}, t)|$ are different. They are random variables. If we assume that the random process which generates the fluctuations Ψ is stochastically homogeneous and isotropic, these phases have a vanishing 2-point correlator for different values of $\mathbf{k}$ and $|\Psi|$ depends only on the modulus $k = |\mathbf{k}|$.

The quantity which we can calculate for a given model and which then has to be compared with observations is the power spectrum, defined below. Power spectra are the 'harmonic transforms' of the 2-point correlation functions.[2] If the perturbations of the model under consideration are Gaussian, a relatively generic prediction from inflationary models, then the 2-point functions and therefore the power spectra contain the full statistical information of the model.

There is one additional problem to consider: one can never 'measure' expectation values. We have only one Universe, i.e. one realization of the stochastic process which generates the fluctuations at our disposal for observations. The best we can do when we want to determine the mean square fluctuation on a given scale λ is to average over many disjoint patches of size λ, assuming that this spatial averaging corresponds to an ensemble averaging; a type of 'ergodic hypothesis'. This works well as long as the scale λ is much smaller than the Hubble horizon, the size of the observable Universe. For $\lambda \sim \mathcal{O}(H_0^{-1})$ we can no longer average over many independent volumes and the value measured could be quite far from the ensemble average. This problem is known under the name 'cosmic variance'.

For an arbitrary scalar variable X in position space, we define the power spectrum in Fourier space by

$$\langle X(\mathbf{k}, t_0) X^*(\mathbf{k}', t_0)\rangle = (2\pi)^3 \delta(\mathbf{k} - \mathbf{k}') P_X(k) . \tag{2.84}$$

The $\langle\ \rangle$ indicates a statistical average, ensemble average, over 'random initial conditions' in a given model. We assume that no point in space is preferred,

[2] The 'harmonic transform' in usual flat space is simply the Fourier transform. In curved space it is the expansion in terms of eigenfunctions of the Laplacian on that space, e.g., on the sphere it corresponds to the expansion in terms of spherical harmonics.

in other words that $X(\mathbf{x}, t_0)$ (and any other stochastic field which we consider) has the same distribution in every point $\mathbf{x}$. Such random fields are called 'statistically homogeneous' (or stationary). We also assume that the distribution of $X(\mathbf{x}, t_0)$ has no preferred direction. This means that the random field X is statistically isotropic. These properties imply that the Fourier transform of the 2-point function is diagonal, i.e. they explain the factor $\delta(\mathbf{k} - \mathbf{k}')$ in Eq. (2.84), and that the power spectrum depends only on the modulus k. (see Ex. 9 below).

Since the perturbation equations are linear and different $\mathbf{k}$'s are decoupled, they are of the form

$$D_{ij}(\mathbf{k}, t) X_j(\mathbf{k}, t) = 0 \tag{2.85}$$

with some linear dirrerential operator D_{ij}. Their solution is of the form

$$X_j(\mathbf{k}, t_0) = T_{ji}(\mathbf{k}) X_j(\mathbf{k}, t_{\rm in}) \,. \tag{2.86}$$

T_{ij} is called the transfer matrix. This transfer matrix can be calculated from the linear perturbation equations and it only depends on the cosmological model, i.e. the cosmological parameters. With its help we can express the power spectra today, $t = t_0$ in terms of the initial power spectra.

Exercice 9 Power spectrum
For a spatial, statistically homogeneous and isotropic random variable $X(\mathbf{x})$ with vanishing mean we define the 2-point function

$$\xi(r) = \langle X(\mathbf{x}) X(\mathbf{x} + r\mathbf{n}) \rangle \ .$$

Homogeneity requires that ξ does not depend on the position of the first point, $\mathbf{x}$ and isotropy means that ξ is independent of the direction $\mathbf{n}$ in which the second point $\mathbf{y} = \mathbf{x} + r\mathbf{n}$ lies. Hence ξ depends only on the distance r. Show that the power spectrum defined in Eq. (2.84) is the Fourier transform of the correlation function ξ.

2.3.1 The matter power spectrum

As a simple example, we consider the matter power spectrum, P_D, in a matter/radiation universe. It is defined by

$$\langle D_m(\mathbf{k}, t_0) \, D_m^*(\mathbf{k}', t_0) \rangle = P_D(k) (2\pi)^3 \delta(\mathbf{k} - \mathbf{k}') \ . \tag{2.87}$$

Since in this case Ψ satisfies a simple second order differential equation and D is related to Ψ via the algebraic Eq. (2.54), we have

$$P_D(k) = T_D^2(k) P_\Psi(k, t_{\rm in}) \,. \tag{2.88}$$

Os subhorizon scale P_D is the power spectrum of matter density fluctuations. However, $P_D(k)$ is usually compared with the observed power spectrum of the galaxy distribution. This is clearly problematic since it is by no means evident what the relation between these two spectra should be. This problem is known under the name of 'biasing' and it is very often simply assumed that the dark matter and galaxy power spectra differ only by a scale independent (but time dependent) factor $b(t)$. The hope is also that on sufficiently large scales, since the evolution of both, galaxies and dark matter is governed by gravity, their power spectra should not differ by much.

The power spectrum of velocity perturbations satisfies the relation

$$\langle V_j(\mathbf{k},t_0)\, V_i^*(\mathbf{k}',t_0)\rangle = \hat{\mathbf{k}}_j\hat{\mathbf{k}}'_i P_V(k)(2\pi)^3\delta(\mathbf{k}-\mathbf{k}')\ , \tag{2.89}$$

$$P_V(k) = f^2\left(\frac{H_0}{k}\right)^2 P_D(k) \qquad \text{with} \tag{2.90}$$

$$f(k) \simeq \Omega_m^{0.6}\ . \tag{2.91}$$

For $\simeq$ we have used that in a matter dominated universe (with possibly a cosmological constant or curvature) $|kV(t_0)| = \dot{D}^{(m)}(t_0) \sim H_0\Omega_m^{0.55}D_g$ on subhorizon scales (see e.g., Peebles, 1993 [21]).

2.3.2 The CMB fluctuation power spectrum

The present universe is actually not quite a matter/radiation universe with a cosmological constant. The reason is that the radiation content of the Universe is no longer in thermal equilibrium. Neutrinos free-stream already since $T \sim 1.4$MeV while photons free-stream since decoupling at $T \simeq 3000\text{K} \simeq 0.26$eV.

Fluctuations of the photon (and neutrino) distribution therefore cannot be given simply by a density and velocity field but they contain higher moments in phase space. We describe them as the temperature fluctuations depending on position $\mathbf{x}$, time t and direction $\mathbf{n}$. We develop the directional dependence in spherical harmonics. Assuming again statistical homogeneity and isotropy the off-diagonal correlators of the expansion coefficients $a_{\ell m}$ vanish and we have

$$\frac{\Delta T}{T}(\mathbf{x}_0,\mathbf{n},t_0) = \sum_{\ell,m} a_{\ell m}(\mathbf{x}_0)Y_{\ell m}(\mathbf{n}), \quad \langle a_{\ell m}\cdot a^*_{\ell' m'}\rangle = \delta_{\ell\ell'}\delta_{mm'}C_\ell\ . \tag{2.92}$$

The C_ℓs are the CMB power spectrum.

The 2-point correlation function, $\mathcal{C}(\mu)$, $\mu = \mathbf{n}\cdot\mathbf{n}'$, is related to the C_ℓs by

$$\begin{aligned}
\mathcal{C}(\mu) &\equiv \left\langle \frac{\Delta T}{T}(\mathbf{n})\frac{\Delta T}{T}(\mathbf{n}')\right\rangle_{\mathbf{n}\cdot\mathbf{n}'=\mu} \\
&= \sum_{\ell,\ell',m,m'} \langle a_{\ell m}\cdot a^*_{\ell' m'}\rangle\, Y_{\ell m}(\mathbf{n})Y^*_{\ell' m'}(\mathbf{n}') \\
&= \sum_\ell C_\ell \underbrace{\sum_{m=-\ell}^{\ell} Y_{\ell m}(\mathbf{n})Y^*_{\ell m}(\mathbf{n}')}_{\frac{2\ell+1}{4\pi}P_\ell(\mathbf{n}\cdot\mathbf{n}')} \\
&= \frac{1}{4\pi}\sum_\ell (2\ell+1)C_\ell P_\ell(\mu)\ ,
\end{aligned} \tag{2.93}$$

where we have used the addition theorem of spherical harmonics for the last equality; the P_ℓs are the Legendre polynomials.

Scalar perturbations

Let us first discuss in somewhat more detail scalar perturbations. We suppose the initial perturbations to be given by a spectrum of the form

$$\langle\Psi(\mathbf{k})\Psi^*(\mathbf{k}')\rangle\, k^3 = (2\pi)^3 k^3 P_\Psi(k)\delta(\mathbf{k}-\mathbf{k}') = (2\pi)^3 A_S(kt_0)^{n-1}\delta(\mathbf{k}-\mathbf{k}')\ . \tag{2.94}$$

We multiply by the constant t_0^{n-1}, the actual comoving size of the horizon, in order to keep A_S dimensionless for all values of the spectral index n. A_S then represents the amplitude of metric perturbations at horizon scale today, $k = 1/t_0$.

As we have seen in the previous section, the dominant contribution on *super-horizon scales* (neglecting the integrated Sachs–Wolfe effect $\int \dot{\Phi} + \dot{\Psi}$) is the ordinary Sachs–Wolfe effect, OSW, which for adiabatic perturbations is given by

$$\frac{\Delta T}{T}(\mathbf{x}_0, \mathbf{n}, t_0) \simeq \frac{1}{3}\Psi(x_{\rm dec}, t_{\rm dec}) \ . \tag{2.95}$$

Since $\mathbf{x}_{\rm dec} = \mathbf{x}_0 + \mathbf{n}(t_0 - t_{\rm dec})$, the Fourier transform of (2.95) gives

$$\frac{\Delta T}{T}(\mathbf{k}, \mathbf{n}, t_0) = \frac{1}{3}\Psi(\mathbf{k}, t_{\rm dec}) \cdot e^{i\mathbf{k}\mathbf{n}(t_0 - t_{\rm dec})} \ . \tag{2.96}$$

Using the decomposition (see [6])

$$e^{i\mathbf{k}\mathbf{n}(t_0 - t_{\rm dec})} = \sum_{\ell=0}^{\infty}(2\ell+1) i^\ell j_\ell(k(t_0 - t_{\rm dec})) P_\ell(\widehat{\mathbf{k}} \cdot \mathbf{n}) \ ,$$

where j_ℓ are the spherical Bessel functions, we obtain ($k = |\mathbf{k}|, \hat{\mathbf{k}} = \mathbf{k}/k$)

$$\begin{aligned}
&\left\langle \frac{\Delta T}{T}(\mathbf{x}_0, \mathbf{n}, t_0) \frac{\Delta T}{T}(\mathbf{x}_0, \mathbf{n}', t_0) \right\rangle \qquad (2.97)\\
&\quad = \frac{1}{(2\pi)^6} \int d^3k\, d^3k'\, e^{i\mathbf{x}_0 \cdot (\mathbf{k} - \mathbf{k}')} \left\langle \frac{\Delta T}{T}(\mathbf{k}, \mathbf{n}, t_0) \left(\frac{\Delta T}{T}\right)^* (\mathbf{k}', \mathbf{n}', t_0) \right\rangle \\
&\quad \simeq \frac{1}{(2\pi)^6 9} \int d^3k d^3k' e^{i\mathbf{x}_0 \cdot (\mathbf{k} - \mathbf{k}')} \langle \Psi(\mathbf{k}) \Psi^*(\mathbf{k}') \rangle \sum_{\ell, \ell'=0}^{\infty} (2\ell+1)(2\ell'+1) i^{\ell - \ell'} \\
&\qquad \cdot j_\ell(k(t_0 - t_{\rm dec})) j_{\ell'}(k'(t_0 - t_{\rm dec})) P_\ell(\hat{\mathbf{k}} \cdot \mathbf{n}) \cdot P_{\ell'}(\hat{\mathbf{k}}' \cdot \mathbf{n}') \\
&\quad = \frac{1}{(2\pi)^3 9} \int d^3k P_\Psi(k) \sum_{\ell, \ell'=0}^{\infty} (2\ell+1)(2\ell'+1) i^{\ell - \ell'} \\
&\qquad \cdot j_\ell(k(t_0 - t_{\rm dec})) j_{\ell'}(k(t_0 - t_{\rm dec})) P_\ell(\hat{\mathbf{k}} \cdot \mathbf{n}) \cdot P_{\ell'}(\hat{\mathbf{k}} \cdot \mathbf{n}') \ . \qquad (2.98)
\end{aligned}$$

In the first equals sign we have used the unitarity of the Fourier transformation. Inserting $P_\ell(\hat{\mathbf{k}}\mathbf{n}) = \frac{4\pi}{2\ell+1} \sum_m Y^*_{\ell m}(\hat{\mathbf{k}}) Y_{\ell m}(\mathbf{n})$ and $P_{\ell'}(\hat{\mathbf{k}}\mathbf{n}') = \frac{4\pi}{2\ell'+1}$ $\sum_{m'} Y^*_{\ell' m'}(\hat{\mathbf{k}}) Y_{\ell' m'}(\mathbf{n}')$, integration over the directions $d\Omega_{\hat{k}}$ gives $\delta_{\ell\ell'}\delta_{mm'} \sum_m Y^*_{\ell m}(\mathbf{n}) Y_{\ell m}(\mathbf{n}')$.

Also using $\sum_m Y^*_{\ell m}(\mathbf{n}) Y_{\ell m}(\mathbf{n}') = \frac{2\ell+1}{4\pi} P_\ell(\mu)$, where $\mu = \mathbf{n} \cdot \mathbf{n}'$, we find

$$\begin{aligned}
&\left\langle \frac{\Delta T}{T}(\mathbf{x}_0, \mathbf{n}, t_0) \frac{\Delta T}{T}(\mathbf{x}_0, \mathbf{n}', t_0) \right\rangle_{\mathbf{n}\mathbf{n}' = \mu} \\
&\qquad \simeq \sum_\ell \frac{2\ell+1}{4\pi} P_\ell(\mu) \frac{2}{\pi} \int \frac{dk}{k} \frac{1}{9} P_\Psi(k) k^3 j_\ell^2(k(t_0 - t_{\rm dec})) \ . \qquad (2.99)
\end{aligned}$$

Comparing this equation with Eq. (2.93) we obtain for *adiabatic perturbations* on scales $2 \le \ell \ll \chi(t_0 - t_{\rm dec})/t_{\rm dec} \sim 100$:

$$C_\ell^{\rm (SW)} \simeq C_\ell^{\rm (OSW)} \simeq \frac{2}{9\pi} \int_0^\infty \frac{dk}{k} P_\Psi(k) k^3 j_\ell^2 \left(k\left(t_0 - t_{\rm dec}\right)\right) \ . \tag{2.100}$$

The function $j_\ell^2\left(k(t_0-t_{\rm dec})\right)$ peaks roughly at $k\,(t_0-t_{\rm dec})\simeq kt_0\simeq\ell$. If Ψ is a pure power law on large scales, $kt_{\rm dec}\lesssim 1$ as in Eq. (2.94) and we set $k(t_0-t_{\rm dec})\sim kt_0$, the integral (2.100) can be performed analytically. For the ansatz (2.94), one finds

$$C_\ell^{(\rm SW)}=\frac{A_S}{9}\frac{\Gamma(3-n)\Gamma(\ell-\frac{1}{2}+\frac{n}{2})}{2^{3-n}\Gamma^2(2-\frac{n}{2})\Gamma(\ell+\frac{5}{2}-\frac{n}{2})}\quad\text{for }-3<n<3\,. \tag{2.101}$$

Of special interest is the *scale-invariant* or Harrison–Zel'dovich (HZ) spectrum, $n=1$. Such a spectrum does not lead to large fluctuations neither on very large, nor on very small scales. Interestingly a spectrum with $n\simeq 1$ is also obtained from inflation. It leads to

$$\ell(\ell+1)C_\ell^{(\rm SW)}=\frac{A_S}{9\pi}\simeq\left\langle\left(\frac{\Delta T}{T}(\vartheta_\ell)\right)^2\right\rangle\,,\qquad\vartheta_\ell\equiv\pi/\ell\,. \tag{2.102}$$

This is precisely (within the accuracy of the experiment) the behaviour observed by the DMR (differential microwave radiometer) experiment aboard the satellite COBE [22] and , much more precisely, with the Planck satellite [2], $n=0.9653\pm 0.0048$ (see Table 3.79) .

Inflationary models predict very generically a HZ spectrum (up to small corrections, i.e. a slightly red spectrum as observed). The DMR discovery and even more the Planck result has therefore been regarded as a great success, if not a proof, of inflation. There are, however, other models such as topological defects (see, e.g. [15]), or certain string cosmology models [23] which also predict scale-invariant, i.e. Harrison–Zel'dovich spectra of fluctuations. These models are outside the class investigated here, since in them perturbations are induced by seeds which evolve non-linearly in time. They are not simply laid down as initial conditions for the fluid perturbations but typically affect the perturbations of a given wavelength until it crosses the Hubble scale. This generically leads to iso-curvature perturbations which are ruled out as the dominant component by present data.

For iso-curvature perturbations, the main contribution on large scales comes from the integrated Sachs–Wolfe effect and (2.100) is replaced by

$$C_\ell^{(\rm ISW)}\simeq\frac{8}{\pi}\int\frac{dk}{k}\,k^3\left\langle\left|\int_{t_{\rm dec}}^{t_0}\dot\Psi(k,t)j_\ell(k(t_0-t))\,dt\right|^2\right\rangle. \tag{2.103}$$

Inside the horizon Ψ is roughly constant (matter dominated). Using the ansatz (2.94) for Ψ inside the horizon and setting the integral in (2.103) $\sim 2\Psi(k,t=1/k)j_\ell^2(kt_0)$, we obtain again (2.101), but with $A_S/9$ replaced by $4A_S$. For a fixed amplitude A_S of perturbations, the Sachs–Wolfe temperature anisotropies coming from iso-curvature perturbations are therefore about six times larger than those coming from adiabatic perturbations (see Fig. 2.1).

On smaller scales, $\ell\gtrsim 100$, the contribution to $\Delta T/T$ is dominated by acoustic oscillations, the first two terms in Eq. (2.81). Instead of (2.103) we then obtain

$$C_\ell^{(AC)}\simeq\frac{2}{\pi}\int_0^\infty\frac{dk}{k}k^3\left\langle\left|\frac{1}{4}D_r(k,t_{\rm dec})j_\ell(kt_0)+V^{(b)}(k,t_{\rm dec})j_\ell'(kt_0)\right|^2\right\rangle\,. \tag{2.104}$$

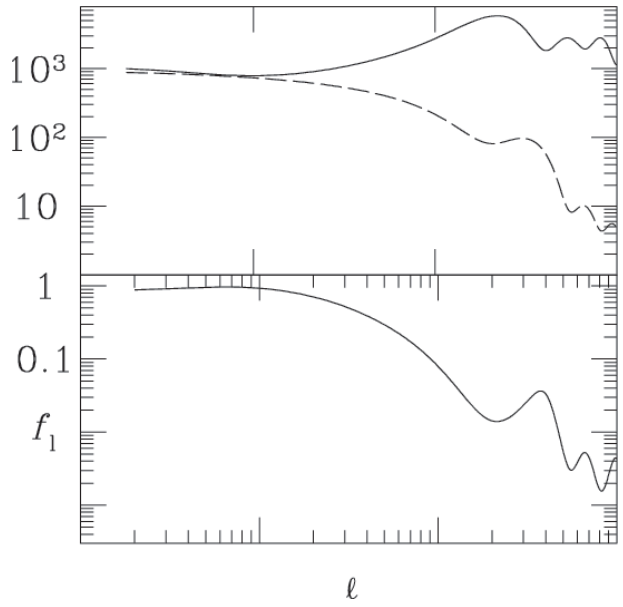

Figure 2.1: Examples of COBE normalized adiabatic (solid line) and isocurvature (dashed line) CMB anisotropy spectra, $\ell(\ell+1)C_\ell/(2\pi)$ in units of $(\mu K)^2$ are shown on the top panel. In the bottom panel the ratio of the isocurvature to adiabatic temperature fluctuations is plotted.

To remove the SW contribution from $D_g^{(r)}$ we have simply replaced it by D_γ which is much smaller than Ψ on super-horizon scales and therefore does not contribute to the SW terms. On subhorizon scales $D_\gamma \simeq D_g^{(\gamma)}$ and V_γ are oscillating like sine or cosine waves depending on the initial conditions. Correspondingly the $C_\ell^{(AC)}$ will show peaks and minima. For adiabatic initial conditions $D_g^{(\gamma)}$ and therefore D_γ also oscillates like a cosine. Its minima and maxima are at $k_n t_{\rm dec}/\sqrt{3} = n\pi$. Odd values of n correspond to maxima, 'contraction peaks', while even numbers are minima, 'expansion peaks'.

These are the 'acoustic peaks' of the CMB anisotropies. Sometimes they are misleadingly called 'Doppler peaks' referring to an old misconception that the peaks are due to the velocity term in the above formula. Actually the contrary is true. At maxima and minima of the density contrast, the velocity (being proportional to the derivative of the density) nearly vanishes. We shall therefore consistently call the CMB peak structure 'acoustic peaks'.

The angle θ_n, which subtends the scale $\lambda_n = \pi/k_n$ at the last scattering surface, is determined by the angular diameter distance to the last scattering surface, $d_A(t_{\rm dec})$ via the relation $\theta_n = \lambda_n/d_A(t_{\rm dec})$. Expanding the temperature anisotropies in spherical harmonics, the angular scale θ_n corresponds (roughly) to the harmonic number

$$\ell_n \simeq \pi/\theta_n = \pi d_A(t_{\rm dec})/\lambda_n = d_A(t_{\rm dec})k_n = n\sqrt{3}\pi d_A(t_{\rm dec})/t_{\rm dec}\ . \qquad (2.105)$$

For a flat matter dominated universe $d_A(t_{\rm dec}) \simeq t_0$ leading to $\ell_n \simeq 180n$. This crude approximation deviates by about 15% from the precise numerical value,

which not only depends, with d_A, strongly on curvature but also on the Hubble parameter and on the cosmological constant. Furthermore, the peak positions depend on the sound speed of the radiation–baryon plasma which we have simply set to $c_s = 1/\sqrt{3}$ in this approximation. The peak position and their spacing therefore strongly depends on the parameters of the underlying cosmological model. For a flat universe, $\Omega = 1$, the nth peak therefore is placed at

$$\ell_n \simeq k_n t_0 \cong n\pi\sqrt{3}\frac{t_0}{t_{\rm dec}}\,. \tag{2.106}$$

For a flat matter dominated universe we have $\frac{t_0}{t_{\rm dec}} \sim \sqrt{z_{\rm dec}} \sim 33.2$ which yields $\ell_1 \sim 180$. Here we have used $z_{\rm dec} \sim 1100$. This approximation is not very good since the Universe is not very well matter dominated at $t_{\rm dec}$. A somewhat more accurate estimate gives $\ell_1 \sim 220$, in good agreement with the numerical value. Subsequent peaks are then given by $\ell_n = n\ell_1$.

Our discussion is only valid in flat space. In curved space the exponentials $\exp(ik(t_0 - t_{\rm dec}))$ have to be replaced with the harmonics of the curved spaces. For the positions of the peaks, this corresponds to replacing $k_n t_0$ by $k_n\chi(t_0)$, hence replacing t_0 by the comoving angular diameter distance to the last scattering surface. Instead of Eq. (2.106) we then obtain the following approximate relation for the peak positions,

$$\ell_n \sim n\pi\sqrt{3}\frac{\chi(t_0)}{t_{\rm dec}}\,. \tag{2.107}$$

For values of Ω close to unity this scales like $1/\sqrt{\Omega}$.

On even smaller scales ($\ell \gtrsim 800$) the acoustic peaks are damped by the photon diffusion, so called Silk damping, which takes place during the recombination process. This effect will be discussed with the Boltzmann equation approach in Section 3.1.4.

Tensor perturbations

For gravitational waves (which are tensor fluctuations), a formula analogous to (2.101) can be derived, see [9]

$$C_\ell^{(T)} = \frac{2}{\pi}\int dk\, k^2 \left|\int_{t_{\rm dec}}^{t_0} dt\, \dot H(t,k)\frac{j_\ell(k(t_0-t))}{(k(t_0-t))^2}\right|^2 \frac{(\ell+2)!}{(\ell-2)!}\,. \tag{2.108}$$

To a very crude approximation we may assume $\dot H^{(T)} = 0$ on super-horizon scales and $\int dt\, \dot H^{(T)} j_\ell(k(t_0-t)) \sim H^{(T)}(t = 1/k) j_\ell(kt_0)$. For a pure power law,

$$k^3\,|H(k, t = 1/k)|^2 = A_T(kt_0)^{n_T}\,, \tag{2.109}$$

one obtains

$$\begin{aligned} C_\ell^{(T)} &\simeq \frac{2}{\pi}\frac{(\ell+2)!}{(\ell-2)!}A_T\int\frac{dx}{x}x^{n_T}\frac{j_\ell^2(x)}{x^4} \\ &= \frac{(\ell+2)!}{(\ell-2)!}A_T\frac{\Gamma(6-n_T)\Gamma(\ell-2+\frac{n_T}{2})}{2^{6-n_T}\Gamma^2(\frac{7-n_T}{2})\Gamma(\ell+4-\frac{n_T}{2})}\,. \end{aligned} \tag{2.110}$$

For a scale-invariant spectrum ($n_T = 0$) this results in

$$\ell(\ell+1)C_\ell^{(T)} \simeq \frac{8}{15\pi}\frac{\ell(\ell+1)}{(\ell+3)(\ell-2)}A_T \ . \tag{2.111}$$

The singularity at $\ell = 2$ in this crude approximation is not real, but there is some enhancement of $\ell(\ell+1)C_\ell^{(T)}$ at $\ell \sim 2$ (see Fig. 2.2).

Since tensor perturbations decay on subhorizon scales, $\ell \gtrsim 60$, they are not very sensitive to cosmological parameters.

Comparing the tensor and scalar result for scale-invariant perturbations we obtain for large scales, $\ell < 50$

$$\frac{C_\ell^{(T)}}{C_\ell^{(S)}} \simeq \frac{24}{5}\frac{A_T}{A_S} \equiv \frac{40}{3}r \tag{2.112}$$

This is the definition of the tensor to scalar ratio r.

Present CMB anisotropy data favour a roughly scale-invariant spectrum with amplitude

$$\ell(\ell+1)C_\ell \simeq 6\times 10^{-10} \quad \text{for} \quad \ell \lesssim 50 \ .$$

If the perturbations are purely scalar, this requires $A_S \simeq 1.7\times 10^{-8}$, if they were purely tensorial (which we know they are not), we would need $A_T \simeq 3.5\times 10^{-9}$. In general observations require

$$\frac{A_S}{9\pi} \simeq 6\times 10^{-10}, \qquad r \leq 0.1 \ . \tag{2.113}$$

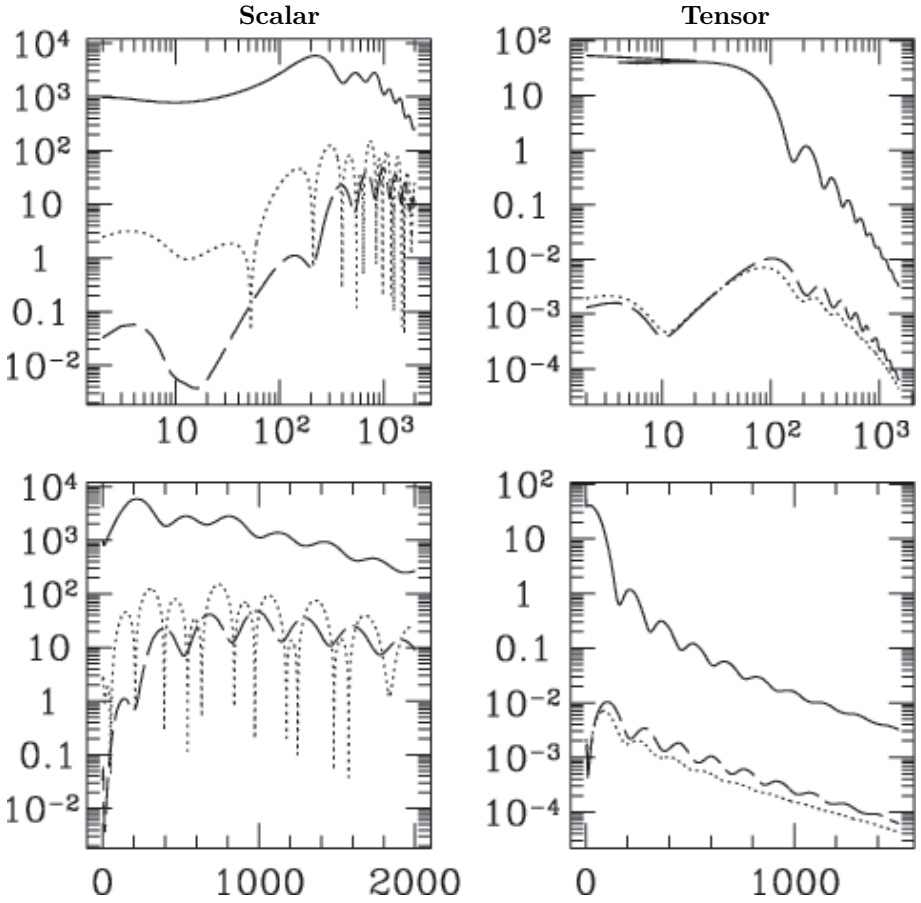

Figure 2.2: Adiabatic scalar and tensor CMB anisotropy spectra are plotted, $\mathcal{D}_\ell = \ell(\ell+1)C_\ell/(2\pi)$ in units of $(\mu K)^2$ as functions of ℓ in log-scale (top panels), where the Sachs–Wolfe plateau is clearly visible and in linear scale (bottom panels) which shows the equal spacing of the acoustic peaks. The solid line shows the temperature spectrum, the dashed line is the polarization and the dotted line shows the temperature–polarization cross correlation (see section 3.2 for a discussion of CMB polarisation). The latter can become negative, the deep spikes in the dotted curves in the left-hand panels are actually sign changes. The left-hand side shows scalar fluctuation spectra, while the right-hand side shows tensor spectra. The observational data are well fitted by a purely scalar spectrum. Comparison of data and a model scalar spectrum are shown in Figs. 2.3–2.5.

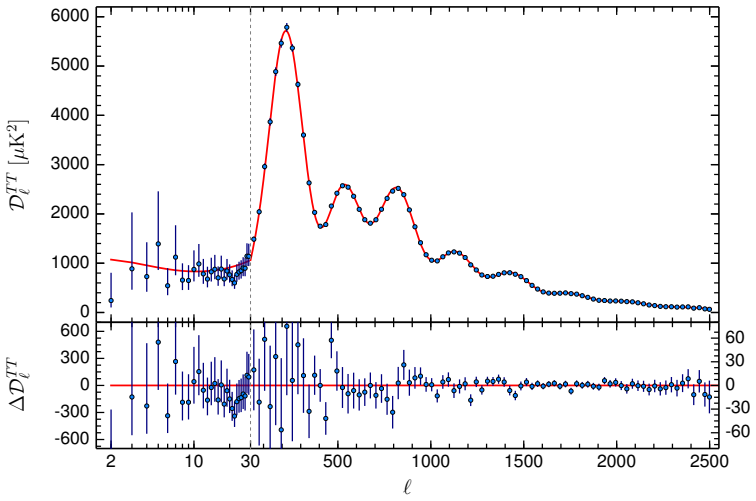

Figure 2.3: The CMB temperature power spectrum, $\mathcal{D}_\ell = T_0^2 \ell(\ell+1)C_\ell/(2\pi)$. Measurements from the Planck satellite are indicated as blue dots with errorbars. The best fitting model from scalar perturbations of a spatially flat ΛCDM universe is shown in red, figure from [2].

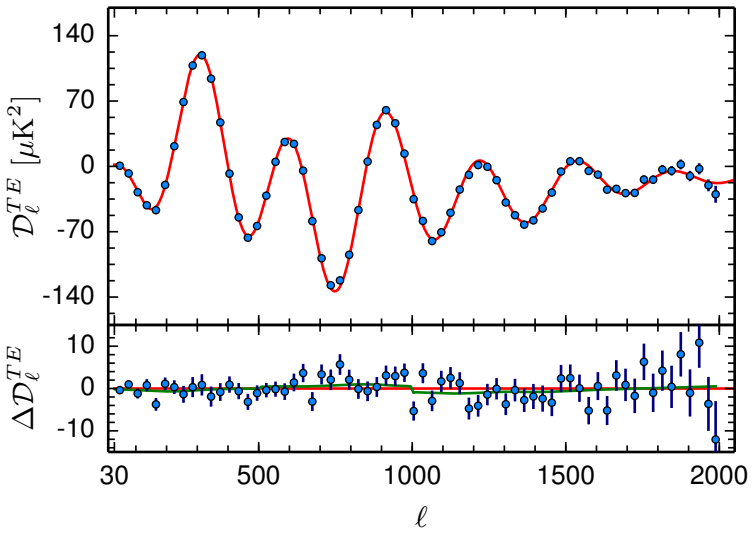

Figure 2.4: The CMB temperature-polarisation cross correlation, $\mathcal{D}_\ell = T_0^2 \ell(\ell+1)C_\ell/(2\pi)$. Measurements from the Planck satellite are indicated as blue dots with errorbars. The best fitting model from scalar perturbations of a spatially flat ΛCDM universe is shown in red, figure from [2].

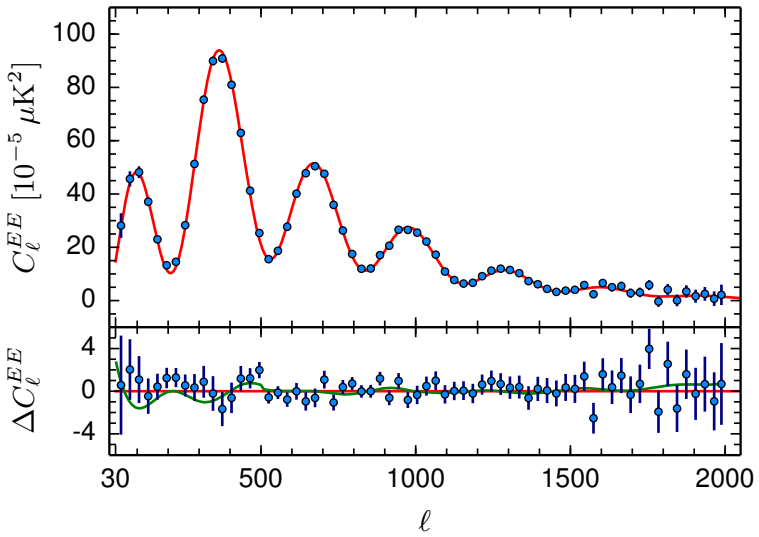

Figure 2.5: The CMB polarisation power spectrum, $\mathcal{D}_\ell = T_0^2 \ell(\ell+1)C_\ell/(2\pi)$. Measurements from the Planck satellite are indicated as blue dots with error-bars. The best fitting model from scalar perturbations of a spatially flat ΛCDM universe is shown in red (Even though the vertical axis is labelled C_ℓ^{EE}, it actually shows $\mathcal{D}_\ell^{EE}$), figure from [2].

Chapter 3

CMB anisotropies and polarisation

3.1 The Boltzmann equation

As we know from statistical mechanics, the distribution function of photons in thermal equilibrium is

$$f(\omega) = \frac{1}{e^{\omega/T} - 1} \ , \tag{3.1}$$

where $\omega = a|\tilde{\mathbf{p}}|$ is the physical photon energy. The comoving photon energy and momentum are denoted by $\tilde{p}^0$ and $\tilde{\mathbf{p}}$ and we have $\tilde{p} = |\tilde{\mathbf{p}}| = \tilde{p}^0 = a^{-1}\omega$. As long as interactions are sufficiently frequent to keep photons in thermal equilibrium, this distribution is maintained. Once there are very few interactions, the distribution is affected only by redshifting photon momenta. As we saw in Section 1.4.1, if we define $T(a) = T_D a_D/a$ after decoupling, where $a(t_D) \equiv a_D$ is the scale factor at decoupling, the distribution retains its form even after decoupling. Of course, after decoupling $T(a)$ is no longer a temperature in the thermodynamical sense but merely a parameter of the distribution function. This point is especially interesting for neutrinos: even if they may have masses of the order of $m_\nu \sim 1\,\mathrm{eV} \gg T_0$, their distribution is an extremely relativistic Fermi–Dirac distribution, since this is what it was at decoupling and it has only changed since by redshifting of neutrino momenta.

3.1.1 Generalities

We first present a brief introduction to relativistic kinetic theory. More details can be found in [24] and [25].

In the context of general relativity on a spacetime $\mathcal{M}$, for a particle species with mass m we define the mass-shell, mass-bundle or 1-particle phase space as the part of tangent space given by

$$P_m \equiv \{(x,p) \in T\mathcal{M} \mid g_{\mu\nu}(x)p^\mu p^\nu = -m^2\} \ . \tag{3.2}$$

This is a seven-dimensional subspace of the tangent space $T\mathcal{M}$. A (three-dimensional) 'fibre' of the mass-bundle at a fixed event $x \in \mathcal{M}$ is defined by

$$P_m(x) \equiv \{p \in T_x\mathcal{M} \mid g_{\mu\nu}(x)p^\mu p^\nu = -m^2\} \ . \tag{3.3}$$

Here $T_x\mathcal{M}$ is the tangent space of $\mathcal{M}$ at point $x \in \mathcal{M}$. The 1-particle distribution function is defined on P_m,

$$f : P_m \to \mathbb{R} : (x,p) \mapsto f(x,p) \ . \tag{3.4}$$

The distribution function is non-negative and represents the phase-space density of particles with respect to the invariant measure $d\mu = 2\delta(p^2+m^2)|g|\, d^4p\, d^4x$. Here g is the determinant of the metric and $p^2 = g_{\mu\nu}\tilde{p}^\mu\tilde{p}^\nu$. The factor 2 is a convention which we adopt here for convenience. We have chosen the coordinate basis $\partial_\mu = \partial/\partial x^\mu$ in tangent space, so that $p = \tilde{p}^\mu\partial_\mu$. We integrate over p^0 to get rid of the Dirac-δ. This yields the measure $d\mu$ on phase space in terms of the phase space coordinates $(\tilde{p}^i, x^\mu)$,

$$d\mu_m = \frac{|g(x)|}{|\tilde{p}_0(x,\tilde{\mathbf{p}})|}\, d^4x\, d^3\tilde{p} = \sqrt{|g(x)|}d\pi_m\, d^4x \ , \quad \text{where} \tag{3.5}$$

$$d\pi_m = \frac{\sqrt{|g(x)|}}{|\tilde{p}_0(x,\tilde{\mathbf{p}})|}\, d^3\tilde{p} \ . \tag{3.6}$$

Here $\tilde{\mathbf{p}} = (\tilde{p}^1,\tilde{p}^2,\tilde{p}^3)$ and $x = (x^0,x^1,x^2,x^3)$; $\tilde{p}_0 = g_{0\mu}\tilde{p}^\mu$ is determined as a function of $(x,\tilde{\mathbf{p}})$ via the mass-shell condition, $p^2 = -m^2$. The measure $\sqrt{|g(x)|}\, d^4x$ is the usual invariant measure on $\mathcal{M}$. Therefore densities on spacetime are obtained by integrating over the momenta with the measure $d\pi_m$. For example the particle flux density is given by

$$n^\mu(x) = \int_{P_m(x)} \frac{\sqrt{|g(x)|}}{|\tilde{p}_0(x,\tilde{\mathbf{p}})|}\frac{\tilde{p}^\mu}{\tilde{p}^0} f(x,\tilde{\mathbf{p}})\, d^3\tilde{p} \ . \tag{3.7}$$

More importantly, the energy–momentum tensor is given by

$$T^{\mu\nu}(x) = \int_{P_m(x)} \frac{\sqrt{|g(x)|}}{|\tilde{p}_0(x,\tilde{\mathbf{p}})|}\tilde{p}^\mu\tilde{p}^\nu f(x,\tilde{\mathbf{p}})\, d^3\tilde{p} \ . \tag{3.8}$$

If the particles are non-interacting, they move along geodesics,

$$\ddot{x}^\mu + \Gamma^\mu_{\nu\alpha}\dot{x}^\nu\dot{x}^\alpha = 0 \ . \tag{3.9}$$

Here the dot denotes the derivative with respect to proper time s defined by the condition $g_{\mu\nu}(x)\dot{x}^\mu\dot{x}^\nu = \dot{x}^2 = -1$. In the case of massless (light-like) particles, the arc length cannot be defined. In this case the dot can be the derivative with respect to some arbitrary affine parameter. The geodesic equation (3.9) for massless particles, $\dot{x}^2 = 0$, is invariant under affine reparametrizations, $s \to As + B$, where A and B are constants.

Equation (3.9) is obtained as the Euler–Lagrange equation of the Lagrangian

$$\mathcal{L}(x,\dot{x}) = \frac{m}{2} g_{\mu\nu}(x)\dot{x}^\mu\dot{x}^\nu \ .$$

For massive particles m denotes the mass, for massless particles it is an arbitrary non-vanishing constant normally set to one. The canonical momentum is then given by

$$\tilde{p}_\mu = \frac{\partial\mathcal{L}}{\partial\dot{x}^\mu} = m\dot{x}_\mu \quad \text{and} \quad \tilde{p}^\mu = m\dot{x}^\mu \ .$$

From the geodesic equation (3.9) we therefore have

$$m\dot{\tilde{p}}^\mu = -\Gamma^\mu_{\nu\alpha}\tilde{p}^\alpha\tilde{p}^\nu \ .$$

If there are no collisions, i.e. no interactions other than gravity, the distribution function remains constant in a 'comoving' volume element of phase space. Therefore

$$\frac{d}{ds}f = \left[\dot{x}^\mu\partial_\mu + \dot{\tilde{p}}^i\frac{\partial}{\partial\tilde{p}^i}\right]f = 0 \ , \tag{3.10}$$

$$\leftrightarrow \qquad \left[\tilde{p}^\mu\partial_\mu - \Gamma^i_{\mu\nu}\tilde{p}^\mu\tilde{p}^\nu\frac{\partial}{\partial\tilde{p}^i}\right]f = 0 \ . \tag{3.11}$$

This is the Liouville equation for collisionless particles. If collisions cannot be neglected, we have to replace the right-hand side by a collision term. Since collisions involve more than one particle, in principle the collision term depends on the 2- or even 3- and 4-particle distribution functions. To continue, one then has to derive an equation of motion for the 2-particle distribution function and so forth. This leads to the well known BBGKY (Bogoliubov–Born–Green–Kirkwood–Yvon) hierarchy of equations. Often, if the particles are sufficiently diluted, the 2-particle distribution function can be approximated by the product of the 1-particle distribution functions,

$$f_2(x, y, \mathbf{p}_x, \mathbf{p}_y) \simeq f(x, \mathbf{p}_x)f(y, \mathbf{p}_y) \ . \tag{3.12}$$

This corresponds to the assumption that the particle positions in phase space are uncorrelated and is called 'molecular chaos'. In this case, the collision term becomes an integral over the momentum of the colliding particle and we obtain the Boltzmann equation,

$$\left[\tilde{p}^\mu\partial_\mu - \Gamma^i_{\mu\nu}\tilde{p}^\mu\tilde{p}^\nu\frac{\partial}{\partial\tilde{p}^i}\right]f = C[f] \ . \tag{3.13}$$

The collision integral $C[f]$ depends on the details of the interactions. We will calculate it for Thomson scattering of electrons and photons.

What we have discussed so far remains valid in the context of general relativity under some conditions on the number of collisions within a small volume which have to be satisfied in order for a coordinate-independent collision integral to exist [24].

In the kinetic approach it is often very useful to use a tetrad basis of vector fields, $e_\mu(x) = e^\nu_\mu\partial_\nu$ with $g(e_\mu, e_\nu) = g_{\alpha\beta}e^\alpha_\mu e^\beta_\nu = \eta_{\mu\nu}$. Here $\eta_{\mu\nu}$ denotes the flat Minkowski metric. With respect to such an orthonormal basis, $p = p^\mu e_\mu$ we have $|p_0| = |p^0| = \sqrt{m^2 - \mathbf{p}^2}$, where $\mathbf{p}^2 = \sum_{i=1}^3 (p^i)^2$, and $d\pi_m = d^3p/|p^0|$, as in flat Minkowski spacetime. This can also be written as

$$\eta_{\mu\nu}p^\mu p^\nu = g_{\mu\nu}\tilde{p}^\mu\tilde{p}^\nu \ .$$

3.1.2 Liouville's equation in a FL universe

We now want to discuss the Liouville equation in a FL universe. We choose the tetrad basis (orthonormal basis of four vector fields)

$$e_0 = a^{-1}\partial_t \quad \text{and} \quad e_i = a^{-1}\partial_i \ , \tag{3.14}$$

The expression for the energy–momentum tensor (with respect to the usual coordinate basis ∂_μ) in a Friedmann universe becomes

$$T^{\mu\nu}(x) = a^4 \int_{P_m(x)} \frac{1}{|\tilde{p}_0|} \tilde{p}^\mu \tilde{p}^\nu f(x, \tilde{\mathbf{p}})\, d^3\tilde{p} \ , \tag{3.15}$$

where we have used $|g| = a^8$.

The Liouville equation in a Friedmann universe in terms of the coordinates $(x^\mu, \tilde{p}^i)$, is given by

$$\tilde{p}^\mu \partial_\mu f|_{\tilde{p}} - \Gamma^i_{\mu\nu} \tilde{p}^\mu \tilde{p}^\nu \frac{\partial f}{\partial \tilde{p}^i} = 0 \ . \tag{3.16}$$

Here we write $\partial_\mu f|_{\tilde{p}}$ in order to indicate that the components $\tilde{p}^i$ are fixed when the derivative w.r.t. x^μ is taken. Next we transform Eq. (3.16) into an equation for f with respect to the new coordinates (x^μ, p^i), i.e. we consider f as a function of (x^μ, p^i). Since the FL universe is isotropic, f depends on the momentum only via[1] $p = \sqrt{\delta_{ij} p^i p^j} = \sqrt{a^2 \delta_{ij} \tilde{p}^i \tilde{p}^j} = a\tilde{p}$. The derivative of the distribution function with respect to t depends on the momentum variable which we keep constant when performing this derivative. We denote by $\partial_\mu f|_p$ the derivative w.r.t. x^μ while keeping constant the momentum components p^i and $\partial_\mu f|_{\tilde{p}}$ the derivative w.r.t. x^μ while keeping constant the momentum components $\tilde{p}^i$. Inserting the Christoffel symbols of the FL universe (see Appendix A.3) $\Gamma^i_{0j} = \Gamma^i_{j0} = \mathcal{H}\delta^i_j$, we find

$$p^\mu \partial_\mu f|_p - \mathcal{H} p^0 p \frac{\partial f}{\partial p} = 0 \ . \tag{3.17}$$

Or, setting $v = ap$ so that $\partial_0 f|_v = \partial_0 f|_p - \mathcal{H}p(\partial f/\partial p)$ and interpreting f as a function of (t, v), we obtain simply

$$\partial_0 f(t, v) = 0 \ . \tag{3.18}$$

The Liouville equation in a FL universe therefore just requires that the distribution function of collisionless particles changes in time only by redshifting of the physical momentum p and therefore is simply a function of the redshift corrected momentum $v = ap$. Normally we shall use the same letter f for $f(t, p)$ and $f(v)$.

We now derive the linear perturbation of Liouville's equation for scalar perturbations in the longitudinal gauge. The perturbed metric is given by

$$ds^2 = -a^2(1 + 2\Psi)\, dt^2 + a^2(1 - 2\Phi)\gamma_{ij}\, dx^i\, dx^j \ . \tag{3.19}$$

The perturbed distribution function is $f = \bar{f}(v) + F^{(S)}(x^\mu, v, \theta, \phi)$, where (θ, ϕ) define the direction of the momentum $\mathbf{p}$. Liouville's equation now becomes, to first order, in the perturbations

$$\tilde{p}^\mu \partial_\mu f - \bar{\Gamma}^i_{\mu\nu} \tilde{p}^\mu \tilde{p}^\nu \frac{\partial f}{\partial \tilde{p}^i} - \delta\Gamma^i_{\mu\nu} \tilde{p}^\mu \tilde{p}^\nu \frac{\partial \bar{f}}{\partial \tilde{p}^i} = 0 \ , \tag{3.20}$$

[1] Here we use p to denote the absolute value of the physical momentum while before we used it to denote the 4-vector p. Since these are very different objects we hope that there is no danger of confusion.

where the perturbations of the Christoffel symbols are given in Appendix A.4, Eqs. (A.44)–(A.47). We We again use a tetrad basis which is now given by

$$e_0 = a^{-1}(1-\Psi)\partial_t \quad \text{and} \quad e_i = a^{-1}(1+\Phi)\partial_i \ . \tag{3.21}$$

We want to transform Eq. (3.20) to the coordinates (x^μ, p^i) with $p^\mu e_\mu = \tilde{p}^\mu \partial_\mu$. So that

$$p^0 = a(1+\Psi)\tilde{p}^0 \quad \text{and} \quad p^i = a(1-\Phi)\tilde{p}^i \ . \tag{3.22}$$

For the transformation we use the derivatives

$$\begin{aligned}
\partial_0 p^i|_{\tilde{p}} &= \left[\mathcal{H}(1-\Phi) - \dot{\Phi}\right] a\tilde{p}^i \quad \text{so that ,} \\
\partial_0 f|_{\tilde{p}} &= \partial_0 f|_p + [\mathcal{H}(1-\Phi) - \dot{\Phi}] a\tilde{p}^i \frac{\partial f}{\partial p^i} \ , \\
\partial_0 f|_{\tilde{p}} &= \partial_0 f|_p + [\mathcal{H} - \dot{\Phi}] p \frac{\partial f}{\partial p} \ , \qquad (3.23) \\
\tilde{p}^j \partial_j f|_{\tilde{p}} &= \tilde{p}^j \partial_j f|_p - \tilde{p}^j \partial_j \Phi p \frac{\partial \bar{f}}{\partial p}. \qquad (3.24)
\end{aligned}$$

As in the previous section, we indicate the momentum variable kept constant. With the help of the Liouville equation for $\bar{f}$, we then find

$$\begin{aligned}
&\tilde{p}^\mu \partial_\mu F^{(S)}\Big|_p - \mathcal{H}\tilde{p}^0 p \frac{\partial F^{(S)}}{\partial p} \\
&\quad = a^{-1} v \frac{d\bar{f}}{dv}[p^i \partial_i \Phi + p^0 \dot{\Phi}] + a^{-1}\delta\Gamma^i_{\mu\nu} p^\mu p^\nu \frac{\partial \bar{f}}{\partial p^i} \ .
\end{aligned} \tag{3.25}$$

Inserting the perturbation of the Christoffel symbols (Eqs. (A.44)–(A.47) of Appendix A.4), the right-hand side becomes

$$a^{-1} v \frac{d\bar{f}}{dv}\left[-p^0\dot{\Phi} + \frac{(\tilde{p}^0)^2}{\tilde{p}^2} p^k \partial_k \Psi\right] \ ,$$

where $\tilde{p}^2 = \sum_k (\tilde{p}^k)^2$ and we have used $p^i(\partial\bar{f}/\partial p^i) = v(d\bar{f}/dv)$.

We now rewrite the Liouville equation in terms of a new variable defined by $\mathcal{F} = F^{(S)} + \Phi v(d\bar{f}/dv)$. In some of the literature (Hu & Sugiyama, 1995 [26]; Hu & White, 1997 [27]) the variable $F^{(S)}$ is used directly. Note, however, that $\mathcal{F}$ and $F^{(S)}$ only differ by an isotropic (direction-independent) term. Hence, once we determine the CMB anisotropies this difference will only be present in the unmeasurable monopole term. The advantage of the variable $\mathcal{F}$ will become clear later.

Setting $\tilde{p}^j = \tilde{p} n^j$ with $1 = \delta_{ij} n^i n^j$ we have to lowest order, $\tilde{p} = p/a = v/a^2$. Defining also

$$q = a^2 \tilde{p}^0 = a\omega = a\sqrt{p^2 + m^2} = \sqrt{v^2 + a^2 m^2} \ , \tag{3.26}$$

we can rewrite the Liouville equation for the function $\mathcal{F}(t, \mathbf{x}, v, \mathbf{n})$ in the form

$$\boxed{q\partial_0 \mathcal{F} + v n^i \partial_j \mathcal{F} = n^i \partial_i \left[q^2 \Psi + v^2 \Phi\right] \frac{d\bar{f}}{dv} \ .} \tag{3.27}$$

Here $v^j = ap^j$ are the redshift corrected physical momentum components and $\mathcal{F}$ is understood as a function of the variables x^μ and $v^j \equiv vn^j$. Since $\mathcal{F}$ and Φ , Ψ are already perturbations, we can use the background relations between $\mathbf{p}$ and $\mathbf{v}$ as well as q.

This is the Liouville equation for collisionless (massive) particles. The equation can be simplified in the massless case where $q = v$, which is relevant for the study of photons.

3.1.3 The Liouville equation for massless particles

The Liouville equation derived in the previous section is actually more important for massive collisionless particles, e.g., massive neutrinos, than for massless particles. In the massless (or ultra-relativistic) case we have $q = v$ and the equations simplify significantly. Let us also introduce the 'longitudinal temperature fluctuation' for a thermal bath of massless particles. 'Longitudinal' indicates that we consider perturbations in the longitudinal gauge. We integrate the perturbed distribution function over energy so that only the dependence on momentum directions, $\mathbf{n}$, remains,

$$\frac{4\pi}{a^4}\int v^3 f\, dv \equiv \bar\rho\,(1+4\Delta(\mathbf{n}))\ . \tag{3.28}$$

We call the variable $\Delta(\mathbf{n})$ the longitudinal temperature fluctuation in direction $\mathbf{n}$. $\Delta(\mathbf{n})$ depends also on $(t,\mathbf{x})$ which we suppress here for brevity. This definition is motivated by the following consideration: for a Planck distribution of photons which has a slightly direction-dependent temperature, but is otherwise unperturbed (especially, it has a perfect blackbody spectrum, $f_B(p,T) = (\exp(p/T)+1)^{-1}$), the perturbed distribution function can be expanded to first order as

$$f(p,\mathbf{n}) = f_B(p,T(\mathbf{n})) = f_B(p,\bar T) - \frac{\delta T}{\bar T}p\partial_p f_B(p,\bar T)\ . \tag{3.29}$$

Observe that f_B is purely a function of p/T so that $\partial_T f_B = -(p/T)\partial_p f_B$. The energy density of this photon distribution is given by

$$\begin{aligned}\rho_\gamma &= \frac{1}{a^4}\int v^3 f(v,\mathbf{n})\, dv\, d\Omega_{\mathbf{n}} = \bar\rho_\gamma - \frac{1}{a^4}\int \frac{\delta T}{\bar T}v^4\partial_v f_B(v,\bar T)\, dv\, d\Omega_{\mathbf{n}}\\ &= \bar\rho_\gamma\left(1+\frac{4}{4\pi}\int\frac{\delta T}{\bar T}d\Omega_{\mathbf{n}}\right) = \bar\rho_\gamma\left(1+\frac{1}{\pi}\int\Delta(\mathbf{n})\, d\Omega_{\mathbf{n}}\right)\ .\end{aligned} \tag{3.30}$$

For the third equals sign we have performed an integration by parts to evaluate the integral over v. We shall see that the Liouville equation for photons leads to a perturbation which can be described entirely by such a direction-dependent temperature fluctuation.

The fact that the perturbation of the photon distribution can be described in such a simple way is not surprising. It is an expression of the 'a-chromaticy' of gravity which is a consequence of the equivalence principle: the deflection and redshift of a photon in a gravitational field are independent of its energy.

As before, we study only scalar perturbations. The corresponding expressions for vector and tensor perturbations are found e.g. in [9]. For massless particles, $v = q$, the Liouville equation (3.27) reduces to

$$\partial_0\mathcal{F} + n^i\partial_i\mathcal{F} = n^j\left[\Psi_{,j} + \Phi_{,j}\right]v\frac{d\bar f}{dv}\ . \tag{3.31}$$

We define

$$\mathcal{M}^{(S)}(t,\mathbf{x},\mathbf{n}) = \frac{\pi}{a^4\bar{\rho}}\int v^3\mathcal{F}\,dv\ . \tag{3.32}$$

In terms of the temperature fluctuation $\Delta(\mathbf{n})$ defined in Eq. (3.28) we get

$$\mathcal{M}^{(S)}(\mathbf{n}) = \Delta^{(S)}(\mathbf{n}) - \Phi\ . \tag{3.33}$$

Up to a (irrelevant) monopole contribution, the momentum integrated distribution function $\mathcal{M}$ is simply the temperature perturbation in the longitudinal gauge. It is not surprising that the monopole terms of $\mathcal{M}(\mathbf{n})$ and $\Delta(\mathbf{n})$ do not agree because they are gauge dependent. Also the dipole terms might differ since they too are gauge dependent. (In a gauge with non-vanishing shear, the dipole contributions to Δ and $\mathcal{M}$ do differ.)

Integrating the Liouville equation (3.31) over momenta and performing an integration by parts on the right-hand side, we obtain the evolution equation for $\mathcal{M}$.

For the scalar part of the distribution function we obtain

$$\partial_t\mathcal{M}^{(S)} + n^i\partial_i\mathcal{M}^{(S)} = -n^j\left[\Psi_{,j} + \Phi_{,j}\right]\ . \tag{3.34}$$

This equation can be solved formally for any given source term $\Phi + \Psi$. One easily checks that the solution with initial condition $\mathcal{M}^{(S)}(t_{\rm in},\mathbf{x},\mathbf{n})$ is

$$\begin{aligned}\mathcal{M}^{(S)}(t,\mathbf{x},\mathbf{n}) &= \mathcal{M}^{(S)}\left(t_{\rm in},\mathbf{x}-\mathbf{n}(t-t_{\rm in}),\mathbf{n}\right)\\ &\quad -\int_{t_{\rm in}}^{t} dt'\,n^i\partial_i(\Psi+\Phi)(t',\mathbf{x}-\mathbf{n}(t-t'))\ .\end{aligned} \tag{3.35}$$

Using

$$\begin{aligned}\frac{d}{dt'}(\Psi+\Phi)(t',\mathbf{x}-\mathbf{n}(t-t')) &= \partial_{t'}(\Psi+\Phi)(t',\mathbf{x}-\mathbf{n}(t-t'))\\ &\quad + n^i\partial_i(\Psi+\Phi)(t',\mathbf{x}-\mathbf{n}(t-t'))\ ,\end{aligned}$$

we can replace the second term on the right-hand side to obtain

$$\begin{aligned}\mathcal{M}^{(S)}(t,\mathbf{x},\mathbf{n}) &= \mathcal{M}^{(S)}\left(t_{\rm in},\mathbf{x}-\mathbf{n}(t-t_{\rm in}),\mathbf{n}\right)\\ &\quad +(\Psi+\Phi)(t_{\rm in},\mathbf{x}-\mathbf{n}(t-t_{\rm in}))\\ &\quad +\int dt'\,\partial_{t'}(\Psi+\Phi)(t',\mathbf{x}-\mathbf{n}(t-t'))+\text{monopole}\ .\end{aligned} \tag{3.36}$$

By 'monopole' we denote an uninteresting $\mathbf{n}$-independent contribution which does not affect the CMB anisotropy spectrum. The Bardeen potentials Ψ and Φ, however, are given via Einstein's equation in terms of the perturbations of the energy–momentum tensor which contain contributions from the photons which are in turn the momentum integrals of $\mathcal{M}$ given below. Therefore, even though it might look like it, this is not really a solution of the Liouville equation. The term on the right-hand side also depends on $\mathcal{M}^{(S)}$.

Let us compare Eq. (3.36) with the result from the integration of light-like geodesics after decoupling in Eqs. (2.79) and (2.81). Here we have solved the Liouville equation which also does not take into account the scattering of photons and is therefore equivalent to our approach in Chapter 2. They both

correspond to the 'sudden decoupling' approximation, where we assume that photons behave like a perfect fluid before decoupling and are entirely free after decoupling. This is a relatively good approximation for all scales which are much larger than the duration of the process of recombination which we shall estimate in the next section. The comparison with Eqs. (2.79) and (2.81) yields

$$\mathcal{M}^{(S)}\left(t_{\rm dec}, \mathbf{x}-\mathbf{n}(t-t_{\rm dec}), \mathbf{n}\right) = \left(\frac{1}{4}D_g + \mathbf{n}\cdot\mathbf{V}^{(b)}\right)\left(t_{\rm dec}, \mathbf{x}-\mathbf{n}(t-t_{\rm dec})\right) , \tag{3.37}$$

and

$$\mathcal{M}^{(S)}(t,\mathbf{x},\mathbf{n}) \equiv \frac{\delta T}{T}(t,\mathbf{x},\mathbf{n}) . \tag{3.38}$$

In other words, the temperature fluctuation defined via the energy shift of photons moving along geodesics corresponds to $\mathcal{M}^{(S)}$ while the temperature fluctuation defined via the energy density fluctuation in longitudinal gauge corresponds to $\Delta^{(S)} = \mathcal{M}^{(S)} + \Phi$. In addition to the energy shift, the latter includes a contribution from the perturbation of the volume element, $\sqrt{|\det(g_{ij})|}\, d^3x = a^3(1-3\Phi)\, d^3x$. The distinction is not very important since it is a monopole which does not show up in the angular power spectrum. However, the corresponding evolution equations are of course different.

The initial condition in the sudden decoupling approximation is a distribution function which contains only a monopole and a dipole. Higher multipoles do not build up in a perfect fluid. In the next section we shall take into account the process of decoupling by studying the Boltzmann equation.

The scalar perturbations of the energy–momentum tensor of the radiation fluid for a given Fourier mode $\mathbf{k}$ can be found from (3.15) and the definitions of the corresponging perturbation variables,

$$\begin{aligned} D_g &= 2\int_{-1}^{1} \mathcal{M}^{(S)}(\mu)\, d\mu = 4\mathcal{M}_0^{(S)} , & (3.39)\\ V &= \frac{3i}{2}\int_{-1}^{1} \mu\mathcal{M}^{(S)}(\mu)\, d\mu = 3\mathcal{M}_1^{(S)} , & (3.40)\\ \Gamma &= 0 , & (3.41)\\ \Pi &= 3\int_{-1}^{1} \left(1-3\mu^2\right)\mathcal{M}^{(S)}(\mu)\, d\mu = 12\mathcal{M}_2^{(S)} . & (3.42) \end{aligned}$$

The general definition of $\mathcal{M}_\ell^{(S)}$ will be given below. We have assumed that $\mathcal{M}^{(S)}(t,\mathbf{k},\mathbf{n})$ depends on the direction $\mathbf{n}$ only via $\mu = \hat{\mathbf{k}}\cdot\mathbf{n}$. We have chosen the z-direction proportional to $\mathbf{k}$ so that $\mu = \cos\theta$ and have performed the integration over φ which simply gives a factor 2π. For statistically isotropic perturbations there is no other vector which could single out a direction and therefore this assumption reflects statistical isotropy.

The exact equality $w = c_s^2 = \frac{1}{3}$ does not allow for any entropy perturbation in a pure radiation fluid.

Exercice 10 *Compute D_g and V explicitly from $\mathcal{M}^{(S)}(\mathbf{n})$.*

The Liouville equation in Fourier space

A Fourier mode of $\mathcal{M}(t, \mathbf{x}, \mathbf{n})$ is given by

$$\begin{aligned} \mathcal{M}(t, \mathbf{k}, \mathbf{n}) &\equiv \int d^3x\, e^{-i\mathbf{k}\cdot\mathbf{x}} \mathcal{M}(t, \mathbf{x}, \mathbf{n}) \ , \text{ and its inverse is} \\ \mathcal{M}(t, \mathbf{x}, \mathbf{n}) &= \frac{1}{(2\pi)^3} \int d^3k\, e^{i\mathbf{k}\cdot\mathbf{x}} \mathcal{M}(t, \mathbf{k}, \mathbf{n}) \ . \end{aligned}$$

The Liouville equation for a Fourier mode is given by

$$(\partial_t + ik\mu)\mathcal{M}(t, \mathbf{k}, \mathbf{n}) = S_G(t, \mathbf{k}, \mu) \quad (\equiv -ik\mu(\Phi + \Psi)(t, \mathbf{k}) \ ) \ , \tag{3.43}$$

where $\mu = \hat{\mathbf{k}} \cdot \mathbf{n}$ is the cosine of the angle between the unit vectors $\hat{\mathbf{k}} = \mathbf{k}/k$ and $\mathbf{n}$. While the first equal sign is valid for all types of perturbations, the term in parenthesis gives S_G for scalar perturbations. The general (formal) solution to this equation for a given source term S_G can be written as

$$\mathcal{M}(t, \mathbf{k}, \mathbf{n}) = e^{-ik\mu(t-t_{\rm in})} \mathcal{M}(t_{\rm in}, \mathbf{k}, \mathbf{n}) + \int_{t_{\rm in}}^{t} dt' e^{-ik\mu(t-t')} S_G(t', \mathbf{k}, \mathbf{n}) \ . \tag{3.44}$$

The function S_G can be decomposed into scalar, vector and tensor perturbations.

As already mentioned, the source term usually depends on $\mathcal{M}$ via Einstein's equations and Eq. (3.44) is not really a solution but simply corresponds to rewriting Eq. (3.43) as an integral equation. But as we shall see, this has serious advantages especially for numerical computations.

From Eq. (3.44) using the decomposition [6]

$$e^{i\mathbf{k}\cdot\mathbf{n}(t-t_{\rm in})} = \sum_{\ell=0}^{\infty} (2\ell + 1) i^\ell j_\ell(k(t - t_{\rm in})) P_\ell(\mu) \ ,$$

one finds the CMB power spectrum, exactly as in Eqs. (2.100)–(2.104) and (2.110). Before we do this, we study Thomson scattering which is the relevant scattering process just before recombination. We will then derive the power spectrum taking into account this scattering process.

3.1.4 The Boltzmann equation

At very early times, long before recombination, scattering of photons with free electrons is very frequent. During recombination, however, the number density of free electrons, i.e. of electrons not bound to an atom, drops drastically and soon the mean free path of photons is much larger than the Hubble scale so that, effectively, photons do not scatter any more. In the previous treatment we assumed this process of decoupling to be instantaneous; now we want to reconsider it in more detail.

The only scattering process which is relevant briefly before decoupling, i.e., at temperatures of a few electron volts and less, is elastic Thomson scattering, where the photon energy is conserved and only its direction is modified. The Thomson scattering rate is

$$\Gamma_T = \sigma_T n_e \ ,$$

where $\sigma_T = 6.6524 \times 10^{-25}\,\mathrm{cm}^2$ is the Thomson scattering cross section and n_e is the number density of free electrons.

Before decoupling, in a matter dominated universe, we find

$$\begin{aligned} \Gamma_T &\simeq 7\times 10^{-30}\,\mathrm{cm}^{-1}\Omega_b h^2(1+z)^3 \quad \text{while} \\ H &\simeq 10^{-28}\,\mathrm{cm}^{-1}h(1+z)^{3/2} \\ \Gamma_T/H &\simeq 0.07\Omega_b h(z+1)^{3/2}\ . \end{aligned}$$

Hence before recombination, which corresponds to redshifts $z > 1100$, say, Thomson scattering is much faster than expansion. During recombination, the free electron density drops and eventually the Thomson scattering rate drops below the expansion rate. To take scattering into account we add a so-called 'collision integral' to the right-hand side of the Liouville equation, which leads us to the Boltzmann equation. To learn more about the Boltzmann equation and the approximations going into it see, e.g., [28]. The collision integral $C[f]$ takes into account that the 1-particle distribution function can change due to collisions which scatter a particle into, f_+, or out of, f_-, a volume element $d^3x\,d^3p$ in phase space,

$$\left[\tilde{p}^\mu\partial_\mu - \Gamma^i_{\alpha\beta}\tilde{p}^\alpha\tilde{p}^\beta\frac{\partial}{\partial\tilde{p}^i}\right] f = C[f] = \frac{df_+}{dt} - \frac{df_-}{dt}\ . \tag{3.45}$$

Here f_+ and f_- denote the distribution of photons scattered into and out of the beam of photons at position $\mathbf{x}$ at time t with momentum $\mathbf{p}$ respectively.

This collision term (integrated over photon energies) is calculated in detail in [9] with the result

$$C[\mathcal{M}] = a\sigma_T n_e\left[\frac{1}{4}D_g^{(\gamma)} - \mathcal{M} - n^i V_i^{(b)} + \frac{1}{2}n_{ij}M^{ij}\right]\ , \tag{3.46}$$

where n_e denotes the free electron density. The pre-factor $a\sigma_T n_e$ is very large before recombination and becomes negligibly small after recombination when photons effectively decouple from electrons. Here

$$\begin{aligned} n_{ij} &= n_i n_j - \frac{1}{3}\delta_{ij} \qquad \text{and} \\ M_{ij} &= \frac{3}{8\pi}\int n_{ij}\mathcal{M}(\mathbf{n})d\Omega_{\mathbf{n}}\,. \end{aligned} \tag{3.47}$$

Using (3.43) and (3.46) we can write the formal solution of the Boltzmann equation as

$$\begin{aligned} \mathcal{M}(t,\mathbf{k},\mathbf{n}) &= e^{-ik\mu(t-t_{\rm in})-\kappa(t_{\rm in},t)}\mathcal{M}(t_{\rm in},\mathbf{k},\mathbf{n}) \\ &\quad + \int_{t_{\rm in}}^t dt'\,e^{ik\mu(t'-t)-\kappa(t',t)}\left[S_G(\mathbf{k},\mathbf{n}) + \dot\kappa\left(\frac{1}{4}D_g^{(\gamma)}(\mathbf{k})\right.\right. \\ &\quad \left.\left. - n^i V_i^{(b)}(\mathbf{k}) + \frac{1}{2}n_{ij}M^{ij}(\mathbf{k},\mathbf{n})\right)\right]\ . \end{aligned} \tag{3.48}$$

Here

$$\kappa(t_1,t_2) = \int_{t_1}^{t_2} a\sigma_T n_e\,dt \quad \text{is the optical depth and} \tag{3.49}$$

$$\dot\kappa(t_1,t_2) = \partial_{t_2}\kappa(t_1,t_2) = a\sigma_T n_e(t_2) \tag{3.50}$$

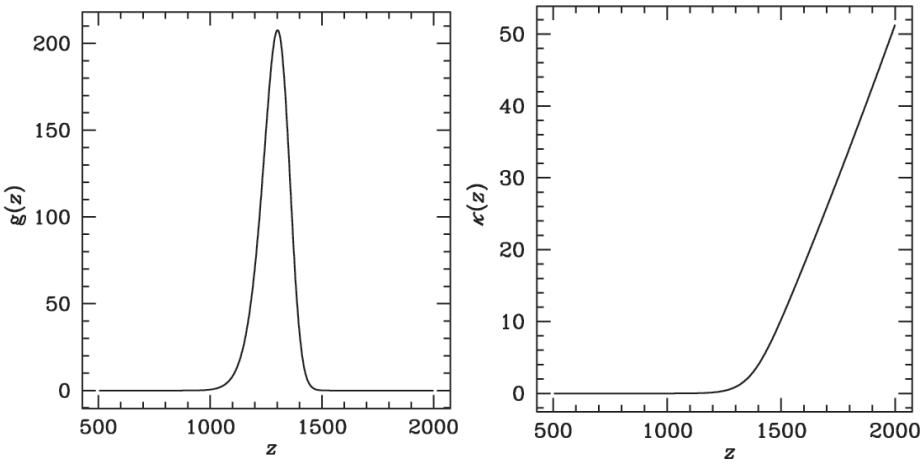

Figure 3.1: The visibility function $g(t) = \partial_t \kappa(t, t_0) \exp(-\kappa(t, t_0)$ (left) is plotted in units of H_0 as a function of redshift. For comparison we show also $\kappa(z) \equiv \kappa(t(z), t_0)$ (right).

is independent of the initial value t_1. In Fig. 3.1 we plot $\kappa(t, t_0)$ as well as the visibility function $g(t) = \partial_t \kappa(t, t_0) \exp(-\kappa(t, t_0)$ as a function of t.

At late time, $z \simeq 6$ the uv radiation from starlight re-ionizes the Universe leading to a slight deviation of $\kappa(t, t_0)$ from zero at low redshift and a slight bump in $g(z)$. But the amplitude of this optical depth due to reonization, called $\tau_{\rm reion}$ is about $\tau_{\rm reion} \sim 0.05$ which is not visible on the scales of Fig. 3.1.

Since the direction dependence enters the evolution equation only via the cosine $\mu = \hat{\mathbf{k}} \cdot \mathbf{n}$, we assume consistently that this is the only direction dependence of the Fourier transform $\mathcal{M}^{(S)}(t, \mathbf{k}, \mathbf{n})$, so that $\mathcal{M}^{(S)}(t, \mathbf{k}, \mathbf{n}) = \mathcal{M}^{(S)}(t, \mathbf{k}, \mu)$. It therefore makes sense to expand $\mathcal{M}^{(S)}$ in Legendre polynomials,

$$\mathcal{M}^{(S)}(t, \mathbf{k}, \mu) = \sum (2\ell + 1)(-i)^\ell \mathcal{M}_\ell^{(S)}(t, \mathbf{k}) P_\ell(\mu) \ . \tag{3.51}$$

Using the orthogonality and normalization of Legendre polynomials, we obtain the expansion coefficients,

$$\mathcal{M}_\ell^{(S)}(t, \mathbf{k}) = \frac{i^\ell}{2} \int_{-1}^{1} d\mu \, \mathcal{M}^{(S)}(t, \mathbf{k}, \mu) P_\ell(\mu) \ . \tag{3.52}$$

Statistical homogeneity and isotropy imply that the coefficients $\mathcal{M}_\ell$ for different values of ℓ and $\mathbf{k}$ are uncorrelated,

$$\left\langle \mathcal{M}_\ell^{(S)}(t, \mathbf{k}) \mathcal{M}_{\ell'}^{(S)*}(t, \mathbf{k}') \right\rangle = M_\ell^{(S)}(t, k)(2\pi)^3 \, \delta^3(\mathbf{k} - \mathbf{k}') \, \delta_{\ell\ell'} \ . \tag{3.53}$$

We want to relate the spectrum $M_\ell^{(S)}(t, k)$ to the scalar CMB power spectrum

$C_\ell^{(S)}$. We use the definition given in Eq. (2.93),

$$\left\langle \frac{\Delta T}{T}(t_0,\mathbf{x}_0,\mathbf{n})\frac{\Delta T}{T}(t_0,\mathbf{x}_0,\mathbf{n}')\right\rangle^{(S)} = \frac{1}{4\pi}\sum_\ell (2\ell+1)C_\ell^{(S)}P_\ell(\mathbf{n}\cdot\mathbf{n}')$$
$$= \frac{1}{(2\pi)^6}\int d^3k\, d^3k' \sum_{\ell_1\ell_2}(2\ell_1+1)(2\ell_2+1)(-i)^{\ell_1-\ell_2}e^{i\mathbf{x}_0\cdot(\mathbf{k}-\mathbf{k}')}$$
$$\times\left\langle \mathcal{M}_{\ell_1}^{(S)}(t_0,\mathbf{k})\mathcal{M}_{\ell_2}^{(S)*}(t_0,\mathbf{k}')\right\rangle P_{\ell_1}(\mu)P_{\ell_2}(\mu')\ ,$$

where $\mu=\hat{\mathbf{k}}\cdot\mathbf{n}$ and $\mu'=\hat{\mathbf{k}}'\cdot\mathbf{n}'$. With Eq. (3.53) we obtain

$$\frac{1}{4\pi}\sum_\ell(2\ell+1)C_\ell^{(S)}P_\ell(\mathbf{n}\cdot\mathbf{n}')$$
$$= \frac{1}{(2\pi)^3}\sum_{\ell_1}\int d^3k\, M_{\ell_1}^{(S)}(t_0,k)(2\ell_1+1)^2P_{\ell_1}(\mu)P_{\ell_1}(\mu')$$
$$= \frac{2}{\pi}\sum_{\ell_1}\int d^3k\, M_{\ell_1}^{(S)}(t_0,k)\sum_{m_1m_2}Y_{\ell_1m_1}(\mathbf{n})Y^*_{\ell_1m_1}(\hat{\mathbf{k}})Y^*_{\ell_1m_2}(\mathbf{n}')Y_{\ell_1m_2}(\hat{\mathbf{k}})$$
$$= \frac{2}{\pi}\sum_{\ell_1m_1}\int dk\, k^2M_{\ell_1}^{(S)}(t_0,k)Y_{\ell_1m_1}(\mathbf{n})Y^*_{\ell_1m_1}(\mathbf{n}')$$
$$= \frac{1}{2\pi^2}\sum_{\ell_1}\left(\int dk\, k^2M_{\ell_1}^{(S)}(t_0,k)\right)(2\ell_1+1)P_\ell(\mathbf{n}\cdot\mathbf{n}')\ .$$

In several steps in this derivation we have applied the addition theorem of spherical harmonics. Comparing the first and the last expressions in the series of equalities above, we infer

$$C_\ell^{(S)} = \frac{2}{\pi}\int dk\, k^2M_\ell^{(S)}(k)\ . \tag{3.54}$$

To calculate the CMB power spectrum, we therefore have to determine the random variables $\mathcal{M}_\ell$. We now derive a hierarchical set of equations for them, the so-called Boltzmann hierarchy.

With Eqs. (3.39)–(3.42), Eq. (3.52) and the explicit expressions of the Legendre polynomials for $\ell\le 2$, one finds the relations of the scalar perturbations of the photon energy–momentum tensor to the expansion coefficients $\mathcal{M}_\ell(t,\mathbf{k}),\ \ell\le 2$,

$$D_g^{(\gamma)} = 4\mathcal{M}_0^{(S)}\ , \tag{3.55}$$
$$V_\gamma^{(S)} = 3\mathcal{M}_1^{(S)}\ , \tag{3.56}$$
$$\Pi_\gamma^{(S)} = 12\mathcal{M}_2^{(S)}. \tag{3.57}$$

Exercice 11 *Using the explicit expressions of the Legendre polynomials for $\ell\le 2$,derive eqs. (3.55) to (3.57).*

Inserting Eq. (3.51) in the definition of M_{ij} and choosing the coordinate system such that $\mathbf{k}$ points in the z direction one can easily compute the integrals

$M_{33} = -\mathcal{M}_2^{(S)}$ and $M_{11} = M_{22} = \mathcal{M}_2^{(S)}/2$ and all off diagonal contributions vanish. With $n_1^2 + n_2^2 = 1 - \mu^2$ this yields

$$\frac{1}{2} n_{ij} M^{ij} = -\frac{1}{2} \mathcal{M}_2^{(S)} P_2(\mu) \ .$$

Also using the fact that for scalar perturbations $\mathbf{V} = i\hat{\mathbf{k}} V$ we obtain the scalar Boltzmann equation

$$\begin{aligned} (\partial_t + ik\mu)\, \mathcal{M}^{(S)}(\mathbf{k}, \mathbf{n}) &= ik\mu(\Phi + \Psi) \\ &\quad + \dot{\kappa} \left[\frac{1}{4} D_g^{(\gamma)}(\mathbf{k}) - \mathcal{M}^{(S)} - i\mu V^{(b)}(\mathbf{k}) - \frac{1}{2} \mathcal{M}_2(\mathbf{k}) P_2(\mu) \right] . \end{aligned} \tag{3.58}$$

With the recurrence relation (see [6])

$$\mu P_\ell(\mu) = \frac{\ell + 1}{2\ell + 1} P_{\ell+1}(\mu) + \frac{\ell}{2\ell + 1} P_{\ell-1}(\mu) \ ,$$

we can convert Eq. (3.58) into the following hierarchy of equations

$$\begin{aligned} &\dot{\mathcal{M}}_\ell^{(S)} + k \frac{\ell + 1}{2\ell + 1} \mathcal{M}_{\ell+1}^{(S)} - k \frac{\ell}{2\ell + 1} \mathcal{M}_{\ell-1}^{(S)} + \dot{\kappa} \mathcal{M}_\ell^{(S)} \\ &\quad = \delta_{\ell 0} \dot{\kappa} \mathcal{M}_0^{(S)} + \frac{1}{3} \delta_{\ell 1} \left[-k(\Phi + \Psi) + \dot{\kappa} V^{(b)} \right] + \dot{\kappa} \frac{1}{10} \delta_{\ell 2} \mathcal{M}_2^{(S)} . \end{aligned} \tag{3.59}$$

Here the source terms on the right-hand side contribute only for $\ell = 0, 1$ and $\ell = 2$ respectively. In Eq. (3.59) each variable $\mathcal{M}_\ell^{(S)}$ couples to its neighbours, $\mathcal{M}_{\ell-1}^{(S)}$ and $\mathcal{M}_{\ell+1}^{(S)}$ via the left-hand side. From Eq. (3.58) it is clear, that the left-hand side actually just describes the free streaming of photons after decoupling.

If we want to determine the CMB power spectrum via the Boltzmann hierarchy, Eq. (3.59), in order to calculate, e.g., C_{1000} we have to know all the other $\mathcal{M}_\ell^{(S)}$s which may influence $\mathcal{M}_{1000}^{(S)}$ via free streaming during a Hubble time, which is certainly more than 1000. Furthermore, at the beginning, when coupling is still relatively tight, we may simply take into account $\mathcal{M}_0^{(S)}$ and $\mathcal{M}_1^{(S)}$ given by the perfect fluid initial conditions and set all the other $\mathcal{M}_\ell^{(S)}$s to zero. They then gradually build up mainly due to free streaming. But using the Boltzmann hierarchy (3.59), we cannot calculate $\mathcal{M}_{1000}^{(S)}$ with any accuracy if we have not determined all the $\mathcal{M}_\ell^{(S)}$s with $\ell < 1000$ with the same (or rather better) accuracy.

On the other hand, if we knew the source term, the right-hand side of Eq. (3.59), we could simply write down the solution, Eq. (3.48). As the source term only depends on the first two moments of the hierarchy, it can usually be obtained with a precision of about 0.1%, see [29], by solving the hierarchy only up to $\ell \simeq 10$. Inserting the corresponding moments into Eq. (3.48) one finds

$$\begin{aligned} \mathcal{M}^{(S)}(t_0, \mathbf{k}, \mu) &= e^{-ik\mu(t_0 - t_{\rm in}) - \kappa(t_{\rm in}, t_0)} \mathcal{M}^{(S)}(t_{\rm in}, \mathbf{k}, \mu) \\ &\quad + \int_{t_{\rm in}}^{t_0} dt\, e^{ik\mu(t - t_0) - \kappa(t, t_0)} \times \left[ik\mu(\Phi + \Psi)(\mathbf{k}) + \dot{\kappa} \left(\frac{1}{4} D_g^{(\gamma)}(\mathbf{k}) \right. \right. \\ &\quad \left. \left. - i\mu V^{(b)}(\mathbf{k}) - \frac{1}{2} P_2(\mu) \mathcal{M}_2^{(S)}(\mathbf{k}, t) \right) \right] . \end{aligned}$$

If the only μ-dependent term was the exponential, we could use its representation in terms of Legendre polynomials and spherical Bessel functions (see [6]) to isolate $\mathcal{M}_\ell^{(S)}$. With this in mind, we use

$$e^{ik\mu(t-t_0)}\mu f(t) = -ik^{-1}\partial_t\left(e^{ik\mu(t-t_0)}\right) f(t) \ ,$$

to get rid of all the μ-dependence in the term in square brackets above. Furthermore, we move the derivative $\partial_{t'}$ onto the function f via integration by parts. We want to choose the initial time $t_{\rm in}$ long before decoupling and t_0 denotes today. Therefore, $\kappa(t_{\rm in}, t_0)$ is huge and we can completely neglect the term from the initial condition. Since early times do not contribute, we can formally start the integral at $t_{\rm in} = 0$. We can also neglect the boundary terms at t_0 since the terms from $t' = t_0$ contribute only to the uninteresting monopole and dipole terms.

Let us introduce the visibility function g, defined by

$$g(t) \equiv (a\sigma_T n_e)(t)e^{-\kappa(t,t_0)} \equiv \partial_t\kappa(t,t_0)e^{-\kappa(t,t_0)} \ . \tag{3.60}$$

This function is very small at early times, when the optical depth, κ is very large. During decoupling, κ becomes smaller but also the pre-factor, $a\sigma_T n_e = \dot\kappa$ then becomes small. Therefore, g is strongly peaked during decoupling and small both before and after, see Fig. 3.1. With the above mentioned integration by parts we then find

$$\mathcal{M}^{(S)}(t_0, \mathbf{k}, \mu) = \int_0^{t_0} dt\, e^{ik\mu(t-t_0)} S^{(S)}(t, \mathbf{k}) \ , \tag{3.61}$$

with

$$\begin{aligned} S^{(S)} \ &= \ -e^{-\kappa}(\dot\Phi + \dot\Psi) + g\left(\Phi + \Psi + k^{-1}\dot V^{(b)} + \frac{1}{4}D_g^{(\gamma)} + \frac{1}{4}\mathcal{M}_2\right) \\ &\quad + k^{-1}\dot g V^{(b)} - \frac{3}{4k^2}\frac{d^2}{dt^2}\left(g\mathcal{M}_2^{(S)}\right) \ . \end{aligned} \tag{3.62}$$

This source term now no longer depends on μ. Rewriting the exponential in terms of Legendre polynomials and spherical Bessel functions, we now obtain simply

$$\mathcal{M}_\ell^{(S)}(t_0, \mathbf{k}) = \int_0^{t_0} dt\, j_\ell(k(t_0 - t)) S^{(S)}(t, \mathbf{k}) \ . \tag{3.63}$$

Together with Eqs. (3.53) and (3.54) this yields the scalar contributions to the CMB power spectrum, once the scalar source term is given.

So far, we still have neglected the effect of polarization which introduces considerable additional complications. We shall discuss it in the next section.

The source term contains Φ and Ψ which we obtain from the Einstein equations where $\mathcal{M}_0$, $\mathcal{M}_1$ and $\mathcal{M}_2$ enter on the right hand side. For a numerical calculation of the CMB anisotropy power spectrum, this method has become the method of choice: first, the source term is calculated via the Boltzmann hierarchy truncated at about $\ell = 10$. Then, the C_ℓs are computed via the line-of-sight integral (3.63) followed by integration over k, Eq. (3.54). Free streaming is now taken care of by the spherical Bessel functions which can be computed

just once and then be stored. This is especially useful if one wants to compute many models for cosmological parameter estimation employing a Monte Carlo method, see [9], Chapter 9.

The C_ℓ spectrum for tensor perturbations is derived in a similar matter, see [9] for details.

3.2 Polarisation

The Thomson scattering cross section depends on the polarization of the outgoing photon. If its polarization vector lies in the scattering plane, the cross section is proportional to $\cos^2\beta$, where β denotes the scattering angle. If, however, the outgoing photon is polarized normal to the scattering plane, no such reduction by a factor $\cos^2\beta$ occurs (see [30], Section 14.7). If photons come in isotropically from all directions, this does not lead to any net polarization of the outgoing radiation. However, if, for a fixed outgoing direction, the intensity of incoming photons from one direction is different from the intensity of photons coming in at a right angle with respect to the first direction and with respect to the direction of the outgoing photon, see Fig. 3.2, this anisotropy leads to some polarization of the outgoing photon beam. As is clear from the figure, it is the quadrupole anisotropy in the reference frame of the scattering electron which is responsible for polarization.

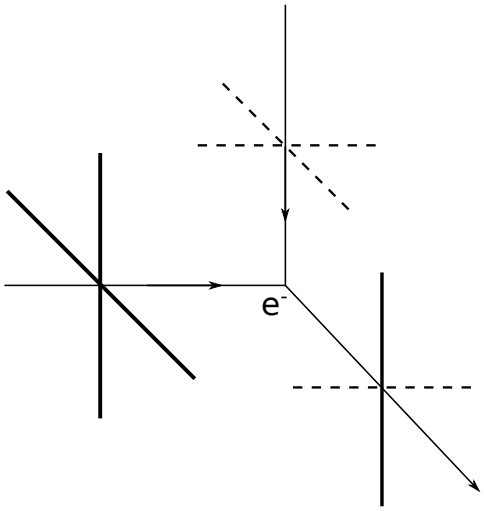

Figure 3.2: More incoming photons from the left than from the top (indicated in the figure with longer polarization directions), lead to a net polarization of the outgoing photon beam. In the situation shown above, where the scattering angle is $\pi/2$, the photons coming in from the left are scattered only if polarized vertically, while the photons coming in from the top are scattered only if polarized horizontally. In this way, an unpolarized photon distribution which exhibits a quadrupole anisotropy generates polarization on the surface of last scattering.

We consider an electromagnetic wave propagating in direction $\mathbf{n}$. We define the polarization directions $\boldsymbol{\epsilon}^{(1)}$ and $\boldsymbol{\epsilon}^{(2)}$ such that $\left(\boldsymbol{\epsilon}^{(1)},\ \boldsymbol{\epsilon}^{(2)},\ \mathbf{n}\right)$ form a right-handed orthonormal system. The electric field of the wave is of the form $\mathbf{E} = E_1\boldsymbol{\epsilon}^{(1)} + E_2\boldsymbol{\epsilon}^{(2)}$. (The polarizations $\boldsymbol{\epsilon}^{(1)}$ and $\boldsymbol{\epsilon}^{(2)}$ are not to be confused with $\mathbf{e}^{(1)}$ and $\mathbf{e}^{(2)}$ which form an orthonormal system with the wave vector $\mathbf{k}$.) The polarization tensor of an electromagnetic wave is defined as

$$P_{ij} = \widetilde{\mathcal{P}}_{ab}\boldsymbol{\epsilon}_i^{(a)}\boldsymbol{\epsilon}_j^{(b)}\ , \quad \text{with} \quad \widetilde{\mathcal{P}}_{ab} = E_a^* E_b\ . \tag{3.64}$$

$\widetilde{\mathcal{P}}_{ab}$ is a hermitian 2×2 matrix and can therefore be written as

$$\begin{aligned}\widetilde{\mathcal{P}}_{ab} &= \frac{1}{2}\left[I\sigma_{ab}^{(0)} + U\sigma_{ab}^{(1)} + V\sigma_{ab}^{(2)} + Q\sigma_{ab}^{(3)}\right] \\ &= \frac{1}{2}I\sigma_{ab}^{(0)} + \mathcal{P}_{ab}\ ,\end{aligned} \tag{3.65}$$

where $\sigma^{(\alpha)}$ denote the Pauli matrices and the four real functions of the photon direction $\mathbf{n}$, I, U, V and Q are the Stokes parameters.

$$\begin{aligned}\sigma^{(0)} &= \begin{pmatrix} 1 & 0 \\ 0 & 1 \end{pmatrix}\ , \qquad \sigma^{(1)} = \begin{pmatrix} 0 & 1 \\ 1 & 0 \end{pmatrix}\ , \\ \sigma^{(2)} &= \begin{pmatrix} 0 & -i \\ i & 0 \end{pmatrix}\ , \qquad \sigma^{(3)} = \begin{pmatrix} 1 & 0 \\ 0 & -1 \end{pmatrix}\ .\end{aligned} \tag{3.66}$$

In terms of the electric field, the Stokes parameters are

$$\begin{aligned} I &= |E_1|^2 + |E_2|^2\ , \quad Q = |E_1|^2 - |E_2|^2\ , \\ U &= (E_1^*E_2 + E_2^*E_1) = 2\mathrm{Re}(E_1^*E_2)\ , \quad V = 2\mathrm{Im}(E_1^*E_2)\ .\end{aligned} \tag{3.67}$$

I is simply the intensity of the electromagnetic wave. Q represents the amount of linear polarization in directions $\boldsymbol{\epsilon}^{(1)}$ and $\boldsymbol{\epsilon}^{(2)}$, i.e., Q is the difference between the intensity of radiation polarized along $\boldsymbol{\epsilon}^{(1)}$ minus the intensity polarized in direction $\boldsymbol{\epsilon}^{(2)}$. The parameters Q and U describe the symmetric traceless part of the polarization tensor while V multiplies the anti-symmetric Pauli matrix $\sigma^{(2)}$. This part describes a phase difference between E_1 and E_2 which results in circular polarization. This is best seen by expressing $\mathcal{P}_{ab}$ in terms of the helicity basis $\boldsymbol{\epsilon}^{(\pm)} = (1/\sqrt{2})\left(\boldsymbol{\epsilon}^{(1)} \pm i\boldsymbol{\epsilon}^{(2)}\right)$, where one finds that V is the difference between the left- and right-handed circular polarized intensities (for details see e.g. [30]). As we shall see below, Thomson scattering does not introduce circular polarization. We therefore expect the V-Stokes parameter of the CMB radiation to vanish. We neglect it in the following discussion. If $V = 0$, we have $\mathcal{P}_{ab} = \mathcal{P}_{ab}^* = \mathcal{P}_{ba}$. Hence $\mathcal{P}_{ab}$ is a real symmetric matrix.

We often also use the quantities

$$P \equiv \mathcal{P}_{++} = 2\mathcal{P}^{ab}\boldsymbol{\epsilon}_a^{(+)}\boldsymbol{\epsilon}_b^{(+)} = Q + iU, \quad \text{and} \tag{3.68}$$

$$\bar{P} \equiv \mathcal{P}_{--} = 2\mathcal{P}^{ab}\bar{\boldsymbol{\epsilon}}_a^{(+)}\bar{\boldsymbol{\epsilon}}_b^{(+)} = 2\mathcal{P}^{ab}\boldsymbol{\epsilon}_a^{(-)}\boldsymbol{\epsilon}_b^{(-)} = Q - iU\ . \tag{3.69}$$

Up to a factor of 2, these are the components of the polarization tensor expressed in the helicity basis. One easily verifies that the off-diagonal terms vanish since they are proportional to V, $\mathcal{P}_{+-} = \mathcal{P}_{-+} \propto V = 0$.

The intensity is proportional to the energy density of the CMB, $\rho = \frac{1}{8\pi} I$ and therefore to our perturbation variable $\mathcal{M} = \delta T/T = \frac{1}{4}\delta\rho/\rho = \frac{1}{4}\delta I/I$. Correspondingly we define the dimensionless Stokes parameters

$$\mathcal{Q} \equiv \frac{Q}{4I} \quad \text{and} \quad \mathcal{U} \equiv \frac{U}{4I} \ . \tag{3.70}$$

Rotating the basis $\left(\boldsymbol{\epsilon}^{(1)}, \boldsymbol{\epsilon}^{(2)}\right)$ by an angle ψ around the direction $\mathbf{n}$ we obtain $\boldsymbol{\epsilon}^{(1)'} = \cos\psi\boldsymbol{\epsilon}^{(1)} + \sin\psi\boldsymbol{\epsilon}^{(2)}$ and $\boldsymbol{\epsilon}^{(2)'} = \cos\psi\boldsymbol{\epsilon}^{(2)} - \sin\psi\boldsymbol{\epsilon}^{(1)}$ so that the coefficients with respect to the rotated basis are $E_1' = E_1\cos\psi - E_2\sin\psi$ and $E_2' = E_2\cos\psi + E_1\sin\psi$. For the Stokes parameters this implies

$$\begin{aligned} I' = I \ , \qquad & V' = V \quad \text{and} \\ Q' = Q\cos 2\psi - U\sin 2\psi \ , \qquad & U' = U\cos 2\psi + Q\sin 2\psi \ , \end{aligned} \tag{3.71}$$

or more simply

$$Q' \pm iU' = e^{\pm 2i\psi}(Q \pm iU) \ . \tag{3.72}$$

Hence $Q \pm iU$ transform like helicity-2 variables with a magnetic quantum number ± 2 under rotations around the $\mathbf{n}$ axis. They depend not only on the direction $\mathbf{n}$, but also on the orientation of the polarization basis $\left(\boldsymbol{\epsilon}^{(1)}, \boldsymbol{\epsilon}^{(2)}\right)$. For example, when rotating the polarization basis by $\pi/4$ we turn U into Q and Q into $-U$. Hence U measures the linear polarization in the basis $\left(\boldsymbol{\epsilon}^{(1)'}, \boldsymbol{\epsilon}^{(2)'}\right)$ which is rotated by $-\pi/4$ from the original basis.

It is not very convenient to work with these basis dependent amplitudes. First of all, the results will depend on the arbitrary choice of $\boldsymbol{\epsilon}^{(1)}$ and $\boldsymbol{\epsilon}^{(2)}$. Therefore, we shall not work directly with the Stokes parameters Q and U. But we make use of the spin weighted spherical harmonic functions ${}_sY_{\ell m}(\mathbf{n})$ which are defined for each integer s with $|s| \leq \ell$ and have the property that they transform under rotations about $\mathbf{n}$ by an angle ψ like ${}_sY_{\ell m}(\mathbf{n}) \to e^{is\psi}\ {}_sY_{\ell m}(\mathbf{n})$. The spin weighted spherical harmonics are the components of a symmetric rank $|s|$ tensor field defined on the tangent space of the sphere in the canonical basis $(\mathbf{e}_\vartheta \equiv \partial_\vartheta,\ \mathbf{e}_\varphi \equiv (1/\sin\vartheta)\partial_\varphi)$. Note that $(\mathbf{e}_\vartheta,\ \mathbf{e}_\varphi)$ are not well defined at the north and south poles. Setting

$$\mathbf{e}^{\pm} = \frac{1}{\sqrt{2}}\left(\mathbf{e}_\vartheta \mp i\mathbf{e}_\varphi\right) \ ,$$

${}_sY_{\ell m}(\mathbf{n})$ transforms like the $+\cdots+$ component of a rank s tensor, if $s > 0$ and like the $-\cdots-$ component of a rank $|s|$ tensor, if $s < 0$. More details about spin weighted spherical harmonics and the full derivation of the results presented here are found in [9].

With respect to the helicity basis $\mathbf{e}^{(\pm)}$, the dimensionless parameters $\mathcal{Q} \pm i\mathcal{U}$ can be expanded as

$$(\mathcal{Q} \pm i\mathcal{U})(\mathbf{n}) = \sum_{\ell=2}^{\infty}\sum_{m=-\ell}^{\ell} a_{\ell m}^{(\pm 2)}\ {}_{\pm 2}Y_{\ell m}(\mathbf{n}) \ , \tag{3.73}$$

$$= \sum_{\ell=2}^{\infty}\sum_{m=-\ell}^{\ell} \left(e_{\ell m} \pm ib_{\ell m}\right)\ {}_{\pm 2}Y_{\ell m}(\mathbf{n}) \ . \tag{3.74}$$

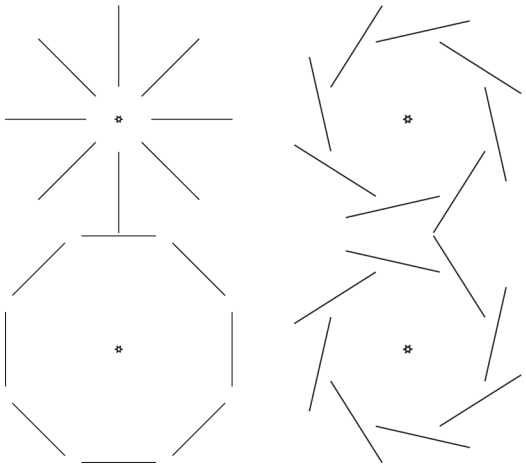

Figure 3.3: E-polarization (left) and B-polarization (right) patterns are shown around the photon direction indicated as the centre. E-polarization can be either radial or tangential, while B-polarization is clearly of curl type.

Hence

$$e_{\ell m} = \frac{1}{2}\left(a^{(2)}_{\ell m} + a^{(-2)}_{\ell m}\right) \ , \quad b_{\ell m} = \frac{-i}{2}\left(a^{(2)}_{\ell m} - a^{(-2)}_{\ell m}\right) \ . \tag{3.75}$$

Under a 'parity' transformation, $\mathbf{n} \to -\mathbf{n}$ the basis vectors $\mathbf{e}^{(\pm)}$ transform as $\mathbf{e}^{(\pm)} \to \mathbf{e}^{(\mp)}$. Hence the coefficient $a^{(2)}_{\ell m}$ turns into $a^{(-2)}_{\ell m}$ and $a^{(-2)}_{\ell m} \to a^{(2)}_{\ell m}$ so that $e_{\ell m}$ remains invariant while $b_{\ell m}$ changes sign.

As we have expanded $\mathcal{M}$ in Fourier components and Legendre polynomials one can now expand $\mathcal{Q} \pm i\mathcal{U}$ in Fourier components and spin weighted spherical harmonics and derive the Boltzmann equation for the corresponding components which we call

$$ {}_{\pm 2}\mathcal{A}^{(m)}_\ell(t,\mathbf{k}) = \mathcal{E}^{(m)}_\ell(t,\mathbf{k}) \pm i\mathcal{B}^{(m)}_\ell(t,\mathbf{k}) \ .$$

Here $\mathcal{E}$ again is parity even while $\mathcal{B}$ is parity odd. Scalar perturbations only generate E-polarisation which corresponds to a gradient field on the sphere while B-polarisation is a curl, see Fig. 3.3.

The Boltzmann equation for $(\mathcal{M}, \mathcal{E}, \mathcal{B})$ now couples $\mathcal{M}$ and $\mathcal{E}$ for vector and tensors perturbations, the evolution of $\mathcal{B}$ is also sources by $\mathcal{E}$, however, scalar perturbations do not generate $\mathcal{B}$. More details and a derivation of the Boltzmann equation using the total angular momentum method can be found in [9]. Fast codes like
CAMB (available at `https://camb.readthedocs.io/en/latest/`) or
CLASS (available at `https://lesgourg.github.io/class_public/class.html`)
calculate these CMB power spectra numerically with sub-percent precision for given cosmological parameters in a few seconds up to $\ell \sim 2000$.

The detection of B-polarisation would be very important as (within the standard model) it is nearly entire due to gravitational waves from inflation.

Exercice 12 *For an electric field normal to* $\mathbf{n}$ *given by* $E_i(\mathbf{n}) = \nabla_i f(\mathbf{n}) + \epsilon_{ij}\nabla_j g(\mathbf{n})$ *determine the* $\mathcal{E}$ *and* $\mathcal{B}$ *polarization. Here* f *and* g *are real functions*

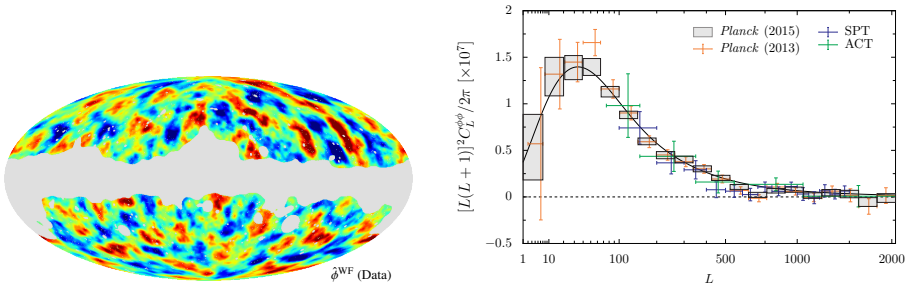

Figure 3.4: The lens map from Planck and the inferred lensing power spectrum are shown. Figs. from [31].

on the sphere; ϵ_{ij} *is the totally anti-symmetric tensor in two dimensions;* $\epsilon_{ij} = \pm \det \gamma$ *if* $(i,j) = (1,2)$ *and* $(i,j) = (2,1)$ *respectively and* $\epsilon_{ij} = 0$ *if two indices are equal. Here* γ *is the standard metric of the two-sphere.*

3.3 CMB lensing

So far, we have only used linear perturbation theory. But there is one second order term which cannot be neglected in a precise CMB calculation and it is also included in the above codes. This is lensing of CMB photons be foreground perturbations of the geometry. We shall again only consider scalar perturbations.

Due to the foreground gravitational potential the CMB temperature anisotropies and polarisation are lensed. The temperature which we see in direction $\mathbf{n}$ actually has been emitted into direction $\mathbf{n} + \delta\mathbf{n}$ and then deflected by an angle $-\delta\mathbf{n}$.

$$T_{\rm obs}(\mathbf{n}) = T(\mathbf{n} + \delta\mathbf{n}), \qquad \delta\mathbf{n} = \nabla\phi, \tag{3.76}$$

$$\phi(\mathbf{n}) = -\int_0^{r_*} dr \frac{(r_* - r)}{r_* r} (\Phi + \Psi)(r\mathbf{n}, \tau_0 - r)\,. \tag{3.77}$$

The function $\phi(\mathbf{n}, z_*)$ is called the lensing potential to the CMB. Its reconstruction from CMB observation is shown in Fig. 3.4 . A derivation of Eqs. (3.76) and (3.77) and be found e.g. in [9]. Lensing of the CMB is a second order effect. If the temperature fluctuations vanish lensing has no effect and if the lensing potential vanishes, the temperature fluctuations are not lensed. Lensing of E polarisation induces B polarisation also from scalar perturbations. These have been observed in several CMB experiments see Fig 3.5.

The fact that the observed B-polarisation spectrum is compatible with lensing of scalar perturbations without any need for a primordial tensor mode yields a limit of about $r < 0.065$ (at 95% confidence at the scale $k = 0.002{\rm Mpc}^{-1}$) for the tensor to scalar ratio, see Fig 3.6.

Lensing of the CMB is very important as it breaks degeneracies for parameter estimation and it provides an integrated measure of the matter distribution. The planned S4 CMB experiments like the Simons array will determine the lensing

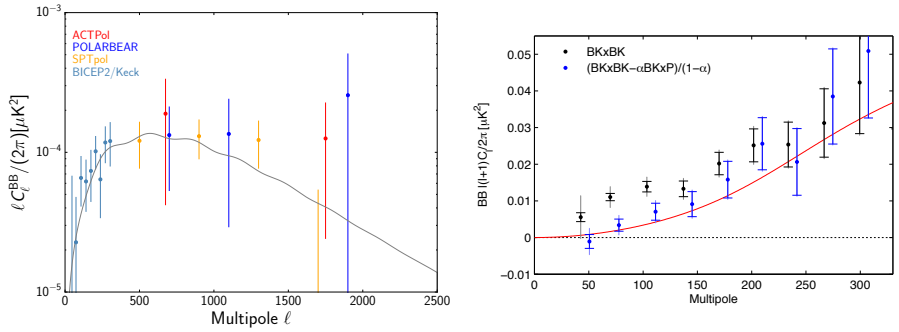

Figure 3.5: The observed B-polarization power spectrum, figures from [32] (left) and [33] (right). The data and the B polarisation spectrum from lensing of scalar perturbations for the Planck best fit model are shown.

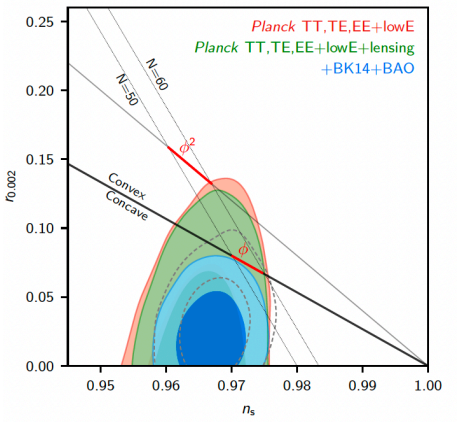

Figure 3.6: The limits on r at the scale $k = 0.002\text{Mpc}^{-1}$ from the Planck data, figure from [34].

potential with high accuracy. This is their primary goal besides measuring or limiting r down to $r_{\rm min} \sim 10^{-3}$, see [35].

3.4 Cosmological parameters from CMB observations

The CMB power spectrum and polarisation from scalar perturbations can formally be written in the form

$$C_\ell = \int dk \Delta^2_\ell(k) P_\Psi(k, t_{\rm in}) \tag{3.78}$$

Here $\Delta^2_\ell(k)$ only depends on cosmological parameters. Assuming a simple initial power spectrum like $k^3 P_\Psi(k, t_{\rm in}) = A_s (k t_0)^{n_s - 1}$, one can therefore use the measured C_ℓ spectrum to estimate cosmological parameters jointly with A_s and n_s.

The fixed parameter of the Planck base model assume

- No curvature, $K = 0$
- No tensor perturbations, $r = 0$
- Three species of thermal neutrinos, $N_{\rm eff} = 3.046$ with temperature $T_\nu = (4/11)^{1/3} T_0$
- 2 neutrino species are massless and the third has $m_3 = 0.06$eV such that $\sum_i m_i = 0.06$eV.
- Helium fraction $Y_{\rm He} = 4 n_{\rm He}/n_b$ is calculated from $N_{\rm eff}$ and ω_b.

The following parameters are estimated from the data via am Markov Chain Monte Carlo procedure (MCMC), see [9] for an explanation how this works in principle. The results given below are from [34].

- Amplitude of curvature perturbations, A_s
- Scalar spectral index, n_s
- Baryon density $\omega_b = \Omega_b h^2$
- Cold dark matter density $\omega_c = \Omega_c h^2$
- Present value of Hubble parameter $H_0 = 100 h$km/sec/Mpc ($\Omega_\Lambda = 1 - \Omega_m = 1 - (\omega_b + \omega_c)/h^2$).
- optical depth to reionization $\tau_{\rm reion}$.

$$\begin{array}{lcr} n_s & = & 0.9652 \pm 0.0042 \\ \Omega_c h^2 & = & 0.1198 \pm 0.0012 \\ \Omega_b h^2 & = & 0.02233 \pm 0.00015 \\ \ln(10^{10} A_s) & = & 3.043 \pm 0.014 \\ h & = & 0.6737 \pm 0.0054 \\ \tau_{\rm reion} & = & 0.054 \pm 0.0074 \\ (\Omega_\Lambda & = & 0.687 \pm 0.0087) \end{array} \tag{3.79}$$

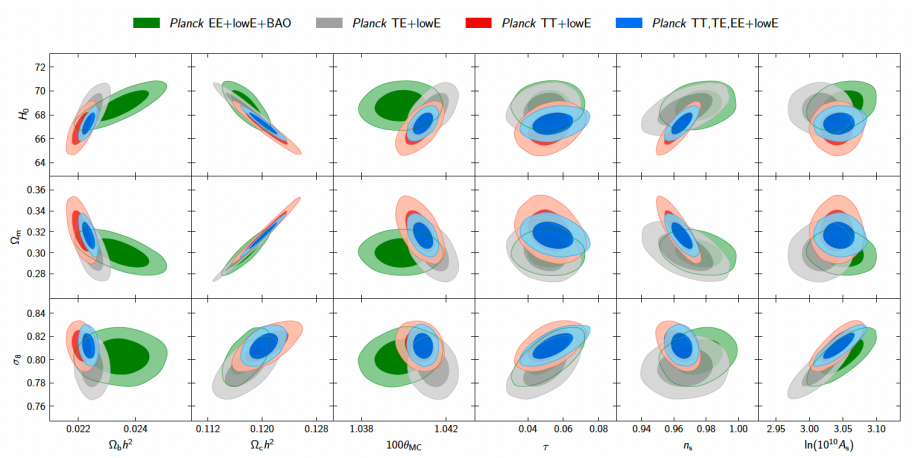

Figure 3.7: The cosmological parameters as obtained from the Planck data within the Planck base model defined above. The mans values with 65% errors are given in the list (3.79). Figure from [34].

3.5 Conclusions

`redo this !`

In this course you have seen how observations of CMB anisotropies and polarisation can be used to determine cosmological parameters as well as the parameters of the initial power spectrum which was generated in the early Universe, probably during a phase of inflation. As an example, from the CMB alone the presence of dark energy is inferred at more than 70σ. The CMB (more than 5000 data points) is compatible with a simple standard model of only 6 independent parameters, ΛCDM.

Nevertheless, the determination of these parameters with CMB observations is model dependent. Allowing for extensions of the standard mode, like e.g. curvature, tensor modes, a more complicated initial power spectrum, will lead to larger error bars on the parameters or may even move them outside the confidence interval of the standard model. For this reason we always talk of 'parameter estimation' and never of 'parameter measurement'. For this reasons it is also very important to confirm the standard model with other, independent observations, for example via large scale structure which is tested in galaxy number counts, weak lensing of H1 intensity mapping.

Already, some tension of cosmological parameters found by other means than the CMB have emerged: Direct measurements of the Hubble constant via Supernovae of type 1a used as 'modified standard candles yield [1]

$$H_0 = 73.04 \pm 1.04\text{km/sec/Mpc}$$

which is nearly 5σ higher than the value obtained by the Planck collaboration. Another tension come from the clustering amplitude measured by weak lensing. It is typically somewhat lower than the one inferred by Planck. More precisely, weak lensing survey are most sensitive to the combination

$$S_8 \equiv \sigma_8 \sqrt{\Omega_m/0.3}\,. \tag{3.80}$$

Here σ_8 is the matter fluctuation at $z = 0$ in a ball of radius $8h^{-1}$Mpc,

$$\sigma_8^2 = \frac{3}{2\pi^2} \int \frac{j_1(kR)}{kR} P_m(k) dk \qquad R = 8h^{-1}\text{Mpc}\,. \tag{3.81}$$

Planck results [34] infer $S_8 = 0.811 \pm 0.011$ while e.g. the KiDS weak lensing survey [36] reports $S_8 = 0.766^{+0.020}_{-0.014}$ which is in tension by about 2σ. The tension with older weak lensing results is somewhat larger.

It is not clear whether non-linearities or, especially baryonic effects which may not be correctly taken into account in weak lensing surveys are the cause of this tension. Also in what concerns the Hubble tension it is still possible that some unaccounted for systematic error in the supernova data or in the CMB might be the origin of the discrepancy. The most exciting prospect, however, is of course that these (or any other) tensions might be due to new physics, deviations from the simple ΛCDM model. So far no convincing alternatives have been proposed in the vaste literature on the subject[2].

To resolve the issue new observations which are as independent as possible from the present measurements are needed on the one side and new theoretical ideas concerning possible systematics in the data or alternative cosmological models are needed.

[2]Searching for 'H_0 tension' in the title I have found 275 papers (on September 19, 2023) on inspire which have collected 12'396 citations!

Appendix A

Appendix

In this appendix a present a brief reminder of General relativity, which is mainly useful to fix the notation but can of course not replace a course on the subject.

A.1 Notation

We consider a four-dimensional pseudo-Riemannian spacetime given by a manifold $\mathcal{M}$ and a metric g with signature $(-,+,+,+)$. For a given choice of coordinates $(x^\mu)_{\mu=0}^3$ the metric is given by the ten components of a 4×4 symmetric tensor,

$$g = ds^2 = g_{\mu\nu}dx^\mu dx^\nu \ . \tag{A.1}$$

Contravariant and covariant tensor fields on a pseudo-Riemannian manifold are equivalent. Their indices can be lowered and raised with the metric, e.g.

$$g_{\beta\nu}T^{\alpha\nu} = T^\alpha_{\ \beta} = g^{\alpha\mu}T_{\mu\beta}. \tag{A.2}$$

Here $g^{\alpha\mu}$ is the inverse of the metric such that $g^{\alpha\mu}g_{\mu\beta} = \delta^\alpha_\beta$, and we adopt Einstein's summation convention: indices which appear as subscripts and superscripts are summed over.

The Christoffel symbols are defined by

$$\Gamma^\mu_{\alpha\beta} = \frac{1}{2}g^{\mu\nu}\left[\partial_\alpha g_{\nu\beta} + \partial_\beta g_{\nu\alpha} - \partial_\nu g_{\alpha\beta}\right]. \tag{A.3}$$

Here ∂_μ indicates a partial derivative w.r.t. the coordinate x^μ, this is sometimes also simply denoted by a comma $\partial_\mu f \equiv f_{,\mu}$. Covariant derivatives are indicated by a semi-colon ';' or by the symbol ∇.

A geodesic $\gamma(t)$ with $X = \dot\gamma$ is a solution to the differential equation

$$\nabla_X X = 0\,, \quad X^\mu\partial_\mu X^\nu + \Gamma^\nu_{\alpha\beta}X^\alpha X^\beta = 0\ , \tag{A.4}$$

where the second equation expresses the first equation in components. The vector field $X = \dot\gamma$ is given by $X = X^\mu\partial_\mu$. We often conveniently identify a vector field with the partial derivative in its direction. A tensor field T of rank (p,q) is parallel transported along the vector field X if

$$\nabla_X T = 0\ , \quad X^\mu T^{\alpha_{i_1}\cdots\alpha_{i_p}}_{\beta_{j_1}\cdots\beta_{j_q};\mu} = 0\ . \tag{A.5}$$

Covariant derivatives of a tensor field are given by

$$T^{\alpha_{i_1}\cdots\alpha_{i_p}}_{\beta_{j_1}\cdots\beta_{j_q};\mu} = T^{\alpha_{i_1}\cdots\alpha_{i_p}}_{\beta_{j_1}\cdots\beta_{j_q},\mu} + \Gamma^{\alpha_{i_1}}_{\mu\sigma} T^{\sigma\cdots\alpha_{i_p}}_{\beta_{j_1}\cdots\beta_{j_q}} + \cdots - \Gamma^{\sigma}_{\mu\beta_{j_1}} T^{\alpha_{i_1}\cdots\alpha_{i_p}}_{\sigma\cdots\beta_{j_q}} - \cdots \ . \quad \text{(A.6)}$$

The Riemann curvature tensor is defined by

$$R^{\alpha}_{\ \beta\mu\nu} = \Gamma^{\alpha}_{\nu\beta,\mu} - \Gamma^{\alpha}_{\mu\beta,\nu} + \Gamma^{\rho}_{\beta\nu}\Gamma^{\alpha}_{\mu\rho} - \Gamma^{\rho}_{\beta\mu}\Gamma^{\alpha}_{\nu\rho} \ . \quad \text{(A.7)}$$

The tensor $R_{\alpha\beta\mu\nu} = g_{\alpha\sigma}R^{\sigma}_{\beta\mu\nu}$ is anti-symmetric in the first $(\alpha\beta)$ and second $(\mu\nu)$ pair of indices and symmetric in the exchange of the pairs, $(\alpha\beta) \leftrightarrow (\mu\nu)$. The Bianchi identities read

$$\Sigma_{(\beta\mu\nu)} R^{\alpha}_{\ \beta\mu\nu} = 0 \qquad \text{1st Bianchi identity} \quad \text{(A.8)}$$

$$\Sigma_{(\mu\nu\sigma)} R^{\alpha}_{\ \beta\mu\nu;\sigma} = 0 \qquad \text{2nd Bianchi identity .} \quad \text{(A.9)}$$

Here $\Sigma_{(\beta\mu\nu)}$ denotes the sum over all cyclic permutations of these three indices.

The Ricci tensor and the Riemann scalar are given by

$$R_{\mu\nu} = R^{\alpha}_{\ \mu\alpha\nu} \ , \qquad R = R^{\mu}_{\mu} = R_{\mu\nu}g^{\mu\nu} \ . \quad \text{(A.10)}$$

With these sign conventions, the curvature of the sphere is positive, and changing the order of covariant derivatives of a vector field X yields

$$\nabla_\mu \nabla_\nu X^\alpha - \nabla_\nu \nabla_\mu X^\alpha = R^{\alpha}_{\ \sigma\mu\nu} X^\sigma \ . \quad \text{(A.11)}$$

The Einstein tensor is defined as

$$G_{\mu\nu} = R_{\mu\nu} - \frac{1}{2} g_{\mu\nu} R \ . \quad \text{(A.12)}$$

The second Bianchi identity and the symmetries of the Riemann tensor imply $G^{\nu}_{\mu;\nu} = 0$.

The field equations of general relativity relate the curvature to the energy–momentum tensor $T_{\mu\nu}$ via Einstein's equation,

$$G_{\mu\nu} = 8\pi G T_{\mu\nu} \ , \quad \text{(A.13)}$$

where G denotes Newton's constant, $G = m_P^{-2}$. The second Bianchi identity ensures that $T_{\mu\nu}$ is covariantly conserved, $T^{\nu}_{\mu;\nu} = 0$. Equation (A.13) can also be derived from an action principle with

$$S = S_{\rm grav} + S_{\rm mat} \ .$$

Here $S_{\rm mat}$ is the usual matter action and

$$S_{\rm grav} = \frac{m_P^2}{16\pi} \int d^4x \sqrt{-g} R \quad \text{(A.14)}$$

is the Hilbert action. A somewhat tedious but standard calculation gives (see e.g. [37])

$$\delta S_{\rm grav} = -\frac{m_P^2}{16\pi} \int d^4x \sqrt{-g} G^{\mu\nu} \delta g_{\mu\nu} \ . \quad \text{(A.15)}$$

The Einstein equation implies then that the energy–momentum tensor can be obtained by varying the matter action w.r.t. the metric,

$$T^{\mu\nu} = \frac{1}{2}\frac{\delta S_{\mathrm{mat}}}{\delta g_{\mu\nu}} \ .$$

By construction, this energy–momentum tensor is always symmetric, but it does, in general, not agree with the canonical energy–momentum tensor. Of course the conserved quantities (if any!) are the same for both definitions.

The Weyl tensor specifies the degrees of freedom of the Riemann tensor which are not determined by the Ricci tensor (or Einstein tensor). It is the traceless part of $R^{\alpha}_{\beta\mu\nu}$. In n dimensions, $n \geq 3$, it is given by

$$\begin{aligned} C_{\alpha\beta\mu\nu} &= R_{\alpha\beta\mu\nu} - \frac{2}{n-2}\left(g_{\alpha[\mu}R_{\nu]\beta} + g_{\beta[\mu}R_{\nu]\alpha}\right) \\ &\quad - \frac{2}{(n-1)(n-2)} R g_{\alpha[\mu}g_{\nu]\beta} \ . \end{aligned} \tag{A.16}$$

Here $[\mu\nu]$ denotes anti-symmetrization in the indices μ and ν. The Weyl tensor has the same symmetries like the Riemann tensor but all its traces vanish. It describes the degrees of freedom of the curvature (gravitational field) in source-free spacetime, hence it describes gravity waves.

An introduction to general relativity can be found e.g. in [38] or [37].

A.2 The Lie derivative

For a vector field X with flux ϕ_t^X the Lie derivative of a tensor field T of arbitrary rank is defined by

$$L_X T = \lim_{\epsilon\to 0} \frac{1}{\epsilon}\left(\left(\phi_\epsilon^X\right)^* T - T\right) \ . \tag{A.17}$$

Here $\left(\phi_\epsilon^X\right)^*$ denotes the pullback of the map $\phi_t^X : \mathcal{M} \to \mathcal{M} : p \mapsto \gamma_p(t)$, where γ_p is the integral curve to X with starting point p. The existence and uniqueness of solutions to ordinary differential equations tells us that for sufficiently small t, ϕ_t^X is a local diffeomorphism. If $T(t)$ denotes the value of the tensor field T at the position $\gamma_p(t)$ we also have

$$L_X T(p) = \left.\frac{d}{dt}\right|_{t=0} T(t) \ . \tag{A.18}$$

Hence the Lie derivative in direction X vanishes if the tensor field T is conserved along integral curves of X. Furthermore, for small t we have

$$\left(\phi_t^X\right)^* T = T + t L_X T + \mathcal{O}(t^2) \tag{A.19}$$

In coordinates the Lie derivative becomes (see e.g. [37])

$$\begin{aligned} L_X T^{\alpha_{i_1}\cdots\alpha_{i_p}}_{\beta_{j_1}\cdots\beta_{j_q}} &= X^\mu T^{\alpha_{i_1}\cdots\alpha_{i_p}}_{\beta_{j_1}\cdots\beta_{j_q},\mu} - X^{\alpha_{i_1}}{}_{,\sigma}\, T^{\sigma\cdots\alpha_{i_p}}_{\beta_{j_1}\cdots\beta_{j_q}} - \cdots \\ &\quad + X^{\sigma}{}_{,\beta_{j_1}}\, T^{\alpha_{i_1}\cdots\alpha_{i_p}}_{\sigma\cdots\beta_{j_q}} + \cdots \ . \end{aligned} \tag{A.20}$$

A.3 Friedmann metric and curvature

The Friedmann metric is given by

$$ds^2 = g_{\mu\nu}dx^\mu dx^\nu = -d\tau^2 + a^2(\tau)\gamma_{ij}dx^i dx^j = a^2(\tau)[-dt^2 + \gamma_{ij}dx^i dx^j] \quad \text{(A.21)}$$

The Christoffel symbols with respect to cosmic or conformal time are

		cosmic time τ	conformal time t	
Γ^0_{00}	$=$	0	$\frac{\dot{a}}{a}$	(A.22)
Γ^i_{00}	$=$	0	0	(A.23)
Γ^0_{i0}	$=$	0	0	(A.24)
Γ^i_{j0}	$=$	$\frac{a'}{a}\delta^i_j = H\delta^i_j$	$\frac{\dot{a}}{a}\delta^i_j = \mathcal{H}\delta^i_j$	(A.25)
Γ^0_{ij}	$=$	$a'a\gamma_{ij}$	$\frac{\dot{a}}{a}\gamma_{ij}$	(A.26)
Γ^k_{ij}	$=$	${}^{(3)}\Gamma^k_{ij} = \frac{1}{2}\gamma^{km}\left(\gamma_{im,j} + \gamma_{jm,i} - \gamma_{ij,m}\right)$	${}^{(3)}\Gamma^k_{ij}$,	(A.27)

where ${}^{(3)}\Gamma^k_{ij}$ denotes the three-dimensional Christoffel symbols of the metric γ which depend on the coordinate system chosen on the spatial slices. The overdot indicates a derivative w.r.t. conformal time t while the prime indicates a derivative w.r.t. cosmic time τ.

The non-vanishing components of the Riemann and Ricci curvature tensors in **cosmic time** τ are then given by

$$\begin{aligned}
R^0_{i0j} &= a''a\gamma_{ij} \ , && \text{(A.28)}\\
R^i_{00j} &= \frac{a''}{a}\delta^i_j \ , && \text{(A.29)}\\
R^i_{jkm} &= {}^{(3)}R^i_{jkm} + (a')^2\left(\delta^i_k\gamma_{jm} - \delta^i_m\gamma_{jk}\right) \ , && \text{(A.30)}\\
R_{00} &= -3\frac{a''}{a} \ , && \text{(A.31)}\\
R_{ij} &= \left[a''a + 2\left(a'^2 + K\right)\right]\gamma_{ij} \ , && \text{(A.32)}\\
R &= 6[\frac{a''}{a} + H^2 + \frac{K}{a^2}] \ , && \text{(A.33)}
\end{aligned}$$

while in **conformal time** t we have

$$\begin{aligned}
R^0_{i0j} &= \left(\frac{\dot{a}}{a}\right)^{\cdot}\gamma_{ij} = \dot{\mathcal{H}}\gamma_{ij} \ , && \text{(A.34)}\\
R^i_{00j} &= \left(\frac{\dot{a}}{a}\right)^{\cdot}\delta^i_j = \dot{\mathcal{H}}\delta^i_j \ , && \text{(A.35)}\\
R^i_{jkm} &= {}^{(3)}R^i_{jkm} + \mathcal{H}^2\left(\delta^i_k\gamma_{jm} - \delta^i_m\gamma_{jk}\right) \ , && \text{(A.36)}\\
R_{00} &= -3\left(\frac{\dot{a}}{a}\right)^{\cdot} = \dot{\mathcal{H}} \ , && \text{(A.37)}\\
R_{ij} &= \left[\dot{\mathcal{H}} + 2\left(\mathcal{H}^2 + K\right)\right]\gamma_{ij} \ , && \text{(A.38)}\\
R &= \frac{6}{a^2}\left[\dot{\mathcal{H}} + \mathcal{H}^2 + K\right] \ . && \text{(A.39)}
\end{aligned}$$

The curvature on the three-dimensional slices of constant time is given by

$$
\begin{aligned}
{}^{(3)}R^i_{jkm} &= K\left(\delta^i_k\gamma_{jm} - \delta^i_m\gamma_{jk}\right) \ , && \text{(A.40)}\\
{}^{(3)}R_{ij} &= 2K\gamma_{ij} \qquad \text{and} && \text{(A.41)}\\
{}^{(3)}R &= 6K \ . && \text{(A.42)}
\end{aligned}
$$

A.4 Scalar perturbations

Here we collect the Christoffel symbols and the curvature tensor for scalar perturbations in longitudinal gauge in Fourier space,

$$ds^2 = a^2\left(-(1+2\Psi)\,dt^2 + (1-2\Phi)\delta_{ij}\,dx^i\,dx^j\right) \ . \qquad \text{(A.43)}$$

A.4.1 The Christoffel symbols

$$
\begin{aligned}
\delta\Gamma^0_{00} = \quad & \dot\Psi \ , \qquad & \delta\Gamma^0_{0j} = ik_j\Psi \ , && \text{(A.44)}\\
\delta\Gamma^j_{00} = \quad & ik^j\Psi \ , \qquad & \delta\Gamma^j_{i0} = -\dot\Phi\delta^j_i \ , && \text{(A.45)}
\end{aligned}
$$

$$
\begin{aligned}
\delta\Gamma^0_{ij} = \quad & \left[-2\mathcal{H}(\Psi+\Phi) - \dot\Phi\right]\delta_{ij} \ , && \text{(A.46)}\\
\delta\Gamma^j_{im} = \quad & -i\Phi\left[\delta^j_i k_m + \delta^j_m k_i - \delta i m k^j\right] \ . && \text{(A.47)}
\end{aligned}
$$

A.4.2 The Riemann tensor

$$
\begin{aligned}
\delta R^0_{00j} &= \delta R^0_{0ij} = 0, && \text{(A.48)}\\
\delta R^0_{i0j} &= -\left[2\dot{\mathcal{H}}(\Psi+\Phi) + \mathcal{H}(\dot\Psi+\dot\Phi) + \ddot\Phi - \frac{k^2}{3}\Psi\right]\delta_{ij}\\
&\quad \Psi k_i k_j \ , && \text{(A.49)}\\
\delta R^0_{ijm} &= -\left[\mathcal{H}\Psi + \dot\Phi\right](\delta_{ij}k_m - \delta_{im}k_j) \ , && \text{(A.50)}\\
\delta R^i_{00j} &= \left[\frac{k^2}{3}\Psi - \mathcal{H}(\dot\Psi+\dot\Phi) - \ddot\Phi\right]\delta^i_j + \Psi k^i k_j \ , && \text{(A.51)}\\
\delta R^i_{0jm} &= i\left[\dot\Phi + \mathcal{H}\Psi\right]\left(\delta^i_j k_m - \delta^i_m k_j\right) \ , && \text{(A.52)}\\
\delta R^i_{j0m} &= -i\left[\mathcal{H}\Psi + \dot\Phi\right]\left(\delta^i_m k_j - \delta_{jm}k^i\right) \ , && \text{(A.53)}\\
\delta R^i_{jmn} &= -2\left[\mathcal{H}^2(\Psi+\Phi) + \mathcal{H}\dot\Phi + \frac{1}{3}k^2\Phi\right]\left(\delta^i_m\delta_{jn} - \delta^i_n\delta_{jm}\right)\\
&\quad \Phi\left(\delta^i_n k_j k_m - \delta^i_m k_j k_n + k^i k_n\delta_{jm} - k^i k_m\delta_{jn}\right) \ . && \text{(A.54)}
\end{aligned}
$$

A.4.3 The Ricci and Einstein tensors

The perturbation if the Ricci tensor is

$$\begin{aligned}
\delta R_{00} &= 3\mathcal{H}(\dot{\Psi}+\dot{\Phi}) - k^2\Psi + 3\ddot{\Phi} \ , && \text{(A.55)}\\
\delta R_{0j} &= 2i\left[\mathcal{H}\Psi + \dot{\Phi}\right]k_j \ , && \text{(A.56)}\\
\delta R_{ij} &= \Big[-2(\dot{\mathcal{H}}+2\mathcal{H}^2)(\Psi+\Phi) - \mathcal{H}\dot{\Psi} + \frac{k^2}{3}\Psi - \ddot{\Phi} - 5\mathcal{H}\dot{\Phi} \\
&\quad - \frac{4}{3}k^2\Phi\Big]\delta_{ij} - (\Phi-\Psi)k_ik_j \ . && \text{(A.57)}
\end{aligned}$$

The perturbation of the Riemann scalar then becomes

$$\delta R = -\frac{2}{a^2}\left[6(\dot{\mathcal{H}}+\mathcal{H}^2)\Psi + 3\mathcal{H}\dot{\Psi} - k^2\Psi + 9\mathcal{H}\dot{\Phi} + 3\ddot{\Phi} + 2(k^2-3K)\Phi\right] \ . \tag{A.58}$$

For the Einstein tensor we find

$$\begin{aligned}
\delta G^0_0 &= \frac{2}{a^2}\left[3\mathcal{H}^2\Psi + 3\mathcal{H}\dot{\Phi} + (k^2-3K)\Phi\right] \ , && \text{(A.59)}\\
\delta G^0_j &= -i\frac{2}{a^2}\left[\mathcal{H}\Psi + \dot{\Phi}\right]k_j \ , && \text{(A.60)}\\
\delta G^j_0 &= i\frac{2}{a^2}\left[\mathcal{H}\Psi + \dot{\Phi}\right]k^j \ , && \text{(A.61)}\\
\delta G^i_j &= \frac{2}{a^2}\left[(2\dot{\mathcal{H}}+\mathcal{H}^2)\Psi + \mathcal{H}\dot{\Psi} - \frac{k^2}{3}\Psi + \ddot{\Phi} + 2\mathcal{H}\dot{\Phi} + \frac{k^2}{3}\Phi\right]\delta^i_j \\
&\quad - \frac{1}{a^2}(\Phi-\Psi)k^ik_j \ . && \text{(A.62)}
\end{aligned}$$

A.4.4 The Weyl tensor

The Weyl tensor from scalar perturbations only has an 'electric' component, i.e. all the components are determined by

$$C^0_{i0j} \equiv -E_{ij} = -\frac{1}{2}(\Phi+\Psi)k_ik_j \ . \tag{A.63}$$

More precisely we have

$$\begin{aligned}
C_{0i0j} &= a^2E_{ij} \ , && \text{(A.64)}\\
C_{0ijk} &= 0 \ , && \text{(A.65)}\\
C_{ijk\ell} &= g_{ik}E_{j\ell} + g_{j\ell}E_{ik} - g_{jk}E_{i\ell} - g_{i\ell}E_{jk} \ . && \text{(A.66)}
\end{aligned}$$

Bibliography

[1] A. G. Riess *et al.*, "A Comprehensive Measurement of the Local Value of the Hubble Constant with 1 km s^1 Mpc^1 Uncertainty from the Hubble Space Telescope and the SH0ES Team," *Astrophys. J. Lett.* **934** no. 1, (2022) L7, arXiv:2112.04510 [astro-ph.CO].

[2] **Planck** Collaboration, P. A. R. Ade *et al.*, "Planck 2015 results. XIII. Cosmological parameters," *Astron. Astrophys.* **594** (2016) A13, arXiv:1502.01589 [astro-ph.CO].

[3] R. R. Caldwell, M. Kamionkowski, and N. N. Weinberg, "Phantom energy and cosmic doomsday," *Phys. Rev. Lett.* **91** (2003) 071301, arXiv:astro-ph/0302506 [astro-ph].

[4] R. R. Caldwell, R. Dave, and P. J. Steinhardt, "Cosmological imprint of an energy component with general equation of state," *Phys. Rev. Lett.* **80** (1998) 1582–1585, arXiv:astro-ph/9708069 [astro-ph].

[5] L. Gradshteyn and L. Ryzhik, *Table of Integrals, Series and Products.* Academic Press, New York, sixth edition ed., 2000.

[6] M. Abramowitz and I. Stegun, *Handbook of Mathematical Functions.* Dover Publications, New York, 9th printing ed., 1970.

[7] **Particle Data Group** Collaboration, K. A. Olive *et al.*, "Review of Particle Physics," *Chin. Phys.* **C38** (2014) 090001.

[8] **Particle Data Group** Collaboration, W. M. Yao *et al.*, "Review of Particle Physics," *J. Phys.* **G33** (2006) 1–1232.

[9] R. Durrer, *The Cosmic Microwave Background, Second Edition.* Cambridge University Press, 2020.

[10] A. Kogut *et al.*, "ARCADE: Absolute Radiometer for Cosmology, Astrophysics, and Diffuse Emission," *New Astron. Rev.* **50** (2006) 925–931, arXiv:astro-ph/0609373 [astro-ph].

[11] D. J. Fixsen, E. S. Cheng, J. M. Gales, J. C. Mather, R. A. Shafer, and E. L. Wright, "The Cosmic Microwave Background spectrum from the full COBE FIRAS data set," *Astrophys. J.* **473** (1996) 576, arXiv:astro-ph/9605054 [astro-ph].

[12] **Planck** Collaboration, N. Aghanim *et al.*, "Planck 2018 results. I. Overview and the cosmological legacy of Planck," *Astron. Astrophys.* **641** (2020) A1, arXiv:1807.06205 [astro-ph.CO].

[13] V. Mukhanov, *Physical Foundations of Cosmology*. Cambridge University Press, 2005.

[14] **Particle Data Group** Collaboration, C. Patrignani *et al.*, "Review of Particle Physics," *Chin. Phys.* **C40** no. 10, (2016) 100001.

[15] R. Durrer, M. Kunz, and A. Melchiorri, "Cosmic structure formation with topological defects," *Phys. Rept.* **364** (2002) 1–81, arXiv:astro-ph/0110348 [astro-ph].

[16] H. Davoudiasl and P. P. Giardino, "Gravitational Waves from Primordial Black Holes and New Weak Scale Phenomena," *Phys. Lett.* **B768** (2017) 198–202, arXiv:1609.00907 [gr-qc].

[17] C. Caprini, R. Durrer, and G. Servant, "The stochastic gravitational wave background from turbulence and magnetic fields generated by a first-order phase transition," *JCAP* **0912** (2009) 024, arXiv:0909.0622 [astro-ph.CO].

[18] E. Lifshitz, "Republication of: On the gravitational stability of the expanding universe," *J. Phys.(USSR)* **10** (1946) 116. [Gen. Rel. Grav.49,no.2,18(2017)].

[19] J. M. Stewart and M. Walker, "Perturbations of spacetimes in general relativity," *Proc. Roy. Soc. Lond.* **A341** (1974) 49–74.

[20] R. Durrer and N. Straumann, "Some applications of the $3+1$ formalism of general relativity," *Helv. Phys. Acta* **61** (1988) 1027–1045.

[21] P. J. E. Peebles, *Principles of Physical Cosmology*. Princeton University Press, 1993.

[22] **COBE** Collaboration, G. F. Smoot *et al.*, "Structure in the COBE differential microwave radiometer first year maps," *Astrophys. J.* **396** (1992) L1–L5.

[23] R. Durrer, M. Gasperini, M. Sakellariadou, and G. Veneziano, "Massless (pseudo)scalar seeds of CMB anisotropy," *Phys. Lett.* **B436** (1998) 66–72, arXiv:astro-ph/9806015 [astro-ph].

[24] *General relativity and kinetic theory*. New York, Academic Press, 1971.

[25] J. Stewart, *Non-equilibrium relativistic kinetic theory*. Springer Lecture Notes. Springer-Verlag, Berlin, 1971.

[26] W. Hu and N. Sugiyama, "Small scale cosmological perturbations: An Analytic approach," *Astrophys. J.* **471** (1996) 542–570, arXiv:astro-ph/9510117 [astro-ph].

[27] W. Hu and M. J. White, "CMB anisotropies: Total angular momentum method," *Phys. Rev.* **D56** (1997) 596–615, arXiv:astro-ph/9702170 [astro-ph].

[28] E. Lifshitz and L. Pitajewski, *Lehrbuch der Theoretischen Physik, vol. X.* Akademie Verlag, Berlin, 1983.

[29] U. Seljak and M. Zaldarriaga, "A Line of sight integration approach to cosmic microwave background anisotropies," *Astrophys. J.* **469** (1996) 437–444, arXiv:astro-ph/9603033 [astro-ph].

[30] J. D. Jackson, *Classical Electrodynamics.* Wiley & Sons, New York, 1975.

[31] **Planck** Collaboration, P. A. R. Ade *et al.*, "Planck 2015 results. XV. Gravitational lensing," *Astron. Astrophys.* **594** (2016) A15, arXiv:1502.01591 [astro-ph.CO].

[32] **ACTPol** Collaboration, T. Louis *et al.*, "The Atacama Cosmology Telescope: Two-Season ACTPol Spectra and Parameters," *JCAP* **1706** no. 06, (2017) 031, arXiv:1610.02360 [astro-ph.CO].

[33] **BICEP2, Planck** Collaboration, P. A. R. Ade *et al.*, "Joint Analysis of BICEP2/*KeckArray* and *Planck* Data," *Phys. Rev. Lett.* **114** (2015) 101301, arXiv:1502.00612 [astro-ph.CO].

[34] **Planck** Collaboration, N. Aghanim *et al.*, "Planck 2018 results. VI. Cosmological parameters," *Astron. Astrophys.* **641** (2020) A6, arXiv:1807.06209 [astro-ph.CO]. [Erratum: Astron.Astrophys. 652, C4 (2021)].

[35] **CMB-S4** Collaboration, K. N. Abazajian *et al.*, "CMB-S4 Science Book, First Edition," arXiv:1610.02743 [astro-ph.CO].

[36] C. Heymans *et al.*, "KiDS-1000 Cosmology: Multi-probe weak gravitational lensing and spectroscopic galaxy clustering constraints," *Astron. Astrophys.* **646** (2021) A140, arXiv:2007.15632 [astro-ph.CO].

[37] R. Wald, *General Relativity.* Chicago University Press, 1984.

[38] N. Straumann, *General Relativity.* Springer Verlag, Berlin, second edition ed., 2013.